

**TRANSCRIPTIONAL REGULATION OF FATTY ACID
BINDING PROTEIN EXPRESSION IN
LOCUST FLIGHT MUSCLE**

by

Jun Mark Zhang

B.Sc., Nankai University, 1986

THESIS SUBMITTED IN PARTIAL FULFILLMENT OF
THE REQUIREMENTS FOR THE DEGREE OF
MASTER OF SCIENCE
IN THE DEPARTMENT OF BIOLOGICAL SCIENCES

© Jun Mark Zhang 1997

SIMON FRASER UNIVERSITY

December 1997

All rights reserved. This work may not be
reproduced in whole or in part, by photocopy
or other means, without permission of the author.



National Library
of Canada

Acquisitions and
Bibliographic Services

395 Wellington Street
Ottawa ON K1A 0N4
Canada

Bibliothèque nationale
du Canada

Acquisitions et
services bibliographiques

395, rue Wellington
Ottawa ON K1A 0N4
Canada

Your file *Voire référence*

Our file *Notre référence*

The author has granted a non-exclusive licence allowing the National Library of Canada to reproduce, loan, distribute or sell copies of this thesis in microform, paper or electronic formats.

The author retains ownership of the copyright in this thesis. Neither the thesis nor substantial extracts from it may be printed or otherwise reproduced without the author's permission.

L'auteur a accordé une licence non exclusive permettant à la Bibliothèque nationale du Canada de reproduire, prêter, distribuer ou vendre des copies de cette thèse sous la forme de microfiche/film, de reproduction sur papier ou sur format électronique.

L'auteur conserve la propriété du droit d'auteur qui protège cette thèse. Ni la thèse ni des extraits substantiels de celle-ci ne doivent être imprimés ou autrement reproduits sans son autorisation.

0-612-24278-1

Canada

APPROVAL

Name: Jun Mark Zhang

Degree: MASTER OF SCIENCE

Title of Thesis:

Transcriptional Regulation of Fatty Acid Binding Protein Expression in Locust Flight Muscle.

Examining Committee:

Chair: Dr. N. Verbeek, Professor

Dr. N. Haunerland, Associate Professor, Senior Supervisor
Department of Biological Sciences, S.F.U.

Dr. B. McKeown, Professor
Department of Biological Sciences, S.F.U.

Dr. S. Lee, Assistant Professor
Department of Biological Sciences, S.F.U.

Dr. T. Williams, Associate Professor
Department of Biological Sciences, S.F.U.
Public Examiner

Date Approved: Dec 10, 1997

PARTIAL COPYRIGHT LICENSE

I hereby grant to Simon Fraser University the right to lend my thesis, project or extended essay (the title of which is shown below) to users of the Simon Fraser University Library, and to make partial or single copies only for such users or in response to a request from the library of any other university, or other educational institution, on its own behalf or for one of its users. I further agree that permission for multiple copying of this work for scholarly purposes may be granted by me or the Dean of Graduate Studies. It is understood that copying or publication of this work for financial gain shall not be allowed without my written permission.

✓
Title of Thesis/Project/Extended Essay

Transcriptional Regulation of Fatty Acid Binding Protein

Expression in Locust Flight Muscle.

Author:

(signature)

Jun Mark Zhang

(name)

December 10, 1997

(date)

ABSTRACT

Fatty acid binding protein (FABP) is the most abundant cytosolic protein in developed flight muscle of adult locusts, but it is completely absent in nymphs. During the two weeks following adult ecdysis, FABP rises to 18 % of the total soluble proteins. FABP mRNA increases steadily up to day 8, before gradually declining to a low concentration at day 15, which remains constant for the rest of the animals life.

In vitro nuclear run-on assays were used to measure the transcriptional status of the FABP gene, but this method was found to be not suitable for locust flight muscle. Instead, an alternative assay was developed (quantitative competitive reverse transcription polymerase chain reaction). Using a PCR primer combination specific for a 600 bp sequence of an intron of the FABP gene, a QC-RT-PCR system was developed to quantify the amount of primary transcript present in muscle tissue at various ages. The FABP gene is not transcribed prior to metamorphosis; its primary transcript rises rapidly during the first two days of adult life, and remains close to maximal until day 5. Subsequently its level rapidly declines, ultimately reaching values of less than 0.02 % of the maximal level. The correlation between primary transcript, mRNA and FABP content were analyzed by modeling transcription, translation and degradation with computer modeling software. The half-lives of FABP protein and its mRNA were estimated as 34 days and 2.3 days, respectively. The computer simulation was in good agreement with the experimentally obtained data, suggesting that the control of FABP expression in locust flight muscle occurs predominantly at the level of transcription initiation.

ACKNOWLEDGMENT

I express my sincerest thanks to Dr. Norbert H. Haunerland, my senior supervisor, for his patient guidance and encouragement throughout my whole project, for his great help in improving my writing. I deeply appreciate the freedom he gave me during my graduate studies. I have learnt a lot in many ways under his supervision over the past four years.

Many thanks go to Dr. Stephen P. Lee and Dr. Brian A. McKeown, my committee supervisors, for their great help, assistance and invaluable advice.

I wish to express my genuine appreciation to Dr. Tony D. Williams and Dr. Nicholas A.M. Verbeek for their kindness in reading my thesis and evaluating my thesis defense.

I also wish to thank Dr. Victor L. Bourne for his technical help on electron microscope; Mr. Akbar Syed for his maintaining the locust colony; Mr. Mei-Keng Yang for his friendship and technical assistance on many instruments.

I also like to thank my labmates and friends who gave me help in many ways.

Special thanks to my family, my wife, Sue, for her care, encouragement and suggestions throughout my studies; my parents, for their support and encouragement all the way in my life.

TABLE OF CONTENTS

APPROVAL	i
ABSTRACT	ii
ACKNOWLEDGEMENTS	iii
TABLE OF CONTENTS	iv
LIST OF FIGURES	vii
CHAPTER 1. GENERAL INTRODUCTION	1
CHAPTER 2. NUCLEI ISOLATION	12
2.1. Introduction	12
2.2. Material and Methods	13
2.2.1. Chemicals and buffers	13
2.2.2. Methods	14
2.2.2.1. Insects	14
2.2.2.2. Nuclei isolation from locust flight muscle	14
2.2.2.3. Electron microscopy	16
2.3. Results	16
2.4. Discussion	20
CHAPTER 3. NUCLEAR RUN-ON ASSAY	22
3.1. Introduction	22
3.2. Material and methods	23
3.2.1. Material	23
3.2.1.1. Plasmid preparation	24
3.2.1.2. Genomic DNA extraction	24
3.2.1.3. cDNA library amplification	24
3.2.1.4. Dot blotting	25
3.2.1.5. Run-on transcription	25

3.2.1.6. Hybridization	26
3.2.1.7. Detection	26
3.2.2. Methods	26
3.2.2.1. Plasmid extraction and purification	26
3.2.2.2. Genomic DNA extraction from locust flight muscle	28
3.2.2.3. Amplifying locust flight muscle cDNA library	28
3.2.2.4. Phage miniprep	29
3.2.2.5. Dot blot on nylon membrane	29
3.2.2.6. Nuclear run on reaction	30
3.2.2.7. Hybridization	30
3.2.2.8. Checking the quality of the DIG detection system	31
3.2.2.9. Detection	31
3.3. Results	32
3.4. Discussion	39

CHAPTER 4. QUANTITATIVE COMPETITIVE REVERSE

TRANSCRIPTION PCR	41
4.1. Introduction	41
4.2. Material and methods	46
4.2.1. Material	46
4.2.2. PCR primer design	46
4.2.3. Internal standard preparation	46
4.2.4. Total RNA isolation	47
4.2.5. Standard curve preparation	48
4.3. Results	49
4.4. Discussion	65

CHAPTER 5. CHANGES IN FABP PRE-MRNA DURING DEVELOPMENT	69
5.1. Introduction	69
5.2. Material and Methods	70
5.2.1. Insects	70
5.2.2. Total RNA isolation	70
5.2.3. Quantitative competitive RT-PCR	70
5.2.4. Detection and quantitation of PCR products	71
5.3. Results	72
5.4. Discussion	78
CHAPTER 6. COMPUTER SIMULATION OF M-FABP GENE EXPRESSION DURING LOCUST DEVELOPMENT	81
6.1. Introduction	81
6.2. Material and methods	83
6.3. Results	84
6.3.1. Determination of protein stability	84
6.3.2. Determination of mRNA stability	88
6.3.3. Complete simulation of mRNA synthesis	92
6.4. Discussion	96
CHAPTER 7. GENERAL DISCUSSION	100
REFERENCE	106

LIST OF FIGURES

Fig. 1-1: Locust lipid transport and utilization.	6
Fig. 2-1: Electron microscope graph of the isolated nuclei from locust flight muscle.	17
Fig. 2-2: Electron microscope graph of the isolated nuclei from locust flight muscle.	18
Fig. 2-3: Electron microscope graph of the isolated nuclei from locust flight muscle.	19
Fig. 3-1: The sensitivity of DIG detection system	34
Fig. 3-2: Nuclear run-on product	35
Fig. 3-3 : Nuclear run-on assay results using different DNA probes	36
Fig. 3-4 : Nuclear run-on assay results using different DNA probes	37
Fig. 3-5 : Nuclear run-on result from 10 day-old locust flight muscle nuclei	38
Fig. 4-1: The restriction map of locust flight muscle fatty acid binding protein gene, <i>Schistocerca gregaria</i>	45
Fig. 4-2: RT-PCR of total RNA and PCR of genomic DNA from 5 day-old locust with primer pair of ex1.5a and ex1.5c	52
Fig. 4-3: Internal standard lower primer (IS1.5I) design	53
Fig. 4-4: Internal standard DNA (IS-DNA)	54
Fig. 4-5: Scheme graph of the internal standard plasmid	55
Fig. 4-6: PCR of IS1.5 clone and genomic DNA with ex1.5a and ex1.5c	56
Fig. 4-7: The exponential character of PCR	57
Fig. 4-8: The exponential character of PCR	58
Fig. 4-9: Quantitative competitive PCRs of known quantity of	

Ex1.5AC and IS-DNA	59
Fig. 4-10: Quantitative competitive PCRs of known quantity of Ex1.5AC and IS-DNA	60
Fig. 4-11: Competitive PCRs of known quantity of Ex1.5AC and IS-DNA	61
Fig. 4-12: RT-PCR of the internal standard RNA	62
Fig. 4-13: QC-RT-PCR of the total RNA from 12 day-old locust flight muscle	63
Fig. 4-14: The plot of QC-RT-PCR products from 12 day-old locust flight muscle	64
Fig. 5-1: RT-PCR of total RNA from flight muscle of different age locusts	74
Fig. 5-2: QC-RT-PCR of the total RNA from 5 day-old locust flight muscle	75
Fig. 5-3: The plot of QC-RT-PCR products from 5 day-old locust flight muscle	76
Fig. 5-4: The transcription regulation during locust development	77
Fig. 6-1: Simulation of FABP translation	86
Fig. 6-2: Simulation of FABP translation	87
Fig. 6-3: Estimation of FABP mRNA half-life	90
Fig. 6-4: Estimation of FABP mRNA half-life	91
Fig. 6-5: Two-compartment model of FABP expression	94
Fig. 6-6: Simulation of FABP expression	95

CHAPTER 1. GENERAL INTRODUCTION

Since ancient times, locust swarms have regularly threatened mankind. Swarms of these migrating insects have invaded African and Asian countries, leaving devastation and famine behind. While there are more than 5,000 different species of grasshoppers, only a few cause economic problems. Two species of locusts which cause perhaps the greatest financial loss are the desert locust (*Schistocerca gregaria*) and the migratory locust (*Locusta migratoria*). While harmless when present at low density, these species undergo marked physiological and morphological changes once their population exceeds a certain density, and the insects change from the solitary to the gregarious phase. Gregarization, which occurs only under favorable conditions approximately once in a decade, causes distinct behavioral changes, namely the formation of swarms that migrate in a coordinated manner. The threat of a locust swarm arises both from the actual quantity of insects and from their mobility. As a locust eats the equivalent of its own weight in vegetation every day, a swarm of several million locusts may consume many tons of food in a day. It was reported that during a major outbreak a swarm of locust contained more than 40,000 million locusts and covered 1,200 km²; it was estimated that such a swarm consumed 80,000 tons of food in one day (Uvarov, 1977). As vegetation is rapidly eliminated along its path, the swarm migrates further to new sources of nutrition. The desert locust is a large, powerful insect, capable of flying at an air speed of 20 km/hour. During migration, the locust can maintain a cruising speed of up to 15 km/hour for a period of 40 hours or longer. Swarms have been found to migrate over extreme distances, for example 11,000 km from African Sahel to West India (Rainey, 1989).

After hatching, locusts develop through 5 wingless nymphal stages. The locusts have fully developed wings only after metamorphosis, when the insects molt from the final nymph stage into adult locusts. For about the first 10 days after the final molt the locust

undergoes a period of somatic growth during which the flight muscles increase in size and become fully functional, and fat is stored simultaneously in the fat bodies. Although the locust may take off during this period, the flight is of short duration, as the insect cannot sustain long distance flight until approximately 2 weeks after adult ecdysis. Subsequently the insect retains its capacity to fly for the rest of its life.

During flight, the locust is kept in the air and propelled by the flapping of the wings. The wings are moved by distortions of the thorax. The depression of the dorsal surface by dorsal-ventral muscles causes the wings to move up because of the nature of their articulation. Bowing upwards of the dorsal surface, resulting from the action of dorsal longitudinal muscles, causes the wings to move down. The muscles producing these effects are known as the indirect flight muscles because they move the wings indirectly as a result of distortion of the thorax (Beenackers et al., 1985). The direct flight muscles, on the other hand, are inserted directly into the bases of the wings. They assist in wing depression, but are also involved in the control of flight by producing twisting movements of the forewings.

Flight is one of the most energy demanding activities found in the animal world. Most metabolic energy needed during flight is consumed by the flight muscles. Rates of oxygen consumption of insects during flight are among the highest measured, varying from 40 to over 150 ml of oxygen per gram of body mass per hour. The power output of insect flight muscles is greater than that of any other animal muscle, producing up to 35 W/kg when the insect is in flight (Casey, 1989). This enormous expenditure of energy depends on the ample supply of fuels and mechanisms facilitating rapid oxidation. The muscles are directly bathed in hemolymph, because locusts, like all other insects, have an open circulatory system, and the hemolymph penetrates between the muscle fibers and into fine channels invaginating them. In order to maintain an adequate supply of fuel to the mitochondria, where oxidation occurs, very high concentrations of fuels are necessary in

the hemolymph. Carbohydrate levels fall at the beginning of flight and are not replenished, indicating that carbohydrates represent the main fuel for flight only for a short time after take-off. The concentration of lipids in the hemolymph, on the other hand, starts to rise after about 10 minutes of flight and is then maintained at a high level, providing the energy needed to sustain longer periods of flight (Wheeler, 1989).

Oxygen is readily supplied directly to the flight muscle cells by the highly developed thoracic tracheal system. The resting pattern of opening and closing of the spiracles is modified during flight to ensure full aerobic respiration at even the highest wing beat frequencies. The main air supply to the flight muscles runs directly from the first thoracic spiracle. Within the flight muscles the tracheae expand into extensive air sacs. Fine tracheae penetrate deep into the flight muscle tissue, indent the muscle membrane and end close to the mitochondria. During flight, the contractions of the flight muscles result in the alternate collapse and expansion of the air sacs so that air is forced out from and drawn in through the permanently opened first spiracle (Wigglesworth, 1983; Van den Hondel-Franken and Flight, 1981). In this way ample supply of oxygen is maintained and the carbon dioxide produced is pumped directly out of the body. Because of the high efficiency of the complex tracheal system, there is no oxygen debt due to the increase in metabolic rate during flight.

The supply of fuel to the flight muscle is, however, more problematic. Insect hemolymph moves in the body cavity in a tidal flow manner and is aided by the movement of the flight muscles. Such a system could create problems in the rapid exchange of fuels, metabolites, and hormones between the tissues and hemolymph. However, insects appear to have successfully avoided this potential handicap by carrying high concentrations of fuels in the hemolymph to ensure steep concentration gradients between the hemolymph and tissues. Carbohydrate and lipid concentrations in hemolymph are typically up to 80 times higher than in vertebrate blood. In vertebrates, however, such high concentrations of

fuels would cause problems due to high osmotic pressure, chemical reactivity, or toxicity. To avoid these complications insects transport their major fuels predominantly in forms that are nonreducing, neutral, and contribute less to the osmotic pressure (Goldsworthy, 1983).

The two main fuels available to a locust are carbohydrates and fats. These are normally present in high concentrations in the hemolymph and stored in the fat body. The main carbohydrate present in locust hemolymph is trehalose. This disaccharide is the predominant source of energy at the start of flight or for flights of short duration. Since the total carbohydrate stored in locusts can provide sufficient energy for a maximum of only about 30 to 45 minutes of continuous flight, and some tissues such as the nervous system have an obligatory requirement for carbohydrate, trehalose is not used during longer flights. During long term flight, hemolymph trehalose levels are maintained at about 50 percent of preflight levels (Jutsum and Goldsworthy, 1976; Van der Horst et al., 1978). There is no doubt that lipids replace carbohydrates as a major energy source during long term flight and migration.

Lipids are primarily stored as triacylglycerol in the fat body. It is well known that the activation and mobilization of the stored lipids during long distance flight is under the control of neuron-hormones, especially the peptide adipokinetic hormone (AKH). AKH is secreted from the corpora cardiaca of insects, a pair of glands found adjacent to the brain. In the desert locust *S. gregaria*, there are two different adipokinetic hormones, AKH I and AKH II. Although their biological activities are similar, AKH I and II are released at different times during flight; at the beginning of flight, most of the AKH released is AKH I, while half an hour later AKH II predominates (Orchard and Lange, 1983). Upon stimulation of AKH, a signal transduction pathway involving Ca^{2+} and cAMP is activated in the fat body that leads to the conversion of triacylglycerol to diacylglycerol (DAG). The resulting free fatty acids are re-esterified to glycerol to produce additional DAG in the fat

body. DAG is the major form of lipid transported in the hemolymph (Beenackers et al., 1985; Chino, 1985).

The generally accepted theory on hemolymph lipid transport is the "reusable shuttle hypothesis", put forward by Chino's group (Chino and Kitazawa, 1981; Chino, 1985), that involves the hemolymph lipoprotein lipophorin. Numerous studies have provided support for this shuttle theory (Downer and Chino, 1985; Van Heusden et al., 1987; Surholt et al., 1991; Van Heusden et al., 1991; Gondim et al., 1992). Once released from the fat body into hemolymph, DAG is bound by high density lipophorin (HDLp). The lipid enriched particle is then stabilized by binding several free apolipophorin III (apoLp-III) molecules, a small apoprotein that has high affinity for the lipid-water interface. Because of the binding of DAG, the size of the lipophorin is increased and its density is decreased; the DAG enriched lipophorin is called low density lipophorin (LDLp). At the flight muscle, LDLp "docks" to the cell surface, and DAG is released and hydrolyzed by a membrane bound lipase. As a result, apoLp-III is removed from the lipophorin particle, leaving behind the DAG depleted HDLp particle which can return to the fat body to pick up more DAG. Similarly, apoLp-III and glycerol, the hydrophilic product of DAG hydrolysis, return to the fat body. The free fatty acid released by the lipase is directly transported into muscle cells where it is ultimately oxidized in the mitochondria to produce ATP to support flight (Fig. 1-1).

Long chain fatty acids are poorly soluble in aqueous media. In the muscle cytosol, the diffusion of free fatty acids is very slow and can never provide enough fatty acids to the mitochondria to meet the energy requirements of flight. Therefore, a cytosolic transport system is needed to supply fatty acids to the mitochondria. Several years ago, Haunerland and Chisholm (1990) found an abundant fatty acid binding protein in the flight muscle of the desert locust that appears to be involved in this fatty acid transport; a similar protein was also shown to be present in *Locusta migratoria* (Van der Horst et al., 1993).

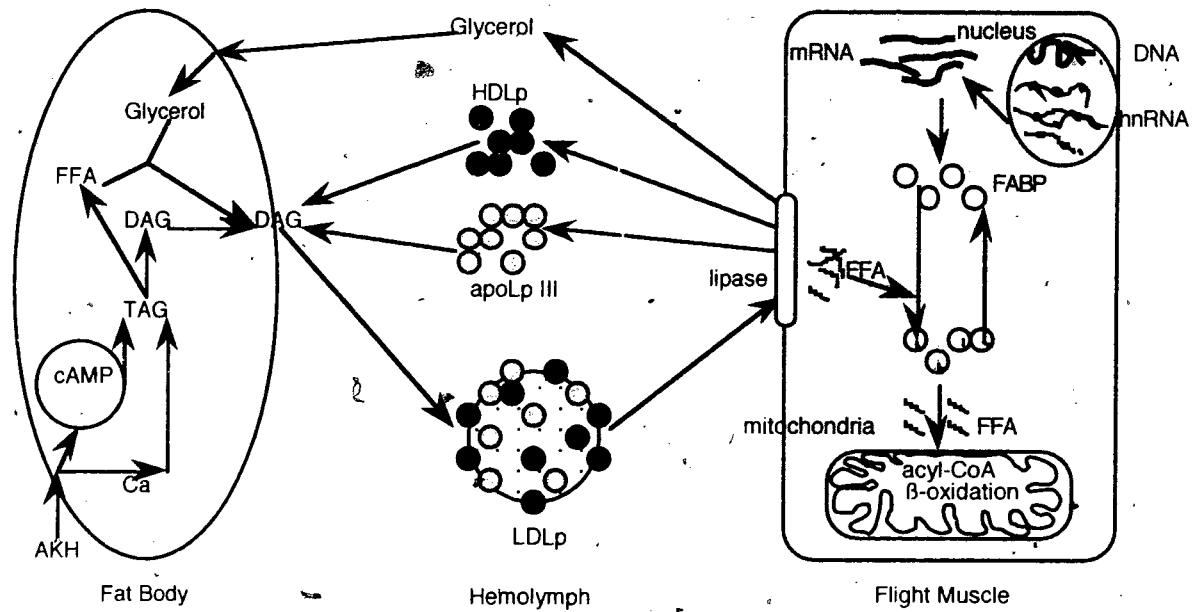


Fig. 1-1: Locust lipid transport and utilization.

FFA: free fatty acid.
TAG: triacylglycerol.
DAG: diacylglycerol.
HDLp: high density lipophorin.
LDLp: low density lipophorin.
apoLp-III: apolipoprotein III.
FABP: fatty acid binding protein.
hnRNA: heterogeneous nuclear RNA.

These fatty acid binding proteins belong to a growing superfamily of lipid binding proteins characterized in many vertebrate tissues, which include FABPs from various tissues as well as myelin P2 protein (MyP2) and cellular retinol and retinoic acid binding proteins (CRBP, CRABP) (reviews: Bass, 1988; Veerkamp et al., 1990; Banaszak et al., 1994; Veerkamp and Maatman, 1995). Several distinct classes of fatty acid binding proteins have been identified in vertebrates, namely hepatic or liver FABP (L-FABP), intestinal FABP (I-FABP), adipocyte FABP (A-FABP), ileal lipid binding protein (I-LBP), epidermal FABP (E-FABP), testis FABP (T-FABP), brain FABP (B-FABP) and cardiac or heart FABP (H-FABP). Since H-FABP is also present in skeletal muscle, it is sometime referred to as M-FABP.

H-FABP was first purified from heart muscle by Fournier et al. (1978). It has been found to be present in different kinds of mammalian tissues, for example in skeletal muscle (Miller et al., 1988), brain, ovary, testis, kidney (Bass and Manning, 1986), aorta (Sarzani et al., 1988), and the mammary gland (Jones et al., 1988; Specht et al., 1996). To date, H-FABP has also been purified and sequenced from other vertebrates such as birds (Guglielmo et al., in press), and fish (Ando et al., in press).

Locust flight muscle M-FABP is an acidic protein with an isoelectric point of 5.2. Its molecular weight is about 15,000 Da. It binds fatty acids stoichiometrically in a 1:1 ratio. Its molecular characteristics, tissue specificity and electrophoretic behavioral are similar to those of mammalian H-FABP (Hauerland and Chisholm, 1990, Hauerland, 1994). Although vertebrates and invertebrates diverged more than 650 million years ago, M-FABP's structure is highly conserved: between locust M-FABP and mammalian heart FABP, more than 40 % of the amino acid residues are identical and an additional 40 % conservatively substituted. This implies that many details of the structure may be required for the identical function in muscle cells of both vertebrates and invertebrates (Price et al.,

1992). Indeed, locust M-FABP is remarkably similar to human H-FABP at the tertiary structure level (Hauerland et al., 1994).

The function of FABP, as the name "fatty acid binding protein" suggests, is primarily to bind fatty acids in the cytosol. It is believed that M-FABP is involved in the transport of fatty acids through the muscle cytosol from the plasma membrane to the mitochondria. In addition, M-FABP may have a cytoprotective function: by binding unesterified fatty acids, it keeps the concentration of free fatty acids low, and thus prevents the pathological effects attributed to the detergent-like action of free fatty acids. There appears to be a correlation between the rate of fatty acid oxidation of a muscle and its FABP content. Of all mammalian muscles, cardiac muscle has the highest fatty acid metabolizing rate, and its FABP content is also the highest found (~6 % of total cytosolic proteins). Migratory birds may encounter twice the metabolic rates during flight, and recent results by Guglielmo et al (1997) indicate an FABP content of 13 %. Locust flight muscle, while similar in structure and physiological properties to mammalian heart muscle (Crabtree and Newsholme, 1975), encounters much higher metabolic rates, up to three times as high during migratory flight; its FABP content can approach 18% of the total cytosolic proteins (Hauerland et al., 1992).

M-FABP is the most prominent protein in mature adult locust flight muscle, but it is completely absent in nymphs and newly emerged adults. Immediately after metamorphosis, FABP synthesis starts and the protein concentration rises rapidly within the first two weeks of adulthood, after which it reaches its maximal level. Afterwards, the FABP concentration remains constant at approx. 18 % of the total cytosolic proteins throughout the entire life time. The content of M-FABP in locust flight muscle is concomitant to the flight ability of the insect. While the mesothorax muscle is already differentiated and prominent in nymphs, these insects can not fly since they have no wings. Newly emerged adults, however, do have wings, but they acquire the capacity of migratory

flight only after a final differentiation and growth period of 10 days (Wang et al., 1993) during which the FABP content increases. Flight periods exceeding 60 min. that rely on fatty acid metabolism are possible only after FABP reached a significant level (day 5 after adult ecdysis, 10 % of total cytosolic protein).

FABP is an adult specific protein; neither FABP nor its mRNA have ever been detected prior to metamorphosis. Supernumerary nymphs, produced after treatment with juvenile hormone, never expressed FABP, although their muscles grew rapidly (Chen et al., 1993). Similarly, after the treatment with the molting inhibitor azadirachtin, insects remained in their final nymphal stage (over-aged nymphs), their muscles increased in size without expressing FABP. It appears that FABP expression is specifically turned on after metamorphosis.

Indeed, the synthesis of FABP is preceded by a rise in its mRNA. FABP mRNA is first visible one day after metamorphosis; it reaches its peak during the first week and decreases in the second week to a relatively low, constant level (Hauerland et al., 1992). The fact that FABP mRNA decreases after day 8 is unusual for a constitutively expressed protein; it suggests some sort of feed-back control mechanism that suppresses FABP synthesis after a certain level has been reached. From the available data on FABP and its mRNA it is not possible to decide whether this regulation is at the transcriptional or post-transcriptional level. FABP transcription could be de-activated if FABP concentration increases, or mRNA stability could be altered.

It is interesting to note that FABP mRNA can again increase in mature adult locusts. Forced locust flight, during which the metabolic rates are 10-fold higher than at rest, result in 8-12 fold higher levels of FABP mRNA in flight muscle (Chen and Hauerland, 1994), even though there is already an extremely high concentration of FABP present in the flight muscle. Similar results were obtained after injection of either AKH or LDLp, which increase the transport of DAG to the flight muscle (Chen and Hauerland, 1994). The

increase of intracellular fatty acid content for a certain period of time may serve as a signal that can trigger the expression of FABP.

To date, it is not known whether the regulation of M-FABP expression in the locust occurs at the transcriptional level. In mammalian muscle, FABP and its mRNA concentration increase with the terminal differentiation of the muscles, although the mRNA level does not decrease afterwards (Crisman et al., 1987). Further evidence suggests that chronic muscle stimulation in skeletal muscle also leads to an increase in FABP content (Kaufman et al., 1989; Veerkamp and van Moerkerk, 1993). In experimental diabetes, which also leads to increased fatty acid oxidation, a marked increase in FABP mRNA has also been observed (Carey et al., 1994). In this study, nuclear run-ons provided some, albeit weak, evidence that FABP gene expression is up-regulated. Otherwise, nothing is known about the regulation of any muscle FABP.

Recently, the genes for H-FABP, which are formerly known as mammary derived growth inhibitor (MDGI) (Treuner et al., 1994), have been cloned, together with 2 kb of upstream sequence, from mouse (Specht et al., 1996) and human (Phelan et al., 1996). The gene for locust M-FABP has also been cloned, but so far without any upstream sequence (Hauerland et al., unpublished). The gene structure of all known FABP genes is highly conserved. All mammalian genes coding for the various FABP types are composed of 4 exons coding for approximately 22, 57, 37, and 17 amino acids respectively; these are separated by introns of variable length, but in exactly the same positions. While the human and mouse H-FABP gene follow this pattern, the locust M-FABP gene has only two introns of 13 kb and 2.3 kb inserted in analogous positions. The second intron is missing (Hauerland et al., unpublished).

The goal of this thesis was to study whether the regulation of FABP expression in the locust occurs at the level of transcription. Thus, it was necessary to develop a method that could measure newly synthesized transcripts, to measure the rates of transcription at

different days in development, and to correlate the findings with the observed steady state mRNA levels. Normally, a nuclear run-on assay is the method of choice for such analysis, but this has only rarely been used in differentiated muscle. While giving excellent results in cell culture or soft tissue like liver and brain, it appears to be difficult to obtain sufficient numbers of transcriptionally active nuclei from harder tissues, such as muscle. One study employed this technique to measure FABP transcription in normal and diabetic rats (Carey et al., 1994), but it was not possible to obtain any quantitative data. Therefore, it was decided to begin with the isolation and characterization of nuclei and to establish favorable conditions for run-on assays in locusts, and if successful, measure changes in transcription rates throughout development.

CHAPTER 2: NUCLEI ISOLATION

2.1. Introduction:

The eukaryotic nucleus, the major site of RNA synthesis, plays a dominant role in the regulation of gene expression. Muscle is a good model system which has been used extensively for the study of cellular differentiation, tissue development, adaptive changes to conditioning and similar processes. It is thought that changes in the expression of specific genes stimulated by a variety of signals are key events during the process. Because of the structure of striated muscles, which contain an abundance of highly organized contractile elements of myofibers, understanding the regulation of such genes has been hampered by the difficulties in isolating of muscle nuclei. It is essential to isolate sufficient pure, intact and transcriptionally active nuclei from muscle tissue for a variety of studies related to the regulation of gene expression, including nuclear run-on transcription for studying the transcription rate of a certain gene, the characterization of DNase I hypersensitive chromatin regions, and the preparation of nuclear extracts for the identification of trans-acting factors (nuclear run-off assay). For the study of fatty acid binding protein expression in locust flight muscle, the isolation of nuclei from locust flight muscle tissue becomes necessary.

Conventional procedures for isolating nuclei from a wide variety of animal soft tissues such as liver, pancreas, kidney and brain (McEwen and Zigmond, 1972; Tata, 1974; Smuckler et al., 1976; Marzluff and Huang, 1984; Nevins, 1987) and cultured cells (Smuckler et al., 1976; David et al., 1978; Mellon and Bhorjee, 1982; Marzluff and Huang, 1984) were not suitable for purifying nuclei directly from striated muscle tissue.

Striated muscle tissue, which include vertebrate heart muscle and skeletal muscle, is different from any other tissues found in animals. Locust flight muscle, also a striated muscle, is similar in structure to vertebrate heart muscle. The muscle cells are multi-

nucleate with numerous peripheral and flattened nuclei aligned in longitudinal rows. The large diameter fibrils are cylindrical in shape and large mitochondria fill the spaces between the fibrils. In flight muscles the multi-nucleate fibers extend the full length of the muscle (Elder, 1975).

The main advantage of using isolated nuclei for transcriptional studies is that this subcellular system is as close to the intact cell as possible. Within the isolated nucleus the chromatin is maintained in its native state. The integrity of the nucleus is maintained during the period of cell free synthesis of RNA, and the newly made RNA remains associated with the nucleus, as it does in the intact cell. Thus, the activity measured reflects the activity of that nucleus in the cell; the same genes are being expressed in the same relative amounts in the isolated nucleus as in the intact cell.

2.2. Material and Methods:

2.2.1. Chemicals and buffers:

All chemicals were from Sigma (St. Louis, MO), unless otherwise indicated. Electron microscopy supplies were from J.B. EM services (Pointe Claire Dorval, PQ).

Buffer I (homogenization buffer): 0.32 M sucrose, 10 mM HEPES, pH 7.6, 15 mM KCl, 0.15 mM spermine, 0.5 mM spermidine, 1 mM EDTA, 10 % glycerol. All the components were fully dissolved and kept at -20 °C. Just before use, 0.5 mM DTT, 0.5 mM PMSF (phenyl-methyl-sulfonyl-fluoride), 1 % aprotinin and the cocktail: 0.1 µg/ml leupeptin, 0.1 µg/ml pepstatin, 0.1 µg/ml antipain, 2 µM TLCK and 2 µM TPCK were added.

Buffer II: 2.2 M sucrose, 10 mM HEPES, pH 7.6, 15 mM KCl, 0.15 mM spermine, 0.5 mM spermidine, 1 mM EDTA, 10 % glycerol. All the components were fully dissolved and kept at -20 °C. Just before use, 0.5 mM DTT, 0.5 mM PMSF

(phenyl-methyl-sulfonyl-fluoride), 1 % aprotinin and the cocktail: 0.1 $\mu\text{g/ml}$ leupeptin, 0.1 $\mu\text{g/ml}$ pepstatin, 0.1 $\mu\text{g/ml}$ antipain, 2 μM TLCK and 2 μM TPCK were added.

Storage buffer: 10 mM HEPES, pH 7.6, 15 mM KCl, 0.15 mM spermine, 0.5 mM spermidine, 1 mM EDTA, 40 % glycerol. All the components were fully dissolved and kept at -20°C . Just before use, 0.5 mM DTT, 0.5 mM PMSF (phenyl-methyl-sulfonyl-fluoride), 1 % aprotinin and the cocktail: 0.1 $\mu\text{g/ml}$ leupeptin, 0.1 $\mu\text{g/ml}$ pepstatin, 0.1 $\mu\text{g/ml}$ antipain, 2 μM TLCK and 2 μM TPCK were added.

DTT: 1 M stock in H_2O .

PMSF: 1 M stock in isopropanol.

Cocktail: Leupeptin, Pepstatin and Antipain: 0.5 mg/ml each in ethanol.

TLCK and TPCK: 10 mM stock in H_2O .

2.5 % glutaraldehyde: 2.5 % v/v in 0.2 M sodium phosphate, pH 7.4.

1.0 % osmium tetroxide: 1.0 % v/v in 0.2 M sodium phosphate, pH 7.4.

2.2.2. Methods:

2.2.2.1. Insects:

Locusts (*Schistocerca gregaria*) were reared in crowded conditions at 32°C under continuous light. The last stage nymphs were collected and immediately dissected for muscle nuclei isolation. Within 12 hours after molting, freshly emerged adults were removed and reared separately until sacrificed for nuclei isolation at the specified age. Individuals between 0 and 24 hours after adult molting are referred to as day 1 adults, with each subsequent day representing an additional 24 hour period.

2.2.2.2. Nucleus isolation from locust flight muscle:

The procedure was modified from Sierra (1990). It was a non stop procedure which required about 5 hours. All the procedures were carried out on ice and in a cold room. After the ultracentrifuge was turned on with vacuum on, the temperature was

equilibrated at 0 °C. The buffers were mixed up with the inhibitor cocktail and no Schlieren line was obvious. 15 ml of buffer II was added to each ultracentrifuge tube to form pads. A few milliliters (10-15 ml) of buffer I were added at the bottom of the homogenizer to prevent the tissue from getting stuck. After the preparation procedure, 12 locusts were dissected to obtain the flight muscles. Every flight muscle was minced as fine as possible and immediately thrown into the homogenization buffer. The muscles were combined together and homogenized by several strokes (7 strokes at 6,000 rpm) in a motor-driven Teflon-tipped Potter- Elvehjem homogenizer (clearance 0.5 mm), keeping the tissue suspended in buffer I at about 1 g/10 ml. After the homogenization, the muscle homogenate was passed through a 100 μ m nylon mesh. The filtrate was centrifuged in an SS34 rotor at 2000 g (4000 rpm) at 0 °C for 10 min. The pellet was resuspended in 20 ml of buffer II, loaded on the top of the cocktail pads in the SW27 ultracentrifuge tubes as fast as possible, and ultracentrifuged at 27,000 g (24,000 rpm in SW27 rotor) for 60 min. in the pre-cooled ultracentrifuge. While spinning, small aliquots of material were checked under a light microscope to confirm that most cells were broken, but most nuclei were intact. After centrifugation, the whole cells and unbroken pieces of tissue and yellow colored fat floated at the surface, nuclei with cytoplasmic tags and broken nuclei stayed in the upper phase of the buffer II, clean nuclei (white or transparent) pelleted at the bottom. The solid floating disc was removed with a spatula, then the liquid was carefully aspirated, and the sides of the tubes were wiped off with Kimwipe. The tube walls were rinsed with distilled water using a syringe which had a long needle with the tip bent about 90 degree attached on it, holding the tube upside down, while avoiding wetting the nuclear pellet. The nuclei were resuspended in 1 ml of storage buffer and counted under a light microscope.

2.2.2.3. Electron microscopy:

The isolated nuclei were fixed in 2.5 % glutaraldehyde at 4 °C for 2 hours. The nuclei were rinsed in 0.2 M sodium phosphate, pH 7.4 and post-fixed in 1.0 % OsO₄. The nuclei were rinsed again in the phosphate buffer and dehydrated in an ethanol series. The nuclei were transferred to propylene oxide and embedded in Epon/Araldite. The ultrathin sections were made with a diamond knife and stained with 5 % uranyl acetate and 2.6 % lead citrate. The sections were observed under a Phillips electron microscope (EM 300, 80 KV).

2.3. Results:

Electron micrographs showed that the purified nuclei were intact. They were usually oval, oblong and flat in shape and had intact double layer nuclear envelope (Fig. 2-1). The length of the nuclei were around 10 μ m, approximately the same size reported for mammalian nuclei (Edelman et al., 1965; Held et al., 1977; David et al., 1978; Jackowski and Liew, 1980; Mellon and Bhorjee, 1982). The ultrastructure of the isolated nuclei was the same as seen in whole muscle (Haunerland, et al., 1992; Chen, et al., 1993). The most electron-dense structure in the nucleus is the nucleolus; all nuclei had one or two distinct nucleoli in the nucleoplasm (Fig. 2-2). Large dense chromatin was aggregated and the loose chromatin dispersed in between. Since a locust has a much larger genome than a mammal, most of the genomes are dormant and are probably contained in the heterochromatin which is electron dense. The active genes constitute the euchromatin, which is the less dense chromatin in the electron micrograph. There are no endoplasmic reticulum tags associated with the nucleus envelope, which indicates that the isolated nuclei were pure (Fig. 2-3).

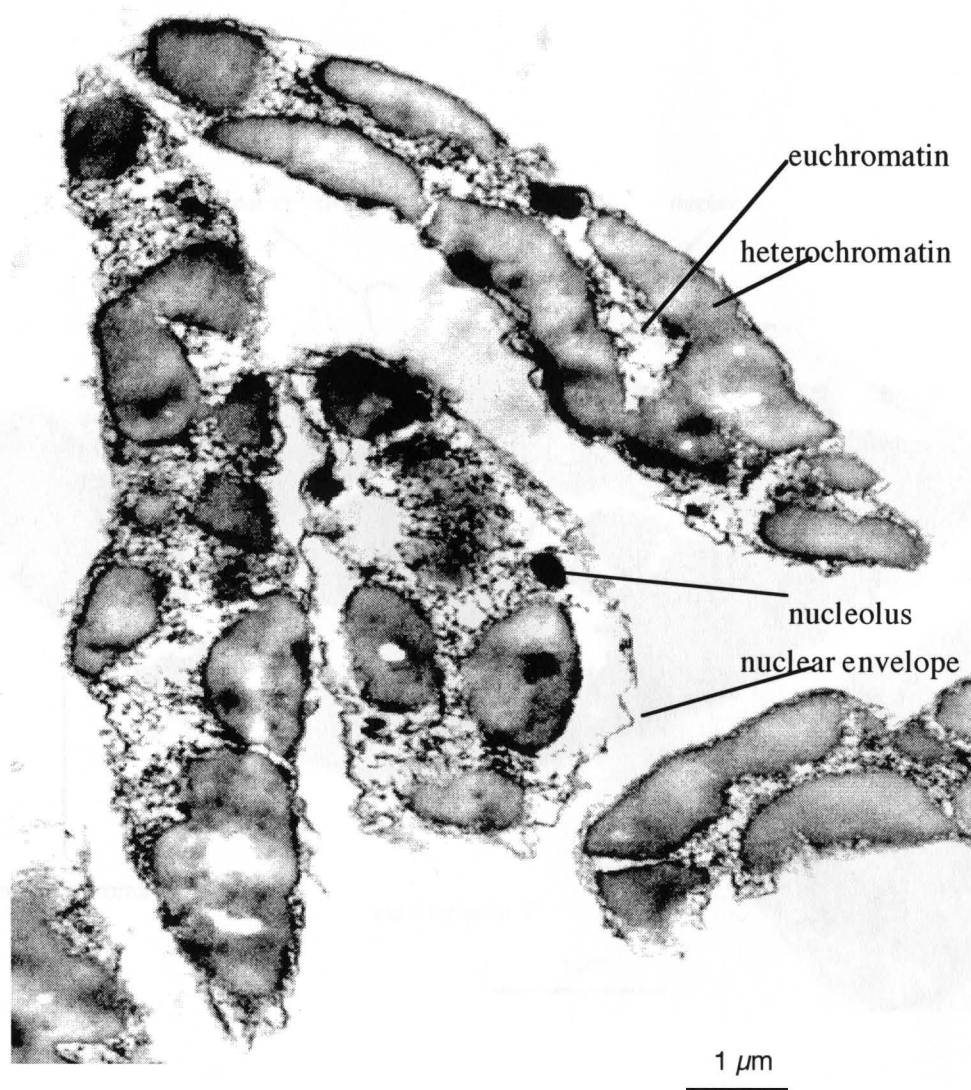


Fig. 2-1: Electron micrograph of isolated nuclei from locust flight muscle.

The nuclei were isolated and fixed as described in Chapter 2.2. (x 8,200).

— 1 μm

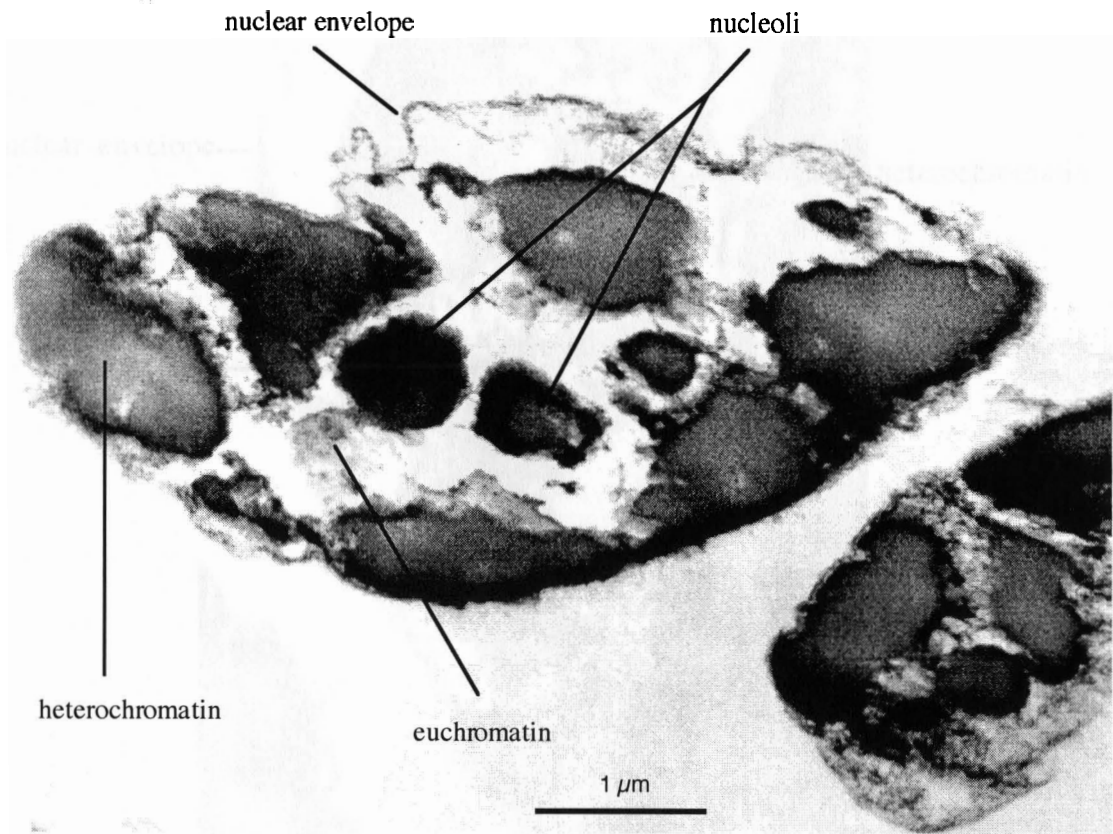


Fig. 2-2: Electron micrograph of isolated nuclei from locust flight muscle.

The nuclei were isolated and fixed as described in Chapter 2.2. (x 12,500).

————— 1 μm

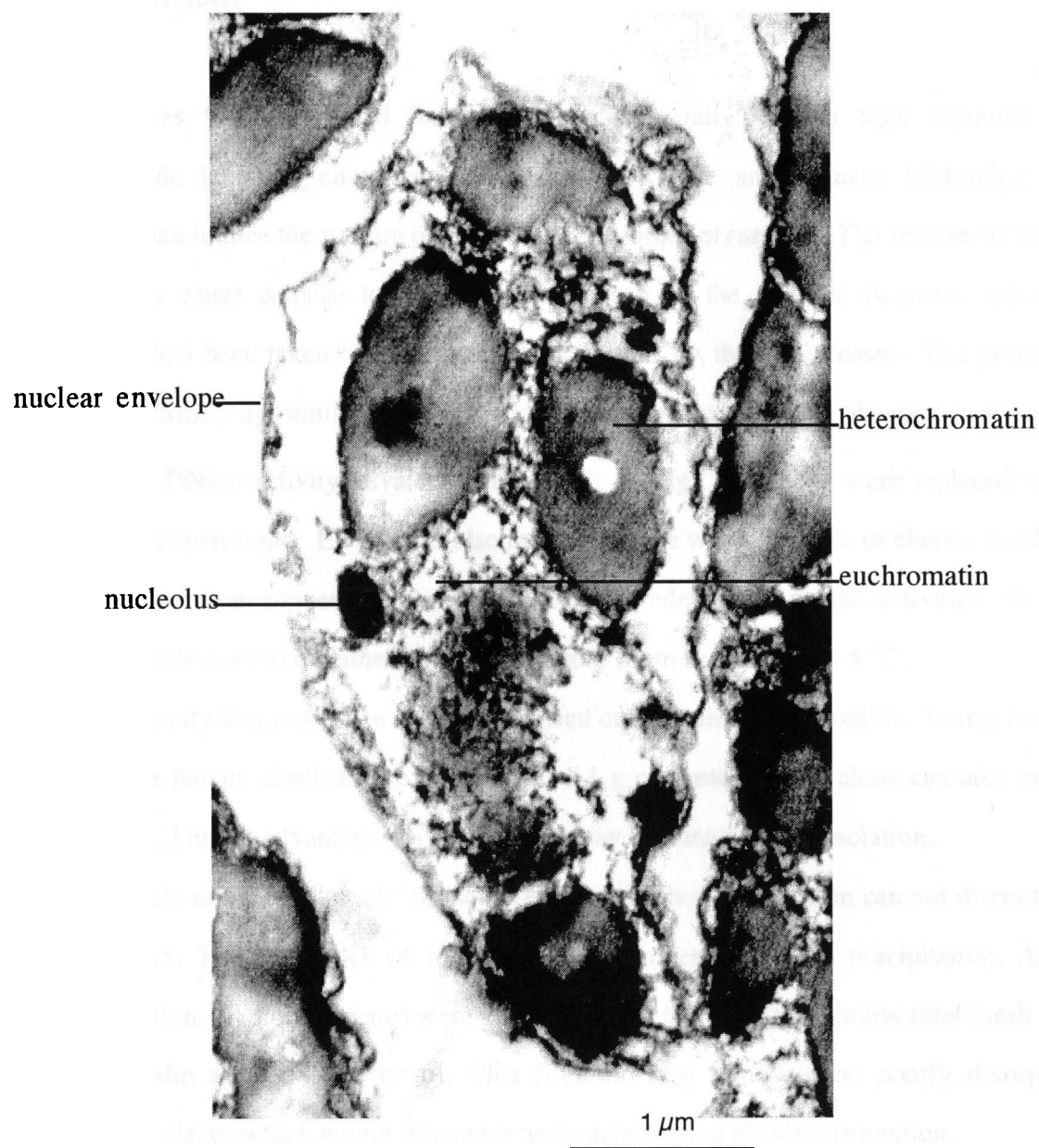


Fig. 2-3: Electron micrograph of isolated nuclei from locust flight muscle.

The nuclei were isolated and fixed as described in Chapter 2.2. ($\times 12,500$).

1 μm

2.4. Discussion:

Tissues freshly isolated from live animals usually contain high amounts of macromolecule degrading enzymes, such as DNase, RNase, and protease. Disrupting the solid tissue can induce the rupture of lysosomes and other organelles. The release of these enzymes can cause damage to the nuclei and result in the loss of function. Several precautions had been taken to limit the damage caused by these processes. The protease inhibitors, PMSF, aprotinin, and the cocktail, were included in all the steps. For the inhibition of DNase activity, divalent cations such as Mg^{2+} and Ca^{2+} were replaced with spermine and spermidine. EDTA was also included in the whole process to chelate divalent cations coming from tissues themselves. In order to reduce the enzyme activities, all the procedures were carried on either on ice or in a cold room maintained at 4 °C.

Generally this procedure should be carried out as quickly as possible. Using locust flight muscle has its disadvantage: dissecting of 1 g of muscle tissue alone can take more than an hour. This disadvantage may explain the low efficiency of the isolation.

Muscle tissue is a "tough" tissue. Even vigorous homogenization can not disrupt all muscle fibers. These bundles of myofibers can hamper the nuclei precipitation. After homogenization, the homogenates were passed through the 100 μ m stainless steel mesh for filtration (Hahn and Covault, 1990). This filtration step removed the poorly disrupted muscle fiber pieces which would otherwise trap nuclei during ultracentrifugation.

The principle of nuclei isolation is based on the different densities of nuclei and other organelles. The muscle nucleus is the most heavy organelle. It has a density of about 1.10 g/ml. Other cell component densities are less than 1.05 g/ml (Hahn and Covault, 1990). When using 2.0 M sucrose gradient solution, the nuclei appeared dirty with the myofiber contamination. However after the sucrose concentration was raised to 2.2 M (density about 1.2 g/ml), pure nuclei could be obtained.

After the conditions of nuclei isolation had been optimized, about 1×10^6 nuclei were obtained from approximately 1 g locust flight muscle. In contrast, Jackowski and Liew (1980) obtained 10 times more nuclei from mammalian skeletal muscle tissue (1×10^7 nuclei per gram). This could be because of the experiment limitation mentioned above, or because locust flight muscle has less nuclei than the mammalian skeletal muscle.

CHAPTER 3: NUCLEAR RUN-ON ASSAY

3.1. Introduction:

The establishment of an *in vitro* system is an essential prerequisite for studies of the mechanism of transcription of specific genes and the processing of primary transcripts in eukaryotic cells. Several *in vitro* techniques, such as *in vitro* transcription have been developed (Manley et al., 1981; Heintz et al., 1983; Dignam et al., 1983; Parker and Topol, 1984; Marzluff and Huang, 1984; Linial et al. 1985; Gorski et al., 1986; Shapiro et al., 1988; McCully and Liew, 1988; Celano et al., 1989; Zahradka et al; 1989; Cornelius et al. 1990). One of the most widely used systems is the nuclear run-on assay, which starts with isolated nuclei and uses endogeneous chromatin as the template for transcription. This approach emphasizes the preservation of cellular activities *in vitro*. The nuclear run-on transcription system provides one of the best methods to measure the relative transcriptional rate of a gene.

The advantage of using isolated nuclei for transcriptional studies is that it is a system which is as close to the intact cell as possible. Within the isolated nucleus the chromatin is maintained in its native state. The integrity of the nucleus is maintained during the cell free synthesis of RNA and the newly made RNA remains associated with the nucleus, as it does in the intact cell. Thus the activity measured reflects the approximate activity of that nucleus in the cell; the same genes are being expressed in the same relative amounts in the isolated nucleus as in the intact cell (Marzluff and Huang, 1984).

For *in vitro* RNA synthesis, nuclei are incubated in the *in vitro* transcription buffer with all four ribonucleoside triphosphates, one of which is labeled, for a certain amount of time. The labeled total RNA transcripts are then purified and hybridized to excess DNA probes, which are immobilized on a nylon membrane. After several washing steps to

remove the unbound RNAs, the amount of the hybridized RNAs can be determined by autoradiography or chemiluminescent detection followed by densitometry of the photographic images. The relative transcription rate of a particular gene can be quantified by comparing the measurement of that RNA transcript with the measurement of total RNAs synthesized *in vitro*, using excess DNA probes blotted on nylon membrane.

Several disadvantages of this method limit its usefulness. The assay requires large numbers of isolated nuclei, which restricts its usefulness in systems where the isolation of large number of nuclei is difficult. The sensitivity of this method has to be considered, in light of the complexity of the RNAs being synthesized; it is believed that 10^4 to 10^5 different genes active in the intact cell are also transcribed in isolated nuclei. The nuclear run-on assay is laborious, time consuming and expensive. The traditional standard procedure involves significant amounts of radioactivity; to handle the hazardous radio-labeled RNAs throughout the whole process is another big disadvantage.

Recently, Merscher et al. (1994) developed a modified protocol, which used Dioxigenin (DIG)-labeled UTP instead of α - ^{32}P labeled UTP to transcribe RNAs *in vitro* and used the chemiluminescent detection method to check the RNA signal after hybridization. The procedure used in this chapter was mainly modified from Merscher et al. (1994).

3.2. Material and Methods:

3.2.1. Material:

All the chemicals were from GIBCO BRL (Burlington, ON) unless otherwise specified. Nylon membrane was from Boehringer Mannheim (Larval, QC). The DIG Detection Kit was from Boehringer Mannheim. Wizard Midiprep kit and Wizard Miniprep kit were from Promega Co. (Madison, WI).

3.2.1.1. Plasmid preparation:

1. LB media (liquid): 10 g bact-tryptone, 5 g yeast extract, 10 g NaCl, in 1000 ml H₂O, pH 7-8, autoclaved
2. LB media (plate): LB media (liquid) plus 15 g agar, pH 7-8, autoclaved
3. Wizard Midiprep kit and Wizard Miniprep kit (Promega Co., Madison, WI)
4. Solution I: 50 mM glucose, 25 mM Tris.Cl (pH 8.0), 10 mM EDTA (pH 8.0)
5. Solution II: 0.2 N NaOH, 1 % SDS
6. Solution III: 60 ml 5 M KOAc, 11.5 ml glacial HOAc, 28.5 ml H₂O
7. Buffer-saturated-phenol (Gibco BRL, Life Science Technology)
8. Chloroform: isoamylalcohol = 24:1
9. TE buffer: pH 8.0, 10 mM Tris.Cl, 1 mM EDTA, add H₂O to 1000 ml, autoclaved.
10. H₂O: instead of using TE, can use autoclaved H₂O to dissolve DNA.

3.2.1.2. Genomic DNA extraction:

1. extraction buffer: 0.1 M Tris.Cl, pH 8.0, 0.1 M EDTA, 0.5 % DEPC
2. 10 % SDS
3. Buffer-saturated-phenol (Gibco BRL, Life Science Technology)
4. 8 M KOAc: make fresh, 19.6 g KOAc, add H₂O to 25 ml
5. sevag: chloroform : isoamylalcohol = 24:1
6. 3 M NaOAc pH 5.5
7. TE pH 7.5-8.0

3.2.1.3. cDNA library amplification:

1. plate for bacterial streak: LB-tetracycline
2. medium for bacterial cultures for titering phage (final concentration): LB with 0.2 % (v/v) maltose and 10 mM MgSO₄
3. 10 mM MgSO₄

4. SM buffer (per liter): 5.8 g NaCl, 2.0 g MgSO₄.H₂O, 50 ml 1M Tris.Cl (pH 7.5), 5.0 ml 2 % (w/v) gelatin
5. DEPC
6. 10 % SDS
7. 1.0 M Tris-HCl (pH 8.5)
8. 0.5 M EDTA
9. 5 M potassium acetate
10. TE

3.2.1.4. Dot blotting:

1. 1 M NaOH: 40 g NaOH, 1000 ml DEPC-H₂O, autoclave
2. 0.4 M NaOH: 16 g NaOH, 1000 ml DEPC-H₂O, autoclave
3. 200 mM EDTA
4. 2 x SSC: 20 x SSC: 175.3 g NaCl, 88.2 g Na citrate, add DEPC-H₂O to 1000 ml, pH 7.0

3.2.1.5. Run-on transcription:

1. 2 x reaction buffer: 10 mM Tris.HCl pH 8.0, 5 mM MgCl₂, 0.3 M KCl, 1 mM DTT, 0.2 mM EDTA, 4 mM each of ATP, GTP, CTP, 3 μ l DIG-UTP (10 nmol/ μ L).
2. DNase I, RNase free: 10 mg/ml (Boehringer Mannheim)
3. 1 M CaCl₂: 54 g CaCl₂.6H₂O, add DEPC-H₂O to 200 ml, sterilized by passage through a 0.22-micron filter, store in 1 ml aliquots at -20 °C.
4. proteinase K: 10 mg/ml, (stock: 20 mg/ml in DEPC-ddH₂O, store at -20 °C, in reaction: 50 μ g/ml, buffer: 0.01 M Tris, pH 7.8, 0.005 M EDTA, 0.5 % SDS, temperature: 37-56 °C) (Boehringer Mannheim)
5. 10 x SET: 5 % SDS, 50 mM EDTA, 100 mM Tris.HCl pH 7.4
6. tRNA

7. NRO buffer II: 4 M GITC (Gibco BRL), 25 mM Na citrate, pH 7.0, 0.5 % sarkosyl, 0.1M, β -mercaptoethanol
8. 2 M NaAc: pH 4.0
9. Phenol and SEVAG
10. 95 % and 70 % ethanol
11. 0.5 % SDS

3.2.1.6. Hybridization:

1. hybridization buffer: 0.1 % (w/v) N-lauroylsarcosine, 0.02 % (w/v) SDS, 1 % blocking reagent, (1/10 volume of blocking solution, 10 x conc.)
2. Washing solution: 1st and 2nd time: 2 x SSC, 0.1 % SDS
3rd and 4th time: 0.1 x SSC, 0.1 % SDS

3.2.1.7. Detection:

1. buffer 1 (maleic acid buffer): 0.1 M maleic acid, 0.15 M NaCl, adjusted to pH 7.5 with solid NaOH
2. washing buffer: buffer 1 plus 0.3 % (v/v) Tween 20
3. blocking stock solution (10 x conc.): 10 % (w/v) blocking reagent in buffer 1, dissolve blocking reagent by constantly stirring at 65 °C, autoclave and store at 4 °C.
4. buffer 2 (blocking solution): the 1 x conc. solution is diluted from the blocking stock solution in buffer 1.
5. buffer 3 (detection buffer): 0.1 M Tris.HCl, 0.1 M NaCl, 50 mM MgCl₂, pH 9.5

3.2.2. Methods:

3.2.2.1. Plasmid extraction and purification:

1. Miniprep: The procedure was derived from a Wizard Miniprep kit (Promega Co.). Three ml of cells were pelleted by centrifugation at top speed in a microcentrifuge for 2 min. The cell pellet was then completely resuspended in 200 μ l of cell resuspension solution, followed by the addition of 200 μ l of cell lysis solution and 200 μ l of

neutralization solution. The mixture was spun at top speed in a microcentrifuge for 5 min. The clear supernatant was transferred to a new microcentrifuge tube. 1 ml of the magic minipreps DNA purification resin was added to the supernatant and mixed by inverting the tube several times. The resin was dried by passing through a minicolumn, and washed with 2 ml of 70 % ethanol. 50 μ l of preheated (70 °C) sterilized deionized distill water were applied to the column. To elute the plasmid, the column was spun at top speed for 1 min in a microcentrifuge. The plasmid DNA was stored at -20 °C

2. Midiprep: The procedure was derived from a Wizard Midiprep kit (Promega Co.). One hundred ml overnight cultured cells were pelleted by centrifugation at 10,000 g at 4 °C for 10 min. The cell pellet was then completely resuspended in 3 ml of cell resuspension solution, followed by the addition of 3 ml of cell lysis solution and 3 ml of neutralization solution. The lysate was centrifuged at 14,000 g at 4 °C for 15 min. The supernatant was transferred to a new tube. Ten ml resuspended purification resin were added to the supernatant and mixed by inverting the tube several times. The resin mixture was dried by passing through a midicolumn with a vacuum. The resin was washed by adding 15 ml of column wash solution. 300 μ l of preheated (70 °C) sterilized deionized distill water were applied to the column. To elute the plasmid, the column was spun at top speed for 1 min in a microcentrifuge. The plasmid DNA was stored at -20 °C.
3. Purified plasmids (with insert (cDNA or part of intron 1 sequence) and without insert) were cut with EcoRI and XhoI at 37 °C for more than 2 hours or overnight. The digestion was run on 1 % low melting point agarose gel to separate the insert and the vector. The insert bands and the pure vector were cut out from the gel and put into sterilized ependorf tubes. The agarose was melted at 65 °C for 10 min, then quickly frozen in liquid nitrogen. The agarose was re-melted at room temperature and spun at top speed for 15 min. The supernatants were removed to new tubes. After phenol-

chloroform-isoamylalcohol extraction, the DNAs were precipitated in an equal volume of isopropanol overnight. The precipitates were centrifuged at top speed in a microfuge for 15 min; the pellets were washed with 70 % ethanol and air dried and dissolved in H₂O.

3.2.2.2. Genomic DNA extraction from locust flight muscle:

One locust flight muscle was ground to a fine powder in liquid nitrogen. The powder was transferred into a 4 ml tube containing 2 ml extraction buffer and 225 μ l 10 % SDS and the mixture was incubated at 65 °C for 30 min with inverting periodically. Then 260 μ l 8M KOAc was added and the tube was placed on ice for 30 min. After spinning at 5,000 rpm in an SS34 rotor for 15 min at 4 °C, the aqueous layer was transferred with enlarged P1000 tip to 4 eppendorf tubes (500 μ l each), and extracted with phenol/chloroform. The genomic DNA was then precipitated with 2 volume cold 100 % ethanol and spun at top speed for 15 min in a microcentrifuge. The pellet was rinsed with 70 % ethanol and air dried. The pellet was resuspended in 50 μ l TE buffer with RNase A and incubated at 37 °C for 1 hour, then at room temperature overnight. Extraction and precipitation was processed again as before. The DNA was resuspended in 50 μ l H₂O and stored at -20 °C.

3.2.2.3. Amplifying locust flight muscle cDNA library:

The locust flight muscle cDNA library was constructed with Gigapack II Packaging Extracts (Stratagene, CA) before and stored at -80 °C. The whole amplification process was derived from Gigapack II Packaging Extracts (Stratagene, CA). The XL1-Blue MRF' host strain glycerol stock was streaked onto LB-tetracycline plates, and incubated at 37 °C overnight. A single colony was grown in LB with 0.2 % (v/v) maltose-10 mM MgSO₄ media at 37 °C for 4-6 hour shaking (O.D.600 < 1.0). The cells were pelleted at 2000 rpm for 10 min. The cells were gently resuspended in half the original volume with sterile 10 mM MgSO₄, and Diluted to O.D.600 = 0.5 with sterile 10 mM MgSO₄. Aliquots of library

suspension containing ~50,000 pfu were mixed with 600 μ l of the cell in Falcon 2059 tubes. The tubes were incubated at 37 °C for 15 min. 6.5 ml of melted LB top agar were mixed with each aliquot of infected cell and spread evenly onto a 150 mm plate of bottom agar. The plates were incubated at 37 °C for 6-8 hour. 8-10 ml of SM buffer were overlaid onto the plates. The plates were stored at 4 °C overnight. The bacteriophage suspension was recovered from each plate and pooled into a sterile falcon tube. The plates were rinsed with an additional 2 ml of SM buffer and pooled. chloroform was added in to a 5 % concentration. The tube was incubated for 15 min at room temperature. Cell debris were removed by centrifugation at 2,000 g for 10 min. The supernatant was transferred to a sterile polypropylene tube and chloroform was added to a 0.3 % final concentration and stored at 4 °C.

3.2.2.4. Phage miniprep:

To 400 μ l of the phage suspension, 5.0 μ l DEPC, 5.0 μ l 20 % SDS, 50.0 μ l 2.0 M Tris pH 8.5 and 20.0 μ l 0.5M EDTA were added and mixed gently by finger vortex. The mixture was placed at 70 °C for 5 min. Then 50 μ l of 5 M potassium acetate were added and placed on ice for at least 30 min. The mixture was centrifuged for 15 min at room temperature. The phage DNA was precipitated with 95 % ethanol at room temperature for 10 min. and then microfuged for 15 min and ethanol poured off and air dried. The DNA was resuspended in 50 μ l of TE.

3.2.2.5. Dot blot on nylon membrane:

The Boehringer Mannheim nylon membrane was cut to the appropriate size, rinsed in H₂O for 10 min. A piece of Whatman 3MM filter paper was cut to the size of the Bio-Rad manifold, rinsed in water and placed in the manifold and laid the membrane on top of it, then the manifold was assembled. To each DNA sample, 1 M NaOH and 200 mM EDTA, pH 8.2 were added to a final concentration of 0.4 M NaOH/10 mM EDTA. The samples were denatured for 10 min in a water bath at 100 °C. With the suction to the

manifold device on, 500 μ l H₂O were applied to each well, and allowed the water to filter through. Then the samples were applied to the wells. For each well, 5 μ g of DNA sample was spotted. After applying the samples, each well was rinsed with 500 μ l 0.4 M NaOH and the manifold dismantled. The membrane was rinsed briefly in 2 x SSC and air dried. The DNAs were immobilized by irradiating for the appropriate time (autocrosslinking) on a UV transilluminator with the DNA-side-down. The membrane was stored dry between sheets of Whatman 3MM filter paper for several months at room temperature.

3.2.2.6. Nuclear run on reaction:

Nuclear run-on assay was performed following the methods of Bentley and Groudine (1986), Celano et al. (1989) and Merscher et al. (1994) with modifications. One hundred μ l of isolated locust flight muscle nuclei was mixed with one volume (100 μ l) of 2 x reaction buffer. The mixture was incubated for 60 min at 32 °C. After incubation, 10 μ l RNase free DNase I, (10 mg/ml, Boehringer Mannheim) and 10 μ l CaCl₂ (20 mM) were added to the mixture, and incubated for 5 min at 26 °C. To digest the enzymes, 25 μ l 10 x SET, 2 μ l proteinase K (10 mg/ml, BM) were added, and the mixture was incubated for 30 min at 37 °C. To help precipitate the synthesized RNAs, 5 μ l of tRNA was added to the mixture. The subsequent steps were addition of 550 μ l NRO buffer II and 90 μ l 2 M NaAc, pH 4.0; the mixture was PCI (phenol-chloroform-isoamylalcohol, 24.5:24.5:1) extraction; then precipitated the supernatant with 1 volume ice cold isopropanol (kept at -20 °C over one hour and spun at the top speed for 20 min at 4 °C); resuspended the pellet in 300 μ l NRO II and 0.2 M NaAc, pH 4.0; reprecipitated in two volumes of cold 100 % ethanol; washed the pellet in 70 % ethanol; resuspended the pellet in 20 μ l 0.5 % SDS.

3.2.2.7. Hybridization:

For prehybridization preparation, an appropriate volume of hybridization buffer (20 ml/100 cm²) was prewarmed to hybridization temperature. The nylon filter was prehybridized at 60 °C for over 60 min with gentle agitation. After prehybridization, the

DIG-RNA was denatured by boiling for 5 min and rapidly cooled on ice. Then the prewarmed hybridization buffer (2.5 ml/100 cm²) was added in and mixed well and the membrane was transferred to the probe-hybridization buffer mixture. The incubation was carried on with gentle agitation at 60 °C over night (over 16 h). After hybridization, the membrane was washed at low stringency (two times for 5 min each in 2 x SSC, 0.1 % SDS at room temperature) and high stringency (two times for 15 min each in 0.1 x SSC, 0.1 % SDS at 65 °C under constant agitation), respectively.

3.2.2.8. Checking the quality of the DIG detection system:

One microliter (5 ng) of the labeled control DNA (Boehringer Mannheim) was serially diluted 10 to 10,000 folds. One microliter of each dilution was spotted directly on a positively charged nylon membrane (Boehringer Mannheim) and processed the detection assay according to the protocol from manufacturer (DIG System User's Guide for Filter Hybridization; Boehringer Mannheim). If a signal was visible after chemiluminescent detection at 1:10,000 dilution, the DIG detection system was sufficiently sensitive.

3.2.2.9. Detection:

The DIG-chemiluminescent detection procedure was performed exactly following the Boehringer Mannheim DIG Detection Kit protocol. Optimal exposure times for X-ray films (Kodak) were between 1-6 hours. In brief, after hybridization and stringency washes, the membrane was rinsed briefly (1-5 min) in washing buffer and incubated for 60 min in 100 ml buffer 2. The anti-DIG-AP conjugate was diluted to 75 mU/ml (1: 10,000) in buffer 2. The membrane was incubated for 30 min in 20 ml antibody solution and washed 2 times each 15 min with 100 ml washing buffer and equilibrated 2-5 min in 20 ml buffer 3. The CSPD was diluted 100 times with buffer 3. The membrane was incubated for 5 min in 10 ml CSPD solution. Excess liquid was dripped off and the membrane was blotted briefly (DNA side up) on Whatman 3MM paper. The damp membrane was sealed in

a hybridization bag and incubate for 5-15 min at 37°C to enhance the luminescent reaction. The membrane was exposed to X-ray film for 1-6 hours at room temperature.

3.3. Results:

The sensitivity of the DIG detection system was checked according to the instruction from the manufacturer. Fig. 3-1 shows the detection results of the control DIG-labeled DNA on the nylon membrane. After 30 min. exposure to X-ray film, the signal of the 1:10,000 dilution was still very strong, indicating that the DIG detection kit was sufficiently sensitive.

In order to check whether the isolated nuclei were still active and the nuclear run-on was efficient, 1×10^6 nuclei isolated from 5 day-old locusts were used in one run-on reaction. After purification, 10 μ l of the nuclear RNAs was spotted directly on to the nylon membrane and UV crosslinked and visualized with the standard detection process. After 30 min. exposure, the signal obtained was weaker than that of 0.5 μ g control DNA (Fig. 3-2). Although the nuclear run-on reaction appeared to be working, the sensitivity of the labeled RNA was not high enough to detect specific gene transcription after hybridization.

To understand the developmental regulation of locust flight muscle, nuclei from different age locusts were isolated as described in Chapter 2. 1×10^6 nuclei obtained from each age were used for the nuclear run-on reaction. The nuclear RNAs were hybridized with the DNA probes for 48 hours. Either locust genomic DNA or the flight muscle cDNA library was used as positive control, while purified Bluescript plasmid vector served as negative control. After 60 min. exposure, the signals were analyzed. Since the FABP mRNA concentration changes during the first two weeks after the final ecdysis, nuclear run-on assays was carried out with nuclei isolated at different ages within this period. Fig.

3-3 shows the results from 5 day old locusts. The FABP signal was slightly stronger than the control actin signal, but there was no signal detectable from the positive genomic DNA control. In contrast, a far more intense signal from the negative control plasmid DNA was detected. Basically the same pattern was obtained with flight muscle cDNA as positive control (Fig. 3-4). The nuclear run-on result from 1×10^6 nuclei of 10 day old locust is shown in Fig. 3-5; there was no signal detected.

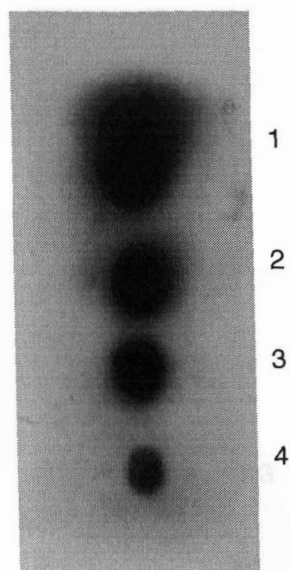


Fig. 3-1: The sensitivity of DIG detection system.

5 ng of labeled control DNA was serial diluted with 1:10 scale.
1 μ l each of the dilutions was spotted on nylon membrane.
After the standard detection process, the membrane was exposed
to X-ray film for 30 min.

- 1: 10 times dilutions (500 pg).
- 2: 100 times dilutions (50 pg).
- 3: 1000 times dilutions (5 pg).
- 4: 10,000 times dilutions (0.5 pg).

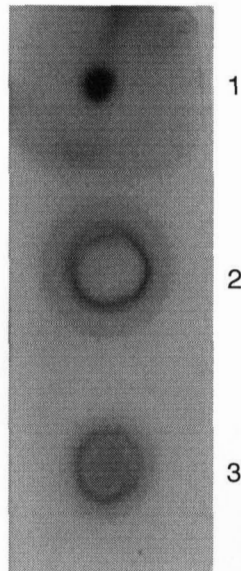


Fig. 3-2: Nuclear run-on product.

5 day-old locusts were dissected for flight muscle nuclei. The nuclear run-on assay was as the protocol described in Chapter 3.2. 10 μ l of the nuclear RNA was spotted directly on membrane. After the standard detection, the membrane was exposed to X-ray film for 30 min.

1: 0.5 pg control DNA.

2 and 3: 10 μ l nuclear run-on RNA.

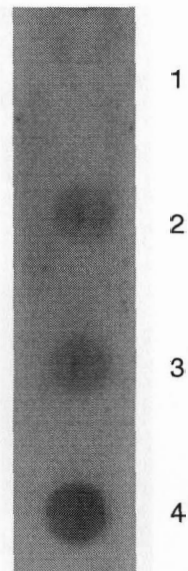


Fig. 3-3: Nuclear run-on assay results using different DNA probes.

Nuclear run-on assay with 5 day-old locust flight muscle nuclei. Hybridization and detection as protocol described in Chapter 3.2.

- 1: 5 μ g genomic DNA.
- 2: 5 μ g FABP cDNA.
- 3: 5 μ g actin cDNA.
- 4: 5 μ g Bluescript plasmid DNA.

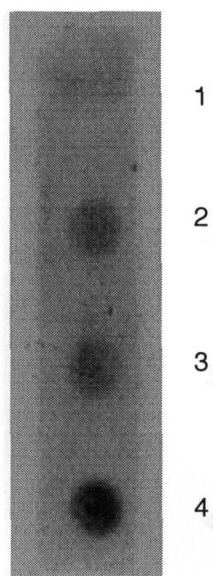


Fig. 3-4: Nuclear run-on assay results using different DNA probes.

Nuclear run-on assay with 5 day-old locust flight muscle nuclei. Hybridization and detection as protocol described in Chapter 3.2.

1: 5 μ g locust flight muscle cDNA library.

2: 5 μ g FABP cDNA.

3: 5 μ g actin cDNA.

4: 5 μ g Bluescript plasmid DNA.

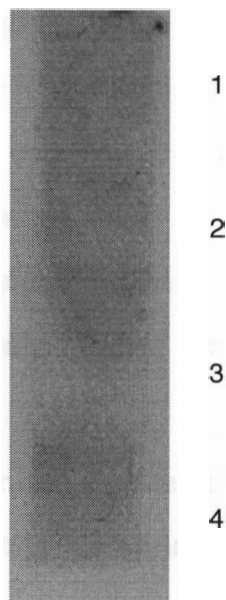


Fig. 3-5: Nuclear run-on result from 10 day-old locust flight muscle nuclei.

The complete process was described in Chapter 3.2.

1: 5 μ g locust flight muscle cDNA library.

2: 5 μ g FABP cDNA.

3: 5 μ g actin cDNA.

4: 5 μ g Bluescript plasmid DNA.

3.4. Discussion:

Nuclear run on experiments were carried out with flight muscle nuclei, but the results were inconsistent and difficult to interpret. While signals were obtained for the transcription product of the FABP gene at times when the FABP gene was suspected to be actively transcribed, these were weak and similar to the intensity of the constitutively expressed actin RNA. Moreover, genomic DNA and muscle cDNA failed to serve as reliable positive control, while plasmid DNA, for unexplained reasons, interacted rather strongly with the probes. The signal to noise ratio was unacceptable under those conditions, and it appears that various factors contributed to the low sensitivity of the assay.

Nuclear run-on assays normally require at least 1×10^7 nuclei for per reaction. However, it was not possible to obtain this amount from locust flight muscle. Instead, only 10 % (1×10^6 nuclei) were available for the assays.

The dissection and purification process was very time consuming, taking at least three hours. This time may have reduced nuclear activity and contributed to a lower sensitivity.

Data obtained from mouse myeloma nuclei showed that the elongation rate *in vitro* is only about 20% of that *in vivo*, at about 5 nucleotides per second *in vitro*, compared with the 30 nucleotides per second *in vivo*. Thus it is obvious that not all RNA polymerase molecules which initiated their RNA transcripts *in vivo* elongate *in vitro* (Mazluff and Huang, 1984). Nuclear run-on assays can quantify the balance of newly synthesized and degraded RNA in a certain amount of time (e.g. 60 min.). Considering the large size of the locust FABP gene (15 kb), its complete transcription *in vitro* requires at least 60 min., if one assumes the above mentioned elongation rate of 5 nucleotides/sec. Nuclei, however,

remain active only for approximately 30-60 min., and this may contribute to the very weak signals obtained with locust nuclei.

Because the nuclear run-on assay involves large amounts of radioactivity, handling the labeled RNA throughout the whole process can be cumbersome. To overcome this disadvantage, we used the Dioxygenin (DIG) labeled UTP to label the newly transcribed RNA. Dioxygenin is a big molecule. Holtke and Kessler (1990) and Heer et al (1994) reported inhibition of SP6 RNA polymerase, T3 and T7 RNA polymerase by DIG-UTP. Thus, partial inhibition of RNA polymerase II by DIG in isolated nuclei may have occurred, and this may have reduced the amount of elongation product.

Although the nuclear run-on assay is stated as the best method to study the transcriptional rate, most of the experimental protocols used to detect the combination of both *in vitro* transcription initiation and the elongation. *In vitro* initiation of transcription is thought to be more difficult to accomplish, and hence it is assumed that run on assays detect mostly elongation products of already partially transcribed RNAs. However, if significant new transcription occurs *in vitro*, the results of a run on assay are not a good measure for the transcription rate *in vivo*.

From the reasons outlined above, it was decided that the nuclear run-on assay was not a suitable method for the intended study of the rate of transcription of the locust flight muscle FABP gene.

CHAPTER 4: QUANTITATIVE COMPETITIVE REVERSE TRANSCRIPTION PCR

4.1. Introduction:

Since the invention of the polymerase chain reaction (PCR) method by Kary Mullis and coworkers (Saiki et al., 1985; Mullis and Faloona, 1987), numerous and diverse PCR applications have been developed. Reverse transcription PCR (RT-PCR), also called RNA PCR, is one particularly useful application which can be used to detect and analyze RNA molecules present in cells and tissues. RT-PCR has been shown to be thousands of times more sensitive than the traditional RNA blotting techniques (Wang et al., 1989). In spite of its impressive sensitivity and specificity, RT-PCR typically only provides an answer as to whether or not a transcript is being expressed. This is primarily due to the fact that RT-PCR involves two sequential enzymatic steps, namely the synthesis of cDNA from an RNA template and the polymerase chain reaction. Because of the exponential nature of the polymerase chain reaction and the liable RNA, it is difficult to obtain quantitative information. However, if specific conditions and proper controls are used, RT-PCR can yield accurate quantitative information of the RNA amount present in a sample.

The amount of PCR product does not directly reflect the number of template molecules used, as a simple PCR reaction is an exponential process. Hence, it is necessary to use a variation of the technique that allows the number of target molecules present to be determined. Numerous methods have been suggested for this purpose. The PCR reaction is an exponential reaction in which small variations in template can yield large changes in the amount of products. As the amplification rate eventually levels off, a plateau effect is observed in later cycles of the PCR reaction. Due to these characteristics, quantitative data must be obtained within the exponential phase, and preliminary experiments must be done

to determine the initial template concentrations and PCR cycle number required. Although some researchers (Singer-Sam et al., 1990) have observed that careful kinetic analysis can be used to determine initial concentrations of mRNA templates by linear regression analysis without internal controls, most quantitative studies include internal controls to eliminate the problem of tube-to-tube variations in amplification efficiency. Internal controls can be an endogenous mRNA which is relatively constant during development and physiological changes, such as actin mRNA. However, since even actin mRNA changes under different physiological conditions quantitative data may be questionable. Exogenous mRNA, synthesized *in vitro* and added prior to reverse transcription, can also serve as internal controls. These standards have the advantage that both target RNA and internal standards share the same primer binding sequences and have similar GC contents so that the amplification efficiencies for both target and standard are identical. As both the internal standard and the sample target template actually compete for the same primers, the amplification takes place in a truly competitive fashion. Hence, this technique is called competitive RT-PCR.

Competitive RT-PCR uses an exogenous template as an internal standard. The internal standard is transcribed and co-amplified with the target in the same reaction. In competitive RT-PCR reactions, a dilution series of either the sample RNA (which contains unknown quantities of the target sequence) or the standard RNA is made, and a constant amount of the other component is added to each of the reactions. After careful quantification, it can be determined at which ratio of added internal standard to target RNA the yield of the two PCR products is identical. If the same quantities of PCR products are obtained from sample and internal standard, it can be assumed that both templates were present at equal amounts at the start. This assumption is only true, however, if the exogenous and the endogenous sequences are amplified with equal efficiency. Moreover,

the two PCR products must be easily distinguishable on a gel, due to different sizes with or without restriction enzyme digestion, or by their hybridization properties.

Among the various quantitative RT-PCR techniques currently in use, competitive RT-PCR is the method of choice. Competitive RT-PCR is accurate to discern the differences in RNA levels as small as 2- or 3-fold. Since the development of quantitative RT-PCR, most investigators have amplified cellular messenger RNA (mRNA) to get insights into gene expression (Hiromichi et al., 1993, Wiesner, 1992, Tarnuzzer et al., 1996, Wang et al., 1989, Klebe et al., 1996, Auboeuf and Vida, 1996, Mitra and Laurence, 1997, Saric and Shain, 1997, Souaz, 1996, Tsai and Wiltbank, 1996, Becker-Andre and Hahlbrock, 1989, Chelly et al., 1988, 1990, Gilliland, 1990, Rappolee et al., 1989, Robinson and Simon, 1991, Singer-Sam et al., 1990). However, the analysis of mature mRNA can only provide indirect measurement of gene transcription, because the mRNA levels represent the balance of both transcription and the post-transcription events (e.g., capping, splicing, transport and degradation). A more direct approach would be to measure the amount of unprocessed primary transcripts in heterogeneous nuclear RNA (hnRNA). Because of the short half-life of primary transcripts, their concentration reflects an equilibrium between transcription and splicing, events that happen only within the nucleus. Because of the small levels of primary transcripts present in the nucleus, classical hybridization techniques are not sensitive enough for such measurements. It should be possible, however, to measure such low levels with PCR-based techniques. As unspliced primary transcripts contain not only the sequence of the expressed proteins but also introns, reverse transcription PCR with primers specific for introns of the gene in question can be used to amplify only unprocessed transcripts. Such measurements have provided useful insight into the transcription status of particular genes (Elferink and Reiners, 1996, Owczarek et al., 1992).

While the most direct way to measure the transcriptional status of a given gene is to carry out *in vitro* nuclear run-on assays, this method is laborious, time consuming, and requires large amounts of isolated nuclei. These disadvantages restrict its use for application where only small amounts of tissue are present, as in locust flight muscle. It was hence necessary to design a more sensitive method that allows to examine the gene expression in locust flight muscle (see chapter 3). Because of the above mentioned potential of PCR techniques, RT-PCR appeared to be a useful alternative technique. This method should be applicable for the study of locust FABP expression. Although the locust FABP gene has not been cloned and sequenced in its entirety, the gene organization and partial sequences of all introns are known. The 15 kb long gene has three exons (22, 94, 17 amino acids respectively) and two introns. The first intron is approximately 12 kb long, and approximately 3 kb of its 3' sequence are known (Hauerland et al., unpublished) (Fig. 4-1). Therefore, there is sufficient information available to develop a RT-PCR based method to quantify primary transcript levels in locust flight muscle.

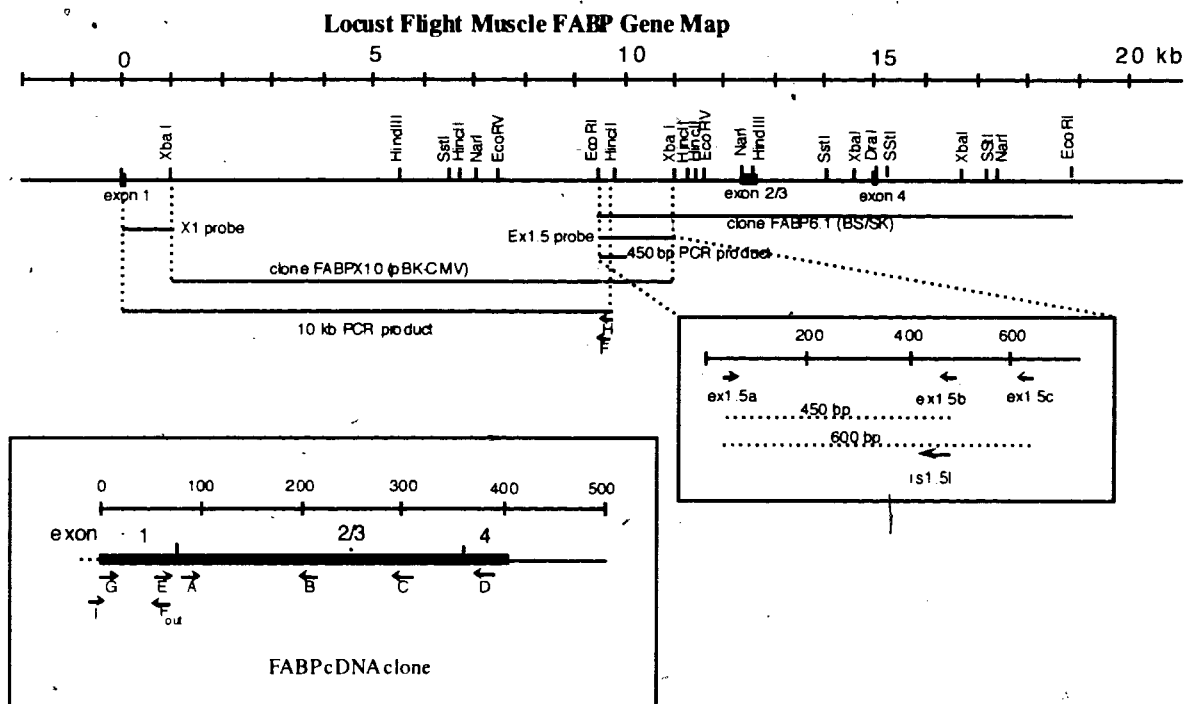


Fig. 4-1: The restriction map of locust flight muscle fatty acid binding protein gene, *Schistocerca gregaria*.

The size of the whole gene is over 15 kb with 3 exons (22, 94, 17 amino acids respective) and 2 introns.

The first intron is about 12 kb and the 2nd intron is about 3 kb.

4.2. Materials and Methods:

4.2.1. Materials:

All the chemicals were from GIBCO BRL (Burlington, ON) unless otherwise specified. Bluescript plasmid was from Stratagene (La Jolla, CA). TA Cloning® kit was from Invitrogen (San Diego, CA). Wizard Miniprep kit were from Promega Co. (Madison, WI). MAXIscript™ In Vitro Transcription Kits.(T7) was purchased from Ambion (Austin, TX). GeneAmp® RNA PCR Kit was from Perkin Elmer (Mississauga, ON). Ultratherm® PCR system was from BIO/CAN (Mississauga, ON). Gel images were taken by the Gel Documentation System and UVP Imagestore 5000 Ultra Violet Products from UVP (San Gabriel, CA).

4.2.2. PCR primer design:

PCR primers were designed from the 2 kb of known 3' sequence of the first intron of the locust FABP gene, which is inserted at the codon for Gly 27 of the protein (Hauerland et al., unpublished results). The forward (upper) primer (ex1.5a) (5' AAG CAA CAC ATC TCC AGA ATC 3') and reverse (lower) primer (ex1.5c) (5' CAA ATT ACA CTA GCA TCT CAG 3') flanked a 555 bp fragment which ends 1722 bp upstream of exon 2.

4.2.3. Internal standard preparation:

In order to produce an internal standard molecule that, when amplified with the same primers as the intron sequence, yielded an amplification product of a distinguishable smaller size, a hybrid lower primer (is1.5l) was constructed (5' CAA ATT ACA CTA GCA TCT CAG TGA GCT CTC GAA GTA TGA TAG 3'). Its 3' 21 nucleotides annealed to a sequence string 150 bp upstream of the original lower primer (ex1.5c), while the 21 nucleotides at its 5' end was identical to the sequence of the original lower primer (ex1.5c).

The primer contains also an XhoI restriction site (GAGCTC), which could be used for checking the insert orientation, as described by Celi et al. (1993).

PCR amplification of the 441 bp internal standard fragment (IS-DNA) was obtained from genomic DNA, with primers ex1.5a and is1.5l (95 °C for 105 sec; 35 cycles for 10 sec at 95 °C, 30 sec at 51.5 °C, 30 sec at 68 °C; 7 min. at 68 °C; hold at 4 °C). The amplified product was directly cloned into PCR™-II vector (TA cloning kit, Invitrogen). After cleaving the vector with EcoRI, the insert was gel purified and ligated into a Bluescript KS (+) vector (Stratagene). Plasmid DNA was digested with XhoI for selecting plasmids where the insert had the right orientation from the T7 promoter. The positive clone was confirmed by PCR with primer pair (T7 and ex1.5c), which could amplify about 525 bp fragment (95 °C for 105 sec; 35 cycles of 10 sec at 95 °C, 30 sec at 51.5 °C, 30 sec at 68 °C; 7 min. at 68 °C; hold at 4 °C).

Internal standard RNA was produced with the MAXIscript in vitro transcription kit (Ambion Inc., Texas). Between 0.5 and 1 µg of the HindIII - linearized, gel purified IS1.5 plasmid was added to 2 µl 10 x buffer, 1 µl each of 10 mM NTP, 5 U RNase inhibitor, 5 U T7-RNA polymerase, and the mixture was brought up to a volume of 20 µl with DEPC treated water. Following *in vitro* transcription for 1 hour at 37 °C the DNA template was removed by DNase I digestion (2 U of RNase free DNase I (Ambion), 30 min. at 37 °C) and subsequently the sample was incubated at 100 °C for 5 min. to denature the enzymes. The resulting RNA was precipitated with ethanol, quantified spectrophotometrically, and checked for presence of DNA contamination by PCR with the primer pair of ex1.5a and ex1.5c (95 °C for 105 sec; 35 cycles of 10 sec at 95 °C, 30 sec at 50 °C, 30 sec at 68 °C; 7 min. at 68 °C; hold at 4 °C). The RNA was kept in single use aliquots at -80 °C.

4.2.4. Total RNA isolation:

Freshly excised flight muscle tissue from locusts of different ages are immediately homogenized in RNA extraction buffer with a mechanical homogenizer (VirTis, New

York, NY). Total RNA was isolated by a one step guanidine isothiocyanate/phenol/chloroform extraction method adapted from Chomczynski and Sacchi (1987). In brief, fresh flight muscle was immediately homogenized in 10 volumes of RNA extraction buffer (4 M guanidium isothiocyanate, 25 mM sodium citrate pH 7.0, 0.5 % sarcosyl, 0.1 M β -mercaptoethanol) and the homogenate extracted with phenol/chloroform/isoamylalcohol; the extraction was repeated once or twice, until the aqueous phase was clear. After centrifugation at 10,000 g, 4 °C for 20 min., the aqueous phase (total RNA phase) was mixed with 1 volume of ice cold isopropanol and held at -20 °C for at least 1 hour. The precipitated RNA was sedimented by centrifugation at 10,000 g, 4 °C for 20 min. Subsequently, the RNA pellet was washed with 70 % cold ethanol, vacuum dried, redissolved in 300 μ l RNA extraction buffer and aliquoted to Eppendorf tubes for single use. In each vial, the RNA was precipitated with 1 volume cold isopropanol or 2 volumes of cold ethanol, washed with 70 % cold ethanol, vacuum dried and redissolved in DEPC treated H₂O. For each data point, the total RNA from each of five individuals was combined into a single sample. All the samples were stored in 100 % ethanol at -80 °C freezer. At the same time every sample was checked to be free of genomic DNA by PCR (95 °C for 105 sec; 35 cycles of 10 sec at 95 °C, 30 sec at 50 °C, 30 sec at 68 °C; 7 min. at 68 °C; hold at 4 °C).

4.2.5. Standard curve preparation:

In order to determine the number of cycles during which the PCR product is produced exponentially, internal standard template DNA (IS1.5 clone, 1×10^9 molecules) was amplified with primers ex1.5a and ex1.5c. Aliquots (5 μ l) were removed after 5, 10, 14, 18, 20, 22, 26, 28, 30, 32, and 35 cycles. The PCR product was separated electrophoretically and quantified by measuring the band densities with the NIH Image 1.61b7 software package (Bethesda, Maryland).

Similarly, constant numbers of IS-DNA molecules and different numbers of Ex1.5AC molecules were mixed and used as template for competitive PCR, in order to establish different target/standard ratios.

4.3. Results:

The primers designed in this study are specific to the sequence in intron 1 of the locust flight muscle FABP gene and work well in the PCR amplification of the enclosed sequence. PCR with primers ex1.5a and ex1.5c and genomic DNA as template resulted in a single PCR product of approximately 600 bp which is virtually identical to the expected size (597 bp) (Fig. 4-2). The same fragment was obtained when using reverse transcribed total RNA extracted from flight muscle of 5 day old adult locusts as template, indicating that primary transcript is indeed present at this stage (Fig. 4-2).

In order to construct an internal standard for quantitative RT-PCR, a 441 bp fragment was amplified from a genomic DNA clone using primers ex1.5a and a new 42 bp long lower primer (5' CAA ATT ACA CTA GCA TCT CAG TGA GCT CTC GAA GTA TGA TAG 3') that annealed to a sequence string 150 bp upstream of the original lower primer (ex1.5c) (Fig. 4-3). The 21 bp at the 5' end of this primer were identical with the sequence of primer ex1.5c, so that the PCR product can be amplified with the primers ex1.5a and ex1.5c to yield a 441 pb long product (Fig. 4-4). The amplified product was directly cloned into PCR™-II vector. After cleaving the vector with EcoRI, the insert was gel purified and ligated into a Bluescript KS (+) vector (Fig. 4-5). Indeed, when this clone was used as template for a PCR reaction with primers ex1.5a and ex1.5c, the expected 441 pb product was obtained which can be easily distinguished from the 600 pb product obtained from the intron sequence (Fig. 4-6).

For accurate quantification it is important that the PCR reaction is within the exponential phase. To determine the optimal number of cycles, 10^9 molecules of internal standard DNA were used as template for amplification. Aliquots of the PCR products after several cycles were run on agarose gels (Fig. 4-7). The band intensities of the PCR products were quantified and plotted against PCR cycle numbers (Fig. 4-8). The amplified products were within the exponential phase from cycle 28 to cycle 32, the linear part of the curve. Therefore, all subsequent PCR reactions were carried out for 30 cycles.

In order to examine whether competitive PCR with these primers was feasible to obtain quantitative data, a constant number of internal standard DNA (IS-DNA) was used together with varying amounts of target DNA (Ex1.5AC) as templates for competitive PCR. As shown in Figs 4-9 and 4-10, the band intensities change with varying ratios of target and standard; similar band intensity should be found at ratios between 1.0 and 1.5. Quantitative evaluation by image analysis revealed that for equal numbers of target and standard DNA a target to standard band intensity ratio of 1.35 was obtained (Fig. 4-11).

In order to proceed to quantitative RT-PCR, internal standard RNA had to be synthesized. The IS1.5 plasmid was cleaved with Hind III just downstream of the insert. After gel purification, the linearized plasmid was used for the *in vitro* synthesis RNA. Since even traces of DNA contamination can cause inaccuracy of the assay, the DNA template was removed after RNA synthesis by adding RNase-free DNase I. The internal standard RNA, when used as template for RT-PCR, resulted in the expected amplification product of 450 bp. No band was detected in a control experiment that omitted the reverse transcription step, proving that the RNA was indeed free of DNA contamination (Fig. 4-12).

Following these preliminary experiments, total RNA from 12-day-old locust flight muscle was used to check the quantitative competitive RT-PCR system. In each reaction, 1.3×10^5 molecules of internal standard RNA were included. Serial dilutions of total RNA

from 2600 ng to 40 ng were used in QC-RT-PCR. The PCR products were separated on 1.5 % agarose gels (Fig. 4-13). The target to internal standard band intensity ratio was plotted against the amount of total RNA used as template on a double logarithmic scale (Fig. 4-14). As the number of template molecules equals that of internal standard molecules when the band intensity ratio is 1.35, it follows that flight muscle from 12 day old locusts contains 308 molecules of FABP primary transcript per ng of total RNA.

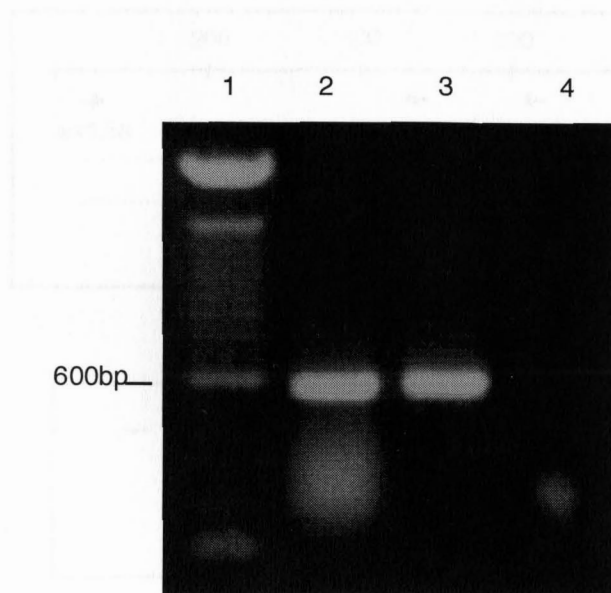


Fig. 4-2: RT-PCR of total RNA and PCR of genomic DNA from 5-day-old locust with primer pair of ex1.5a and ex1.5c.

RT-PCR and PCR procedure was described in Chapter 4.2. PCR of total RNA was as the negative control. No DNA contamination.

Lane 1: 100 bp ladder.

Lane 2: RT-PCR of total RNA from 5-day-old locust flight muscle.

Lane 3: PCR of genomic DNA.

Lane 4: negative control; PCR of RNA from 5-day-old locust.

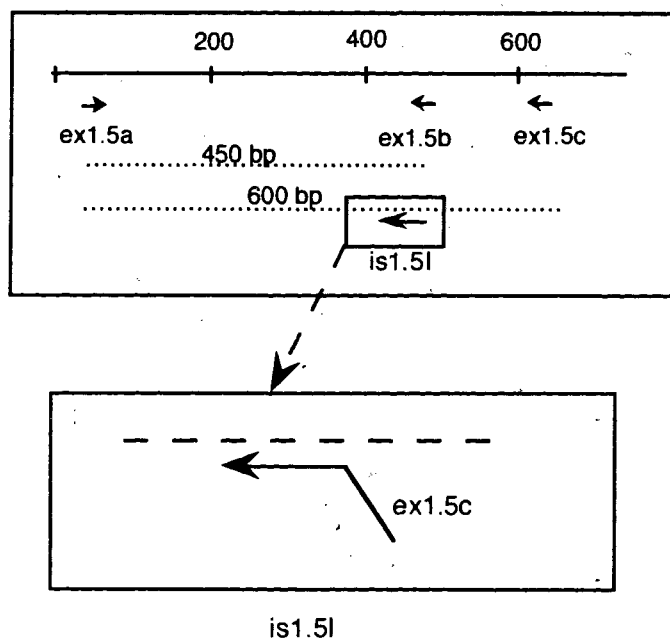


Fig. 4-3: Internal standard lower primer (is1.5l) design.

The new 42 bp long lower primer (5' CAA ATT ACA CTA GCA TCT CAG TGA GCT CTC GAA GTA TGA TAG 3') was synthesized that annealed to a sequence string 150 bp upstream of the original lower primer (ex1.5c). The 21 bp at the 5' end of this primer were identical with the sequence of primer ex1.5c.

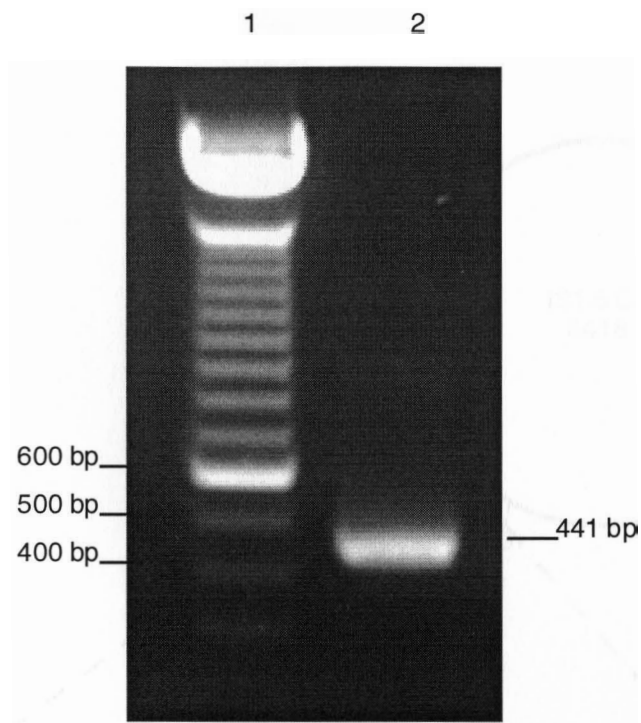


Fig. 4-4: Internal standard DNA (IS-DNA).

With the primer pair of ex1.5a and is1.5l, a 441 bp DNA fragment was amplified as described in Chapter 4.2. which could share the same primer set as target DNA.

Lane 1: 100 bp ladder.

Lane 2: IS-DNA,

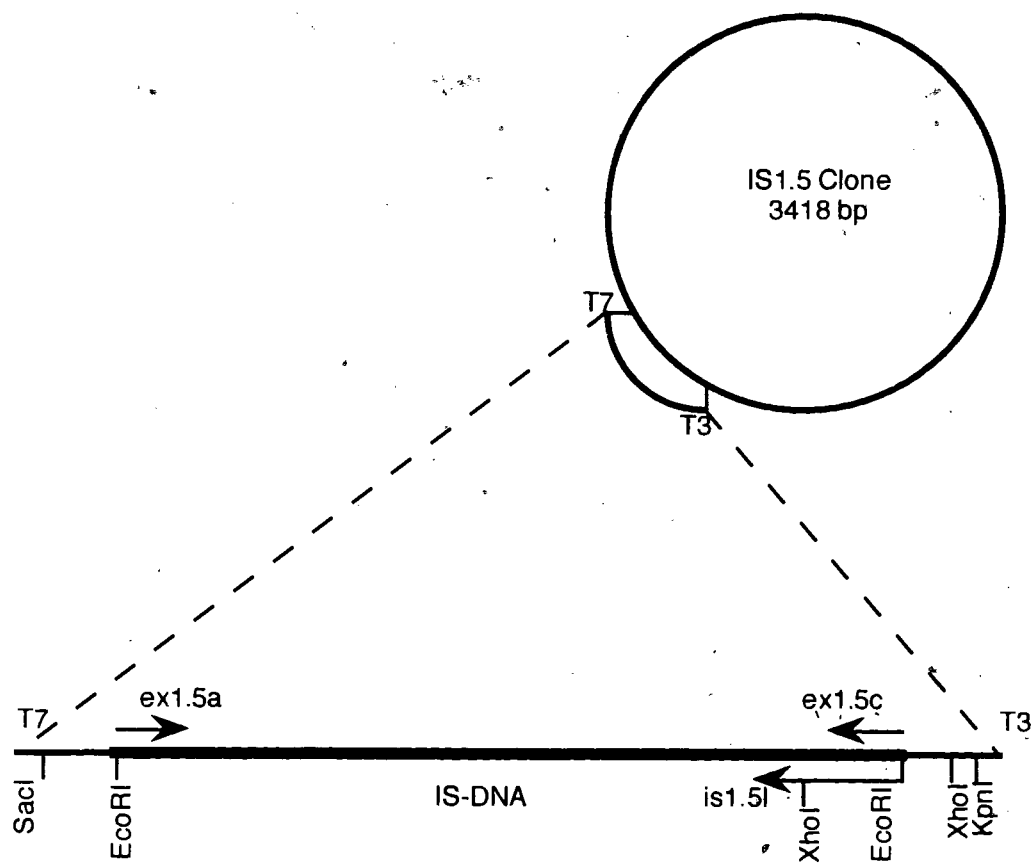


Fig. 4-5: Scheme graph of the internal standard plasmid.

IS-DNA was synthesized by PCR and cloned directly into pCR™ 2.1 vector. The IS-DNA was cut out by EcoRI and religated into pBluescript KS(+). The direction of insert could be checked with XhoI digestion.

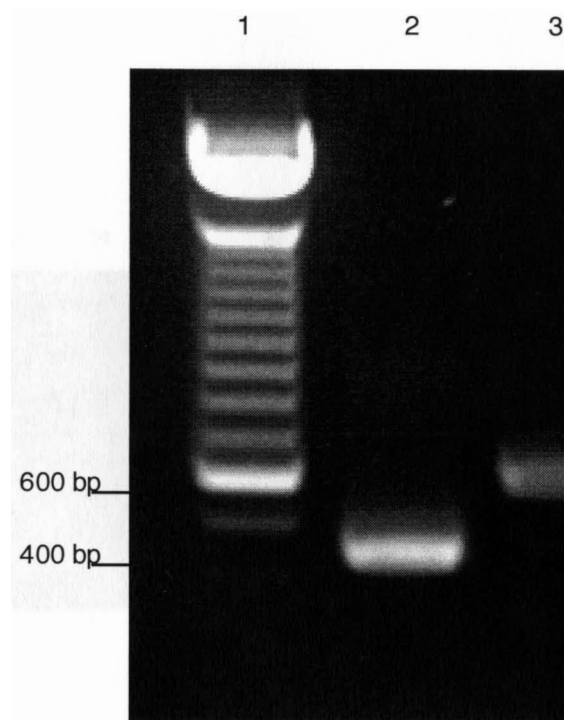


Fig. 4-6: PCR of IS1.5 clone and genomic DNA with ex1.5a and ex1.5c.

Procedure as described in Chapter 4.2.

Lane 1: 100 bp ladder.

Lane 2: PCR product from IS1.5 clone.

Lane 3: PCR product from genomic DNA.

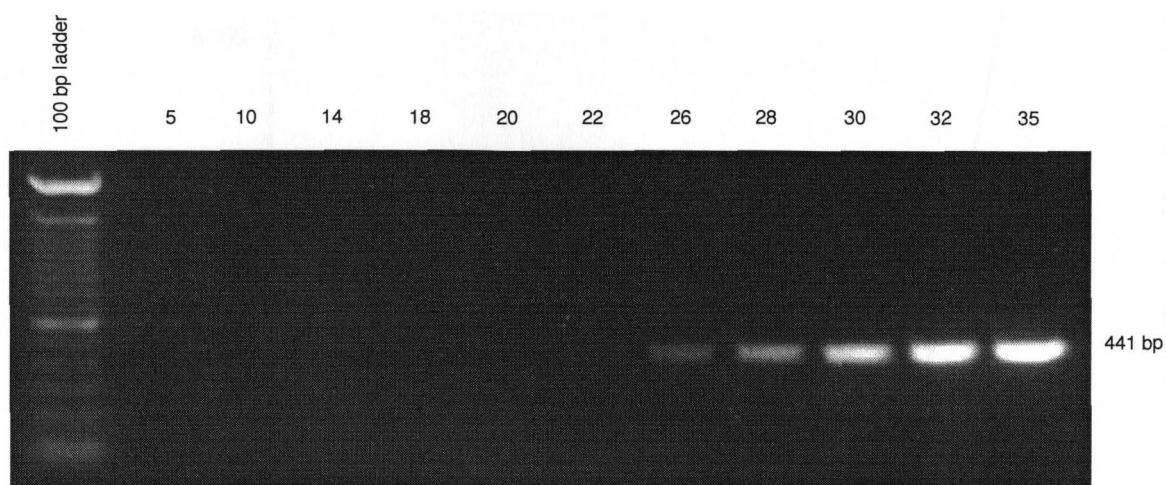


Fig. 4-7: The exponential character of PCR.

PCR of 1×10^9 molecules of IS1.5 clone with primer pair of ex1.5a and ex1.5c as described in Chapter 4.2. $5 \mu\text{l}$ of PCR product was removed at different cycles and run on 1.5% agarose gel.

The lane orders from left to right: 100 bp ladder, cycle 5, cycle 10, cycle 14, cycle 18, cycle 20, cycle 22, cycle 26, cycle 28, cycle 30, cycle 32, cycle 35, respectively.

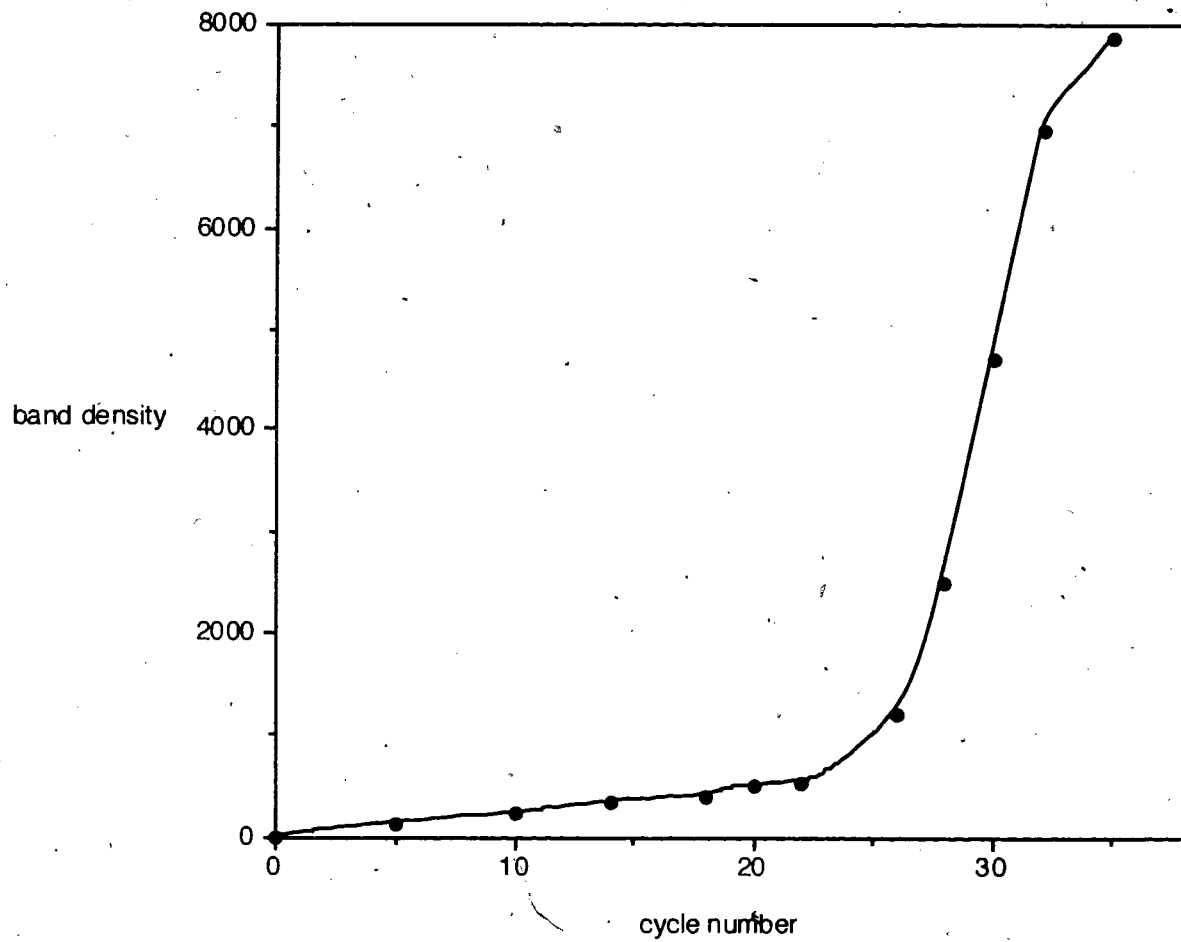


Fig. 4-8: The exponential character of PCR.

The gel image from Fig.4-7 was analyzed with NIH Image 1.61b7. Between cycle 28-cycle 32, the amplification was within exponential phase.

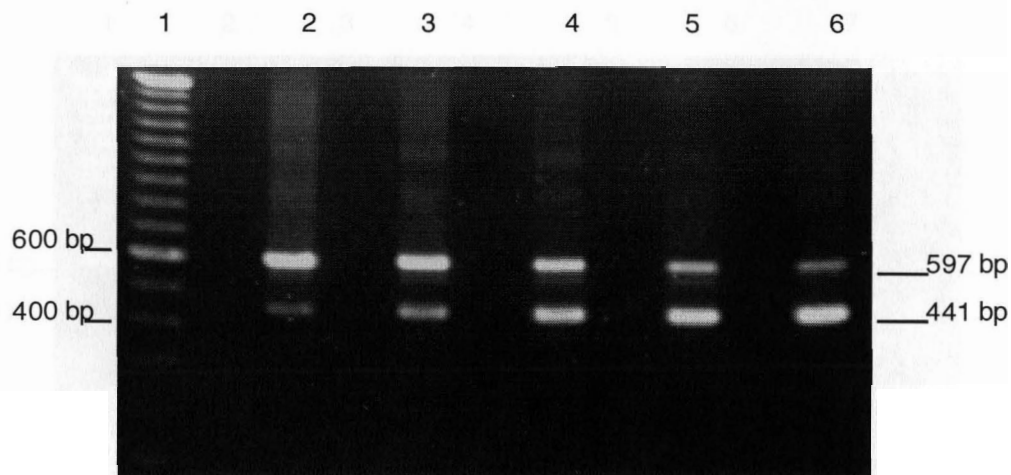


Fig. 4-9: Quantitative competitive PCR of known quantities of Ex1.5AC and IS-DNA.

6×10^7 IS-DNA molecules and known numbers of Ex1.5AC DNA molecules were added as templates, PCR reaction was described in Chapter 4.2. $10 \mu\text{l}$ of each PCR product were run on 1.5% agarose gel.

Lane 1: 100 bp ladder.

Ex1.5AC number:

Lane 2: 2.2×10^8

Lane 3: 1.1×10^8

Lane 4: 5.6×10^7

Lane 5: 2.8×10^7

Lane 6: 1.4×10^7

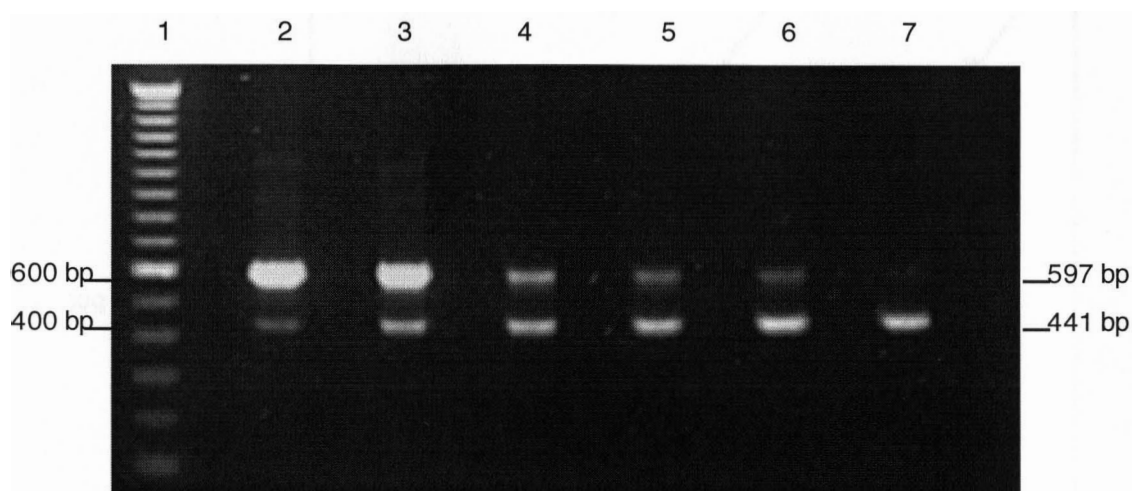


Fig. 4-10: Quantitative competitive PCR of known quantities of Ex1.5AC and IS-DNA,

5×10^6 IS-DNA molecules and known numbers of Ex1.5AC DNA molecules were added as templates, PCR reaction was described in Chapter 4.2. $10 \mu\text{l}$ of each PCR product were run on 1.5% agarose gel.

Lane 1: 100 bp ladder.

Ex1.5AC number:

Lane 2: 1.4×10^7

Lane 3: 7.2×10^6

Lane 4: 3.6×10^6

Lane 5: 1.8×10^6

Lane 6: 9×10^5

Lane 7: 4.5×10^5

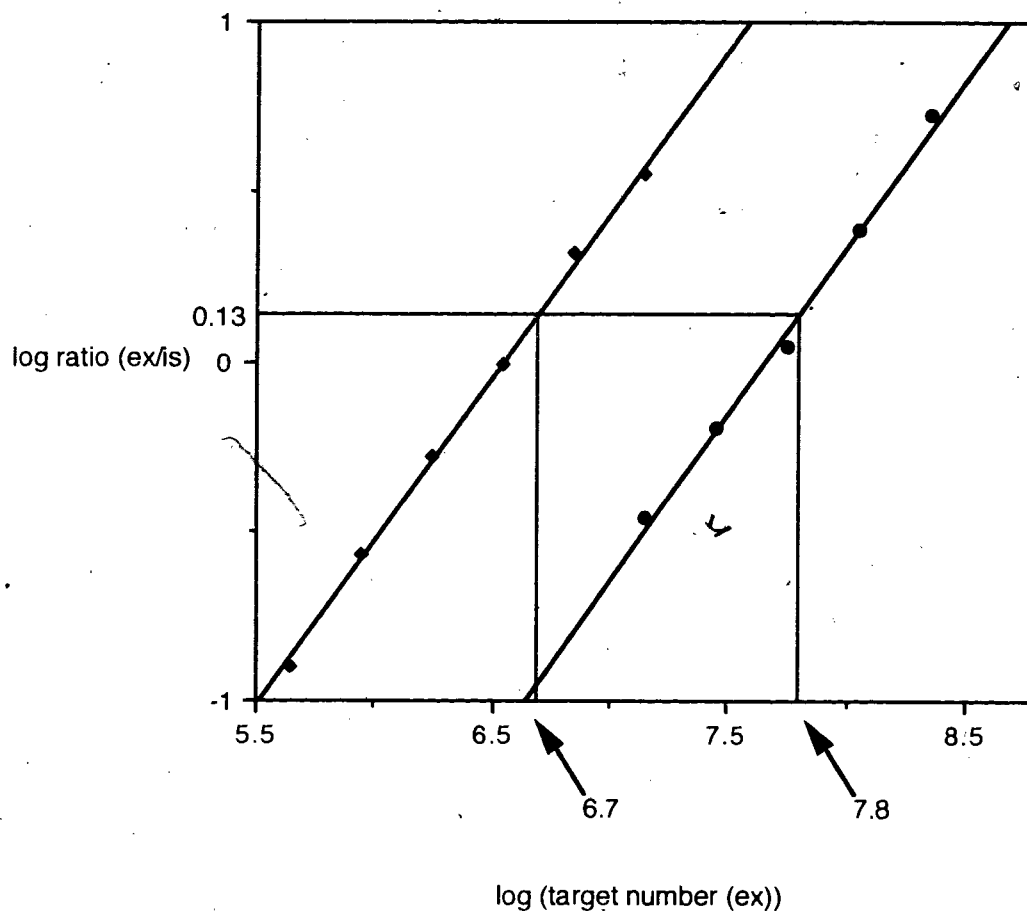


Fig. 4-11: Competitive PCR of known quantity of Ex1.5AC and IS-DNA.

Gel images were analyzed as described in Chapter 4.2. At ratio = 1.35, the target molecule number was equal to the standard molecule number. The calculated IS-DNA numbers (5×10^6 and 6×10^7 , respectively) were identical to the numbers input.

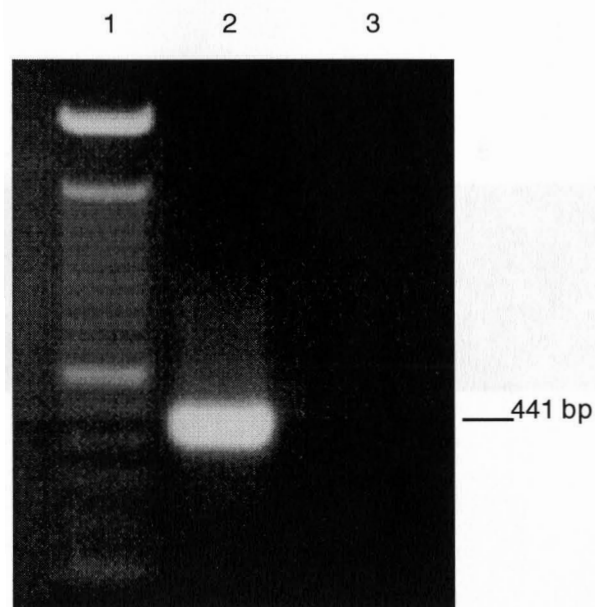


Fig. 4-12: RT-PCR of the internal standard RNA.

After *in vitro* transcription of linearized IS1.5 plasmid, the IS-RNA was reverse transcribed and amplified as described in Chapter 4.2. IS-RNA without reverse transcription was as negative control. There was no IS-DNA contamination left in the IS-RNA product.

Lane 1: 100 bp ladder.

Lane 2: IS-RNA.

Lane 3: IS-RNA PCR without RT as negative control.

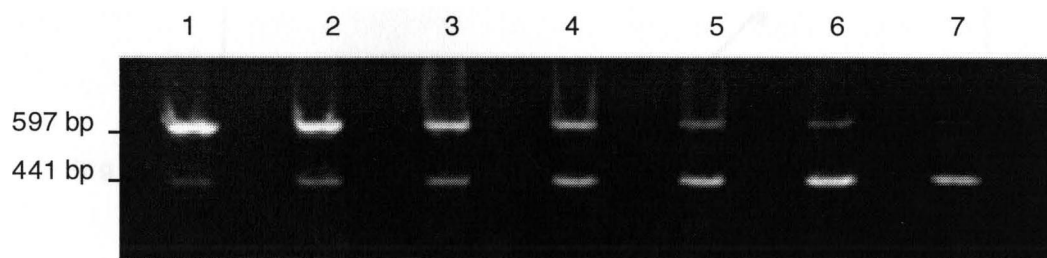


Fig. 4-13: QC-RT-PCR of the total RNA from 12-day-old locust flight muscle.

1.3×10^5 internal standard RNA molecules were used in every reaction. RNA sample was serial diluted and QC-RT-PCR procedure was described in Chapter 4.2.

Lane 1: 2600 ng total RNA

Lane 2: 1300 ng

Lane 3: 650 ng

Lane 4: 325 ng

Lane 5: 162.5 ng

Lane 6: 81.25 ng

Lane 7: 40.625 ng.

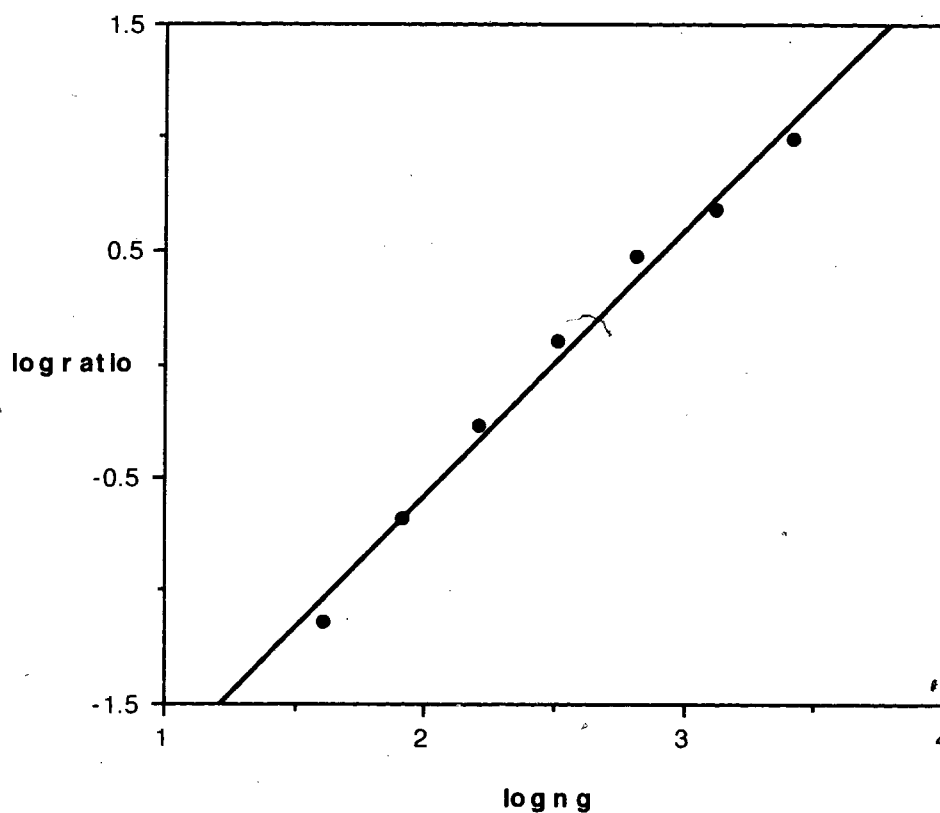


Fig. 4-14: The plot of QC-RT-PCR products from 12-day-old locust flight muscle.

The products were quantified and plotted as described in Chapter 4.2. At ratio = 1.35, the template molecule numbers equal internal standard molecule numbers. After calculation, there was 308 molecules of M-FABP primary transcript per ng of total RNA in 12-day-old locust flight muscle. (421-ng contains 1.3×10^5 molecules).

4.4. Discussion:

A good internal standard for competitive RT-PCR must compete with the target for the PCR primers in reverse transcription and PCR. Hence, it is necessary that standard and target react with the same primers and that the amplification takes place with similar efficiency. This requires that the PCR products to be similar in base composition. To achieve this, frequently an internal standard is produced by cutting out a small part of the target DNA via a convenient restriction site. Since no useful sites were found in the selected target sequence, a simple and efficient alternative approach was chosen here. As PCR is a good method to produce a deletion, a 42 bp hybrid lower primer (is1.5l) was constructed which can amplify a somewhat smaller fragment distinguishable from the Ex1.5AC. Its 3' 21 nucleotides annealed to a sequence 150 bp upstream of the original lower primer (ex1.5c), while the 21 nucleotides at its 5' end were identical to the sequence of the original lower primer (ex1.5c). This primer contained also an XhoI restriction site (GAGCTC), which could be used for checking the insert orientation. The PCR product amplified with the upper primer ex1.5a and this hybrid primer (is1.5l) is 35 % smaller than the target, but contains similar sequence and identical 3' and 5' ends as the target intron sequence. Thus, both target and internal standard should be amplified with similar efficiency, as required in quantitative competitive RT-PCR.

The internal standard DNA was initially used to evaluate the technique. The results were in line with theoretical predictions, as outlined below.

Exponential amplification is characteristic for PCR reactions. The products from one cycle of amplification serve as substrates for the next; hence, from cycle n the number of molecules is doubled after cycle $(n+1)$. The relation of PCR product to cycle number can be expressed as

$$M = 2^n * M_0$$

where M is the number of amplified molecules

M_0 is the initial molecule number

and n represents the PCR cycle number.

These theoretical numbers however cannot be reached in reality, since the amplification efficiency is never 100%. To correct for this, one can rewrite the equation to

$$M = (1+e)^n * M_0$$

where e represents the amplification efficiency.

In competitive RT-PCR, an exogenous competitor is introduced as the internal standard. Both the target sequence and the internal standard sequence share the same primer sites; they have homologous sequences and use identical reaction condition. Therefore, the amplification efficiency of both target and internal standard should be identical.

The equation for target sequence can be expressed as

$$M_t = (1+e_t)^n * M_{0t}$$

(t: target)

while the equation for internal standard sequence is

$$M_{is} = (1+e_{is})^n * M_{0is}$$

(IS: internal standard).

Since

$$e_{is} = e_t$$

the ratio

$$M_t/M_{is} = M_{0t}/M_{0is}$$

The absolute initial amount of target molecules can be determined if the amount of the initial internal standard molecules that compete with the target for primer binding is known. Because the internal standard sequence is shorter than the target, and longer sequences incorporate more ethidium bromide, a corresponding correction must be made in the calculation of initial target molecule numbers. In this case the correction number was $(597/441)=1.35$.

Competitive RT-PCR requires RNA competitor as the internal standard. Since the efficiency of synthesis complementary DNA is less than 100 %, using DNA as competitor would not be accurate. This RNA competitor must be included before reverse transcription. Therefore, *in vitro* transcription was necessary to synthesize competitor RNA. Using this competitor RNA and total RNA extracted from locust muscle at one point in development, it was demonstrated that this method works as well in the RT-PCR setting. Twelve day old locusts were chosen since FABP expression in the flight muscle should be well below the maximum as FABP mRNA levels decline at this age (Haunerland et al., 1992). The QC-RT-PCR method worked as expected, to determine the concentration of pre-mRNA molecules present in flight muscle RNA. Approximately 300 molecules of primary transcript were present in 1 ng of total RNA (Fig. 4-13, Fig. 4-14). Hence, this method appears to be much more sensitive than the nuclear run-on assays. The results also prove that this QC-RT-PCR system can be used in a wide concentration range; 10^6 - 10^8 molecules of primary transcript can be quantified with similar accuracy and efficiency (Fig. 4-11).

The construction of this quantitative competitive reverse transcription polymerase chain reaction (Q-C-RT-PCR) system thus provides a feasible method to study FABP gene

expression at the level of transcription in locust flight muscle tissue. Because of the high sensitivity, this methodology has the potential to be used in other tissues and organisms where either the amount of tissue is limited or the transcription level is too low for nuclear run on assays.

CHAPTER 5: CHANGES IN FABP PRE-MRNA DURING DEVELOPMENT

5.1. Introduction:

FABP level and its mRNA changes rapidly during locust maturation. It is completely absent in nymphs and newly emerged adults. Neither FABP nor its mRNA have ever been detected prior to metamorphosis. Immediately after metamorphosis, FABP synthesis starts and the protein concentration rises rapidly within the first two weeks of adulthood after which it has reached its maximal level. The FABP concentration remains constant afterwards at approx. 18 % of the total cytosolic proteins for the rest of the locust's life. The synthesis of FABP is preceded by a rise in its mRNA. FABP mRNA is first visible one day after metamorphosis; it reaches its peak after one week and decreases during the second week to a relatively low, constant level (Hauerland et al., 1992).

This expression pattern suggests that FABP mRNA is effectively regulated. Changes in gene expression involve changes in the transcription of the gene, which may be activated or inhibited, depending on the required level of gene expression. However, it is also possible that the gene transcription occurs at a constant level, and that the observed rise and decline in mRNA levels is the consequence of altered mRNA stability. To decide whether altered gene transcription is responsible for the observed changes in FABP mRNA, it is necessary to measure the level of transcription at different times in development.

Normally, *in vitro* nuclear run-on assays are used to measure the transcriptional status of a given gene. However, as shown in chapter 3, this method is not suitable for locust flight muscle. Instead, an alternative assay was developed (QC-RT-PCR), as described in chapter 4; which indirectly measures the actual transcription rates. In most

eukaryotic cells, RNA polymerase II synthesizes various RNAs that are collectively referred to as heterogeneous nuclear RNAs (hnRNAs). Pre-mRNAs are the subset of hnRNAs which are interrupted by intervening sequences or introns and eventually are converted into mRNAs by a series of RNA processing reactions. The mature mRNAs are then transported out of the nucleus into the cytosol. Since pre-mRNAs are unstable intermediates of mRNA synthesis, the level of FABP pre-mRNA at any time in development should reflect the ongoing rate of transcription of its gene. In this chapter, the determination of FABP pre-mRNA through the period of muscle development is described.

5.2. Material and Methods:

5.2.1. Insects:

Insects were reared as described in chapter 2.2.2.1. The last stage nymphs were collected and immediately dissected for total RNA isolation. Within 12 hours after molting, freshly emerged adults were removed and reared separately until sacrificed for total RNA isolation at specific ages. Individuals between 0 and 24 hours after adult molting are referred to as day 1 adults, with each subsequent day representing an additional 24 hour period.

5.2.2. Total RNA isolation:

Total RNA was isolated as described in chapter 4.2.4. For each data point, the total RNA from each of five individuals was combined into a single sample.

5.2.3. Quantitative competitive RT-PCR:

The RNA samples, stored in 100 % ethanol, were removed from the -80 °C freezer and spun at 14,000 x g at 4 °C for 20 min. The pellets were washed with 70 % cold ethanol and dried in a Speed-vac system (Savant). The dried RNA was subsequently dissolved in RNase-free H₂O and adjusted to a concentration to 3 µg per µl.

RT-PCR was performed with the GeneAmp PCR System 2400 from Perkin-Elmer. Reverse transcription was carried out using the GeneAmp RNA PCR Kit (Perkin-Elmer, NJ) using the conditions described by the manufacturer. The 20 μ l reaction mixture contained 1 x PCR buffer II, 5 mM MgCl₂, 1 mM each of dNTP, 1 U of RNase inhibitor, 2.5 U of MuLV reverse transcriptase, 2.5 μ M ex1.5c downstream primer, 3 ng-3 μ g total sample RNA and 1×10^5 - 1×10^7 molecules of the internal standard RNA (IS1.5RNA). The reaction was carried out for 60 min. at 42 °C after 10 min. pre-incubation at 25 °C. The reaction was terminated by heating to 99 °C for 5 min. then cooling to 4 °C.

The reverse transcription product was used immediately for PCR amplification. The 100 μ l reaction mixture contained 2 mM MgCl₂, 1 x PCR buffer II, 0.5 μ M ex1.5a upstream primer, 2.5 U AmpliTaq DNA polymerase and 20 μ l of reverse transcription product. The mixture was denatured at 95 °C for 105 sec. PCR was carried out for 10 sec at 95 °C, 30 sec at 50 °C, 30 sec at 68 °C for 30 cycles with a final 7 min. extension at 68 °C. Subsequently, the samples were held at 4 °C. Aliquots (10 μ l) of the products were analyzed by gel electrophoresis on 1.5 % agarose containing ethidium bromide. The absence of DNA contamination was routinely ascertained by carrying out the RT-PCR reactions as above, but in absence of MuLV reverse transcriptase.

5.2.4. Detection and quantitation of PCR products:

The gel image was visualized on a UV transilluminator and documented with a UVP 5100 camera system (UVP, San Gabriel, CA). Images were saved as TIFF files and analyzed on a Macintosh computer with the NIH Image software package (version 1.61b7, NIH, Bethesda, Maryland). The ratio of the densities measured for the template and internal standard bands were plotted against the amount of total RNA used as template on a double logarithmic scale. As the 597 bp template is 35 % larger than the 441 bp internal standard, a ratio of 1.35 indicates equal number of template and internal standard.

5.3. Results:

In order to investigate the developmental changes of FABP primary transcripts, total RNA was isolated from flight muscles at various time points during the first 20 days after adult ecdysis; and the primary transcript levels were analyzed with the quantitative competitive reverse transcription polymerase chain reaction. Initially, the reactions were carried out without internal standard. While these results do not allow quantitation, it is clear that dramatic changes occur during muscle development (Fig. 5-1). In flight muscle of the 5th instar nymph, no FABP pre-mRNA was detectable even when more than 3 μ g of total RNA were used as template. A strong band representing the amplification product of the primary transcript is visible in 2 day old adults. While the band appeared even more intense in 5 day old adults, it was considerably weaker in 10 day old insects and weak, but still clearly detectable in 20 day old adults.

In order to quantify these changes, a series of RT-PCR reactions with varying concentrations of target RNA were carried out in the presence of known amounts of internal standard molecules, as described in the previous chapter. As the amount of total RNA used as template is limited to a range between 25 ng and 3 μ g, the number of standard molecules had to be adjusted so that equal numbers of target and standard were present within this range. In 2 to 6-day-old locusts, where the largest number of pre-mRNA template was present, 1.3×10^7 internal standard molecules (IS-RNA) were used in each reaction. For 8-day-old locust, 1.3×10^6 molecules were used, while for day 1 and 10, 12, 20-day-old locusts, 1.3×10^5 molecules of IS-RNA were included in each reaction. With these adjustments, the target to standard band intensity ratios always covered at least the range of 0.5 to 1.5.

The results for day 12, where only 300 copies of primary transcript were detected, were already shown in the previous chapter (Fig. 4-13). In contrast, much higher levels are

present at day 5 (Fig. 5-2). The ratio of the densities between the target bands to the internal standard bands was plotted against the amount of total RNA used on a double logarithmic scale (Fig. 5-3). At the target to standard intensity ratio of 1.35, the numbers of target molecules and internal standard are identical. From this point, the primary transcript copy number per ng RNA was calculated. In 5-day-old locust flight muscle, 1.3×10^7 molecules of target RNA were present in 25 ng of total RNA; hence, the primary transcript concentration was 520,000 copies/ng of total RNA.

Similar experiments were carried out on other days of development (Fig. 5-4). The transcript numbers were similar in two to six day old insects, but much smaller at day 8. The concentration continued to decline over the next few days. At day 20, FABP pre-mRNA was still detectable, but at less than 0.01 % of the value found at day 5. No primary transcript was detectable in insects immediately before metamorphosis, even in 3 μ g of total RNA, when only 10^4 molecules of standard were used. Therefore, if the FABP gene was transcribed at all, it would be at a very low rate, resulting in less than 3 molecules of target RNA per ng of total RNA.

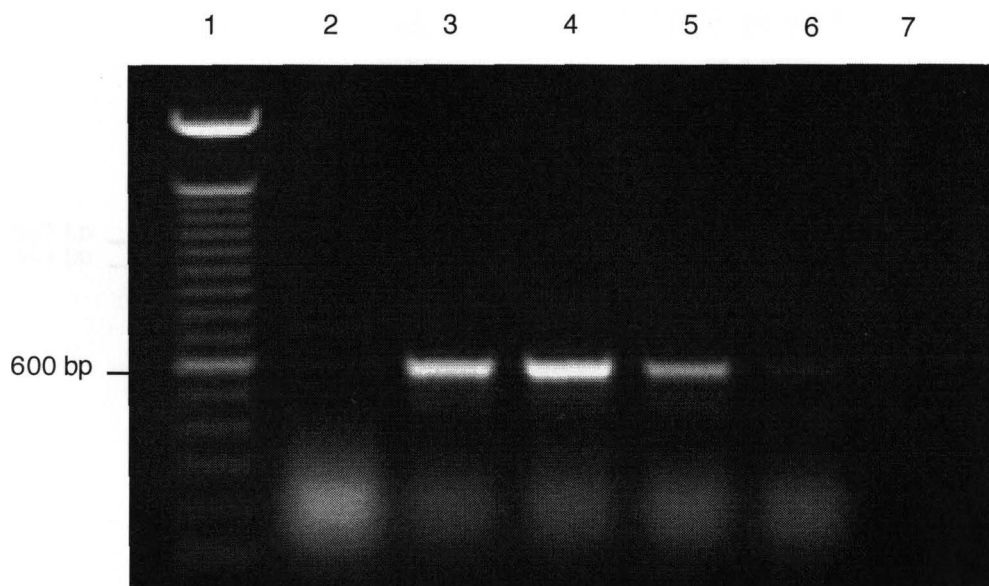


Fig. 5-1: RT-PCR of total RNA from flight muscle of different age locusts.

3 μ g of total RNA was used in each reaction. RT-PCR procedure was described as in Chapter 5.2.

Lane 1: 100 bp ladder

Lane 2: 5th instar nymph

Lane 3: 2-day-old adult

Lane 4: 5-day-old adult

Lane 5: 10-day-old adult

Lane 6: 20-day-old adult

Lane 7: negative control

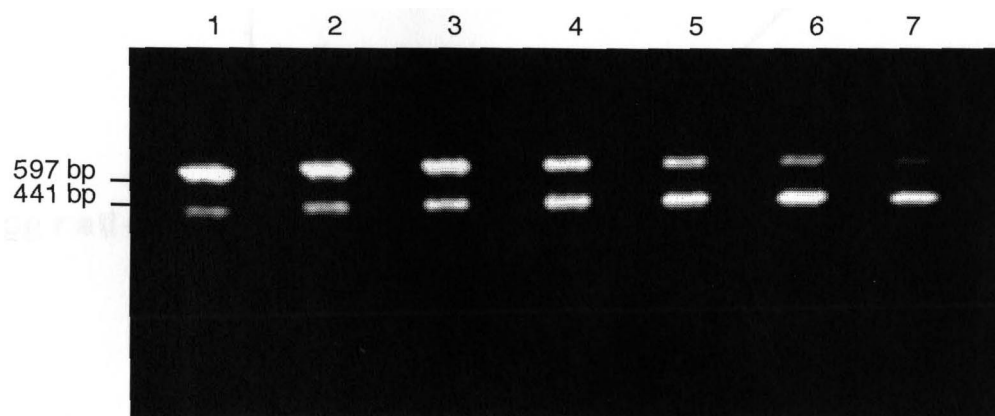


Fig. 5-2: QC-RT-PCR of the total RNA from 5-day-old locust flight muscle.

1.3×10^7 internal standard RNA molecules were used in every reaction. RNA sample was serial diluted and QC-RT-PCR procedure was described in Chapter 5.2.

Lane 1: 128 ng total RNA

Lane 2: 64 ng

Lane 3: 32 ng

Lane 4: 16 ng

Lane 5: 8 ng

Lane 6: 4 ng

Lane 7: 2 ng

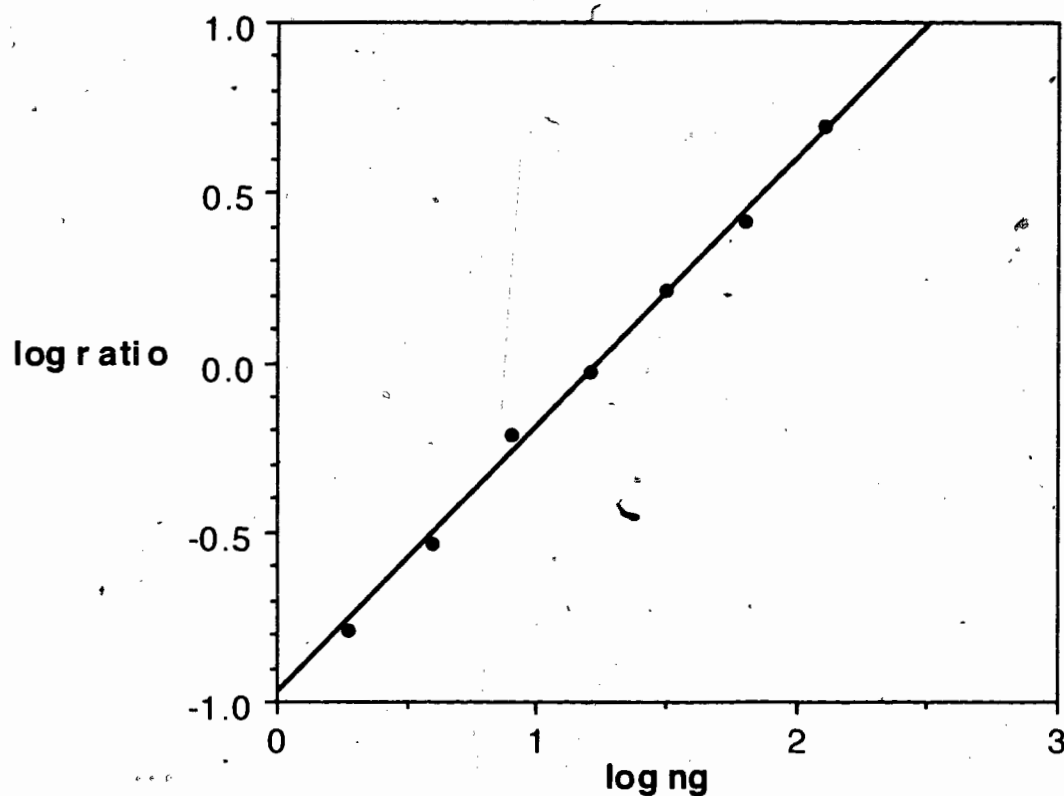


Fig. 5-3: The plot of QC-RT-PCR products from 5-day-old locust flight muscle.

The products were quantified and plotted as described in Chapter 5.2. At ratio = 1.35, the template molecule numbers equal internal standard molecule numbers. After calculation, there was 520000 molecules of M-FABP primary transcript per ng of total RNA in 5-day-old locust flight muscle (25 ng contains 1.3×10^7 molecules).

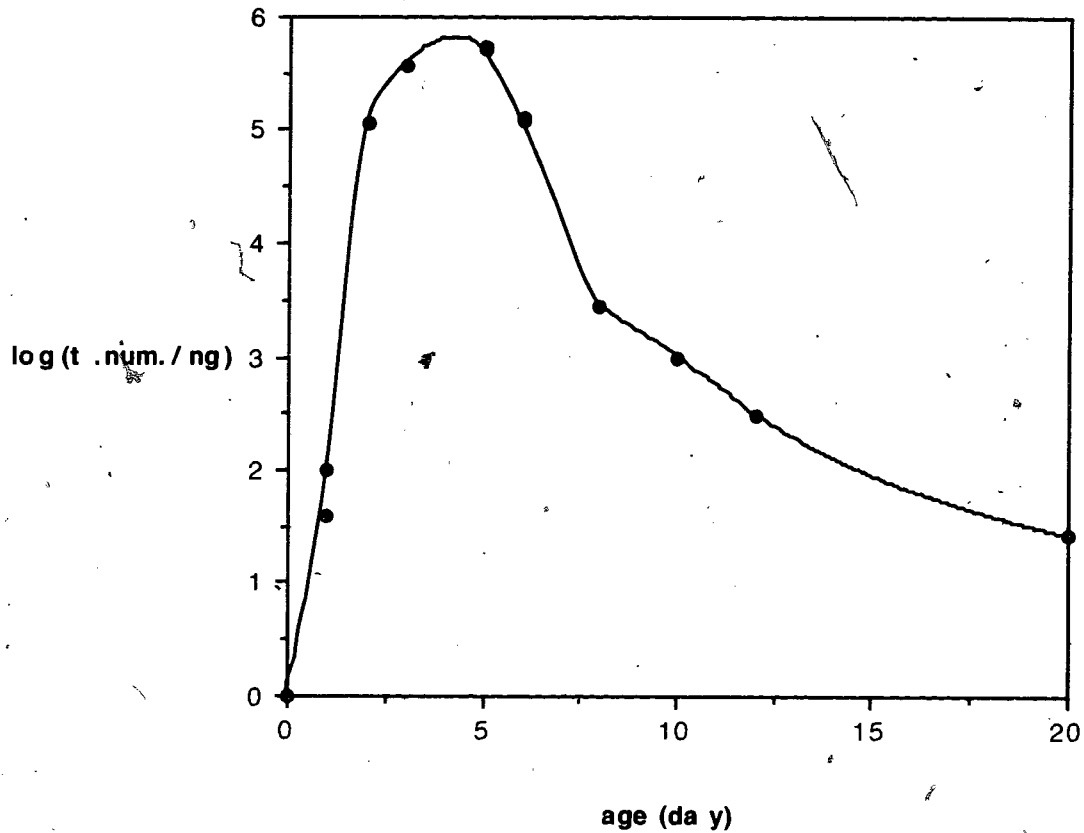


Fig. 5-4: The transcription regulation during locust development.

Total RNA was isolated from different ages of locust. The M-FABP primary transcript was quantified with QC-RT-PCR system. The quantitative data were then plotted. The nymph does not express M-FABP. Within one week after adult ecdysis, the M-FABP expression reaches its peak. Its expression is decreased during the second week to a constant low level.

5.4. Discussion:

In the current study, a quantitative competitive RT-PCR method was used to measure the rate of gene expression in the differentiated flight muscle from desert locust. This method proved to be suitable to quantify pre-mRNA levels over a wide concentration range. Our data clearly show that the observed pattern of FABP mRNA and protein accumulation during adult development of the locust is the consequence of changes in transcription of the FABP gene. FABP pre-mRNA was measured in the total RNAs isolated from last instar nymphs up to 20-day-old adult locust flight muscle. No pre-mRNA is detectable in nymphs, indicating that the FABP gene is not transcribed prior to metamorphosis. This had already been suggested by Haunerland et al. (1992), based on the fact that neither FABP nor its mRNA were detectable before the final ecdysis. Immediately after the final molt, within a few hours, the primary transcript becomes detectable. However, at only about 100 pre-mRNA molecules per ng total RNA, the number of primary transcript molecules is relatively low at the first day. This suggests a delay in the full activation of the gene, possibly due to the need to synthesize other factors required for optimal transcription. The pre-mRNA levels increase dramatically during the next day and remain very high from day 2 until day 5. In 5 day old locusts, the FABP primary transcripts reached its peak with more than 500,000 copies in one ng total RNA. Assuming that each copy detected here represents the full 15 kb primary transcript, FABP pre-mRNA accounts for approximately 0.01 % of the total RNA. These large amounts of primary transcript are present at a time when FABP mRNA levels are still increasing; at day 5, mRNA has reached approximately 90 % of its peak level (Haunerland et al., 1992), while only a third of the final FABP has accumulated. Subsequently, the concentration of primary transcript declined rapidly. At day 8, when FABP mRNA is still near its maximum, the

pre-mRNA level is reduced to approximately 2000 molecules per ng total RNA, and between day 12 and 20 only less than 300 copies were detected. At this time, FABP has reached its maximum, and its mRNA has returned to a constant level of less than 20 % of its maximum. In contrast to the mRNA levels, the pre-mRNA changes from a large factor to less than 0.1 % of the maximal levels.

These results prove that the quantitation of primary transcript can give insights into the control of gene expression similar to those obtained from nuclear run on assays. In contrast to nuclear run-on assays, which require tissue disruption and lengthy purification of nuclei prior to measuring transcriptional activity *in vitro*, this QC-RT-PCR method allows the determination of transcriptional activity present *in vivo*. Moreover, it is far more sensitive than nuclear run-on analysis, which usually requires more than 10^7 nuclei. In contrast, less than 10 mg of tissue are needed to isolate 3 μ g of total RNA, in which fewer than 10,000 molecules of primary transcript can be measured.

Since variations between individual insects of identical age have not been determined, the measured values cannot be taken as exact values. The high sensitivity and wide concentration range over which primary transcript was determined should also result in considerable variations, as the accuracy of the assay depends on the exact quantitation of RNA and internal standard and large dilution factors. Nevertheless, it is clear that the gene is transcribed at very high rates until day 5. Because of the above mentioned errors, the differences between 2 and 5 day old insects might not be significant. Hence, it can be assumed that the FABP gene is activated during this period and expressed at a very high level. Soon afterwards, however, the transcription of the gene is reduced to a very low level, which presumably is sufficient to maintain the stable mRNA content found in insects older than two weeks. The relatively low mRNA level, in turn, may be required to maintain the FABP levels of 18 % of all cytosolic proteins. While the observed changes in FABP pre-mRNA clearly show that FABP expression is regulated at the transcriptional level, it is

worthwhile to analyze the accumulated data further, in order to gather insights into the stability of FABP and its mRNA. Computer simulation was used to carry out such an analysis, which is described in the following chapter.

CHAPTER 6: COMPUTER SIMULATION OF M-FABP GENE EXPRESSION DURING LOCUST DEVELOPMENT

6.1. Introduction:

In the previous chapter, the primary transcript of the FABP gene was quantified by a competitive quantitative RT-PCR assay at different times in locust development. As the half-life for RNA processing in the nucleus and its transport into the cytosol is very short (approx. 10 min.), the number of unspliced RNA molecules provide a good measure for the actual transcriptional activity. The data clearly show that the observed pattern of FABP mRNA and protein accumulation during adult development of the locust is a consequence of changes in transcription of the FABP gene. Changes in the number of primary transcript molecules effects changes in mRNA and FABP levels. Analysis of the quantitative connection can give insights into the RNA and protein stability.

Such analysis normally requires numerous data points and a solid background in mathematics, as various differential equations are involved in the mathematical description of these connections. However, in recent years computer simulation has been used increasingly to provide similar answers. Computer simulation enables molecular biologists to take advantage of this powerful, contemporary method for quantitative modeling. Kinetic models can be constructed that are useful for interpreting the data and to investigate the kinetic processes of gene expression and genetic information flow.

One of the most commonly used computer simulation programs is called *System Thinking, Experimental Learning Laboratory with Animation* (STELLA II, High Performance Systems, Hanover, NH). Based on its ease of operation and user friendly interface, STELLA II is a good choice for simulations of genetic information flow and gene expression. If the quantitative relationships have been supplied, the result is a

computer program that immediately permits simulations to be performed. If an appropriate modeling system is set up, the simulation should closely match the experiment results, and enable predictions about the likely outcome of specific changes. In this way, computers provide a new tool for thinking and encourage an understanding of relationships that are not obvious.

The STELLA II program can build models of gene expression. There are four modeling building blocks: stocks; flows, connectors and converters. Stocks are accumulations, such as FABP mRNA and FABP protein. The function of flows is to fill and drain the accumulations, such as pre-mRNA processing and transport, mRNA decay, translation and protein decay. The arrow head indicates the direction of the flow. The function of connector is to connect model elements. Converter functions as a utility, it holds values for constants, defines external inputs to the model, calculates algebraic relationships, and serves as the repository for graphical functions. In general it converts inputs into outputs (STELLA II, High Performance Systems, Hanover, NH).

One of the reasons for modeling is to formulate and test hypotheses by determining whether the experimental results fit with predictions based on current knowledge. In order to construct a model, assumptions are needed. Based on the single-compartment model, and extended to the two-compartment model (Hargrove, 1993), researchers assume that a product is formed at a fixed rate under initial conditions, and is eliminated at a rate that is proportional to its concentration. This assumption is commonly expressed as zero-order synthesis and first-order degradation. The transfer rates between compartments are related to half-lives; the rates of degradation are equivalent to the rate of transfer. The transfer rate can be expressed as $R = 0.693/t_{1/2}$. (R: transfer rate, $t_{1/2}$: half-life). Therefore, as the fraction of a product transferred or eliminated from a compartment per time interval increases, the shorter the half-life becomes, the quicker the system approaches its new equilibrium.

6.2. Material and Methods:

Data of FABP pre-mRNA from flight muscle of developmental locust were obtained with quantitative competitive RT-PCR as described in previous chapters (4.2. and 5.2.). Data of FABP mRNA and protein were derived from Haunerland et al. (1992).

Data were analyzed by computer simulation (Hargrove, 1994) with the Software package STELLA II (version 4.0, High Performance System, Hanover, NH). The single- and two-compartment model of FABP gene expression were constructed, assuming zero-order synthesis and first order decay for mRNA and FABP. mRNA synthesis was treated as a function of the primary transcript concentration measured, and proteins synthesis as a function of the mRNA concentration. The model was defined by the following equations and parameters:

$$\text{FABP}(t) = \text{FABP}(t - dt) + (\text{translation} - \text{fabp decay}) * dt$$

$$\text{initial FABP} = 0$$

$$\text{translation} = \text{mRNA} * 1$$

$$\text{FABP decay} = \text{FABP} * (0.693/34)$$

$$\text{mRNA}(t) = \text{mRNA}(t - dt) + (\text{processing \& transport} - \text{mRNA decay}) * dt$$

$$\text{initial mRNA} = 0$$

$$\text{processing \& transport} = \text{pre-mRNA} * 1$$

$$\text{mRNA decay} = \text{mRNA} * (0.693/2.3)$$

$$\text{processing \& transport} = \text{pre-mRNA}/(\text{pre-mRNA}+0.2)$$

$$\begin{aligned} \text{mRNA} = & 2.8 + \text{STEP}(7,0.5) + \text{STEP}(13.8,1) + \text{STEP}(33.4,2) + \text{STEP}(17,3) + \\ & \text{STEP}(12,4) + \text{STEP}(7.8,5) + \text{STEP}(6.2,7) + \text{STEP}(-5.8,9) + \text{STEP}(-7.5,11) + \\ & \text{STEP}(-32.8,13) + \text{STEP}(-40.9,15) + \text{STEP}(5,17) + \text{STEP}(1.3,19) \end{aligned}$$

pre-mRNA = 0+STEP(1.397,1)+STEP(20.346,2)+STEP(48.319,3)+
STEP(29.938,5)-STEP(86.492,6)-STEP(12.632,7)-STEP(0.558,8)-
STEP(0.122,10)-STEP(0.136,12)-STEP(0.04,15)-STEP(0.035,20)

pre-mRNA = 100-STEP(38.4,10)-STEP(42.8,12)-STEP(10,15)

FABP half-life = 34 days.

FABP mRNA half-life = 2.3 days

K_m = 0.2 %

6.3. Results:

As no kinetics were measured in this thesis, the absolute values for synthesis and breakdown cannot be calculated. Nevertheless, it should be possible to determine the quantitative relation between synthesis and breakdown, and relative changes during development. To analyze the quantitative connections between pre-mRNA, mRNA, and FABP, all data were expressed relative to the maximal value encountered. Pre-mRNA was maximal at day 5 (100 % = 520,000 copies/ng total RNA), mRNA peaked at day 8 (100 % = the FABP mRNA/actin mRNA ratio determined at day 8), while FABP reached its maximal value after day 15 (100 % = 18 % of total cytosolic proteins).

6.3.1. Determination of protein stability:

Assuming a linear relationship between mRNA and FABP, the stable level obtained after day 15 can be maintained with a relative mRNA concentration of approximately 15 % of the maximal value. In contrast, maximum synthesis of FABP is seen at day 8, when the mRNA concentration is maximal. As mRNA = 100 % causes

synthesis of more than 15 % of the maximal FABP concentration/day (difference between day 8 and day 10), the mRNA after day 15 should be sufficient for the synthesis of only one seventh of the FABP synthesis found between day 8 and day 10, i.e. around FABP = 2 % of maximum. Since only 2 % of the total FABP are synthesized in order to maintain the maximal value; the breakdown should be approximately 2 %, which is equivalent to a half-life of around 34 days ($0.693/0.02$). This initial calculation, however, does not include the breakdown rate in estimating FABP synthesis.

The equations that describe both synthesis and breakdown are:

$$\text{FABP synthesis: } d\text{FABP}/dt = a * \text{mRNA} \quad (\text{Eq. 6.1})$$

$$\text{FABP breakdown: } -d\text{FABP}/dt = b * \text{FABP} \quad (\text{Eq. 6.2})$$

where a and b are constant factors, describing synthesis and breakdown rate, respectively. The value for a is irrelevant, as only relative changes are considered. The only parameter that can be varied is the breakdown rate b.

A simple one compartment model was constructed that describes these connections (Fig. 6-1).

Using the measured relative mRNA values, computer simulation was carried out from this model. The best correlation between the simulated and the previously measured FABP values were obtained for a breakdown rate of 2 %/day, a value equivalent to a protein half-life of 34 days (Fig. 6-2).

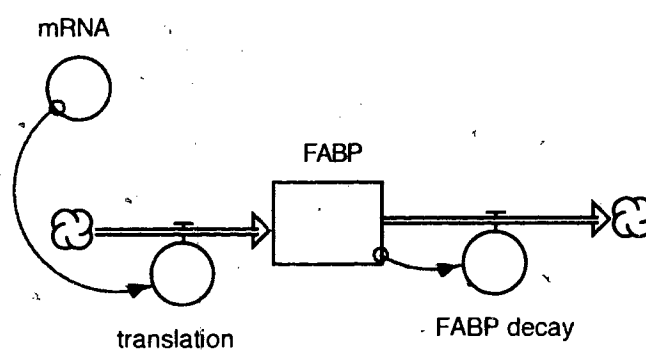


Fig. 6-1: Simulation of FABP translation.

Single-compartment model of locust flight muscle FABP translation during development with STELLA II simulation program was constructed.

mRNA data acquired from Haunerland et al., 1992. Translation is proportional to mRNA concentrations.

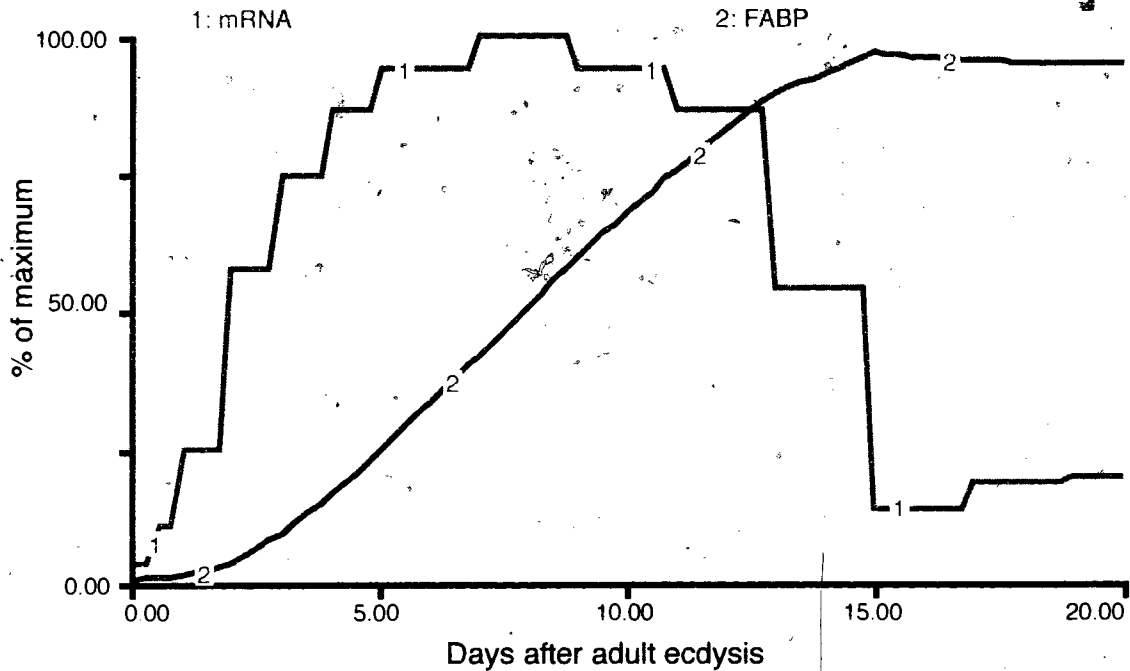


Fig. 6-2: Simulation of FABP translation.

The measured mRNA values during locust development were used in the single-compartment model depicted in Fig. 6-1. The following parameters were used:

$$\text{mRNA} = 2.8 + \text{STEP}(7.0, 5) + \text{STEP}(13.8, 1) + \text{STEP}(33.4, 2) + \text{STEP}(17, 3) + \text{STEP}(12, 4) + \text{STEP}(7.8, 5) + \text{STEP}(6.2, 7) + \text{STEP}(-5.8, 9) + \text{STEP}(-7.5, 11) + \text{STEP}(-32.8, 13) + \text{STEP}(-40.9, 15) + \text{STEP}(5, 17) + \text{STEP}(1.3, 19).$$

$$\text{translation} = \text{mRNA} * 1$$

$$\text{initial FABP concentration} = 0$$

$$\text{FABP decay} = \text{mRNA} * (0.693/34)$$

$$\text{FABP half-life } t_{1/2} = 34 \text{ days}$$

curve 1: mRNA

curve 2: FABP protein

6.3.2. Determination of mRNA stability.

Similar considerations for the relationship between pre-mRNA and mRNA lead to:

$$\text{mRNA synthesis: } \frac{dmRNA}{dt} = c * \text{pre-mRNA} \quad (\text{Eq. 6.3})$$

$$\text{mRNA breakdown: } -\frac{dmRNA}{dt} = d * \text{mRNA} \quad (\text{Eq. 6.4})$$

After day 12, the mRNA value is stable at around 15 %, and pre-mRNA is very low, between 50 and 300 copies (0.01-0.06 %). Considering the inaccuracies of these values, an approximate value of 0.05 % was chosen. If 0.05 % of maximal pre-mRNA can account for replacing the proportion of the constant mRNA value of 15 % that breaks down, then 100 % pre-mRNA should lead to a 2000-times larger synthesis rate. That would be consistent with the observed mRNA pattern only if the mRNA was extremely stable. However, the decline of mRNA between day 12 and 15 suggests that the half-life cannot be much greater than 2 days, as during this period the mRNA values are halved every two days. Moreover, mRNA still increases between day 6 and day 8, although the pre-mRNA values have declined to between 5-20 % of its maximum. It is thus obvious that the relationship between pre-mRNA and mRNA is not linear, at least not over the entire 20 days.

At very high pre-mRNA concentrations, saturation of pre-mRNA processing and mRNA trans-nuclear envelope transport may occur, leading to a non-linear relationship. However, at low concentrations equation 6.3 should still be valid. As the mRNA concentration does not appear to change significantly around day 8, it can be assumed that the pre-mRNA at that time (2000 molecules/ng, or 0.4 % of the maximal levels) is approximately what is needed to counter mRNA breakdown. Hence, a simple one compartment model was constructed to cover only the period after day 8 (Fig. 6-3). In

addition to equations 6.3 and 6.4, it was assumed that before day 8 mRNA was constant at 100 %, and pre-mRNA was also constant at the same value as found at day 8 (which was, for this model, assumed as 100 %). Since under those conditions the amount of mRNA produced is exactly what is needed to replace decaying mRNA, the model can be used to determine the half-life of mRNA.

The simulation was carried out for various breakdown rates, until an optimal fit between the simulated and the measured values for RNA after day 8 was obtained (Fig. 6-4).

A good match between the measured and simulated data was obtained for a mRNA breakdown rate of 30 %/day. Since

$$\text{breakdown rate} = 0.693/t_{1/2},$$

the half life of mRNA is approximately 2.3 days.

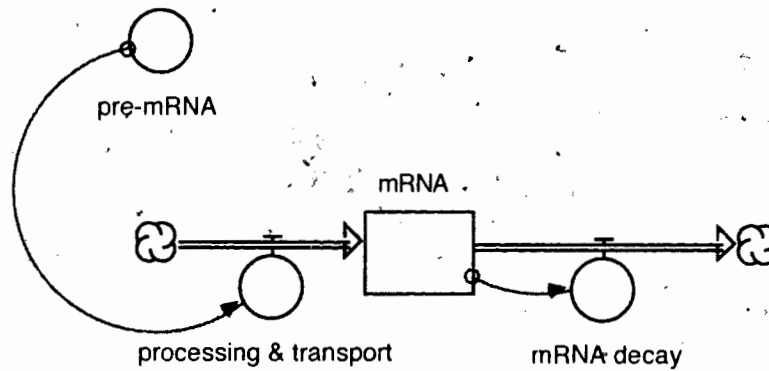


Fig. 6-3: Estimation of FABP mRNA half-life.

Single-compartment model of locust flight muscle FABP mRNA synthesis during development with STELLA II simulation program was constructed.

pre-mRNA: pre-mRNA values from day 8 to day 20 were used in the model.

mRNA synthesis is the function of transcription and processing and transport.

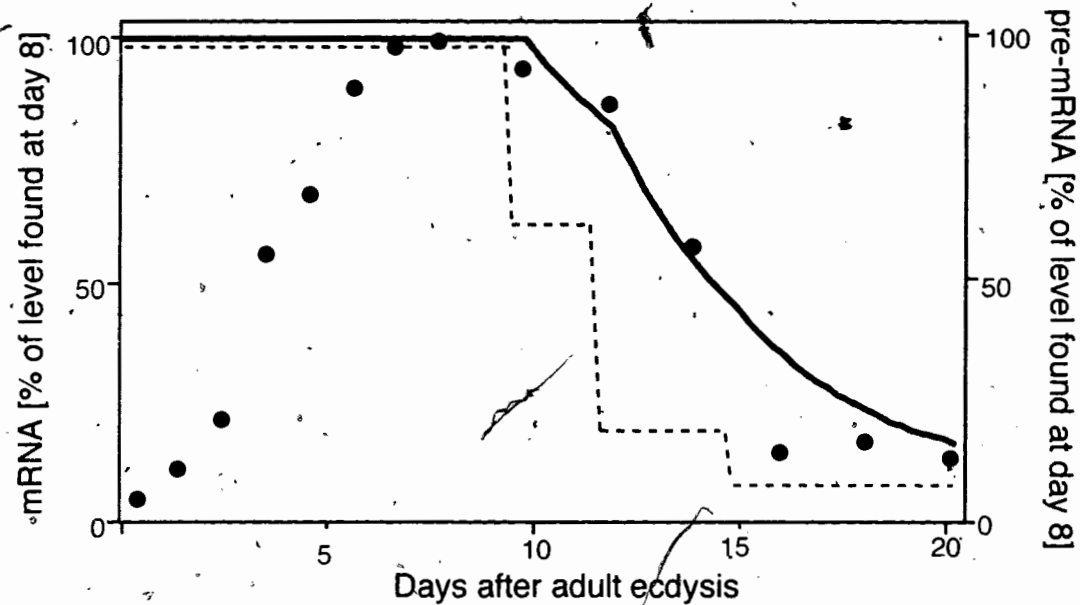


Fig. 6-4: Estimation of FABP mRNA half-life.

The measured pre-mRNA values from day 8 to day 20 during locust development were used in the single-compartment model depicted in Fig. 6-3. The following parameters were used:

$$\text{pre-mRNA} = 100 - \text{STEP}(38.4, 10) - \text{STEP}(42.8, 12) - \text{STEP}(10, 15)$$

$$\text{processing \& transport} = \text{pre-mRNA} * 1$$

$$\text{initial mRNA concentration} = 100$$

$$\text{mRNA decay} = \text{mRNA} * (0.693/2.3)$$

$$\text{mRNA half-life } t_{1/2} = 2.3 \text{ days}$$

● mRNA values from Haunerland et al. (1992)

----- pre-mRNA values used for computer simulation

———— mRNA values from computer simulation

6.3.3. Complete simulation of mRNA synthesis:

As mentioned before, substrate saturation may occur when pre-mRNA is present in large amounts. While many enzyme reactions and the transport out of the nucleus into the cytosol are involved in the conversion from pre-mRNA to mRNA, for the purpose of this simulation these can be all considered as one process. Processing and transport involve enzymatic reactions that should behave according to normal enzyme kinetics, that are described by the Michaelis-Menten equation:

$$V = V_{\max} \frac{[S]}{[S] + K_M} \quad (\text{Eq. 6.5})$$

where

V	=	reaction rate;
V_{\max}	=	maximal reaction rate
$[S]$	=	substrate concentration
K_M	=	Michaelis constant.

Adapted for the synthesis of mRNA, this equation becomes

$$d \text{ mRNA}/dt = V_{\max} \frac{[\text{pre-mRNA}]}{[\text{pre-mRNA}] + K_M} \quad (\text{Eq. 6.6})$$

Since no absolute values were measured, but all results were normalized against the maximal value, the factor V_{\max} is irrelevant. Hence, a simplified model was constructed based on the equation

$$d \text{ mRNA}/dt = \frac{[\text{pre-mRNA}]}{[\text{pre-mRNA}] + K_M} \quad (\text{Eq. 6.7})$$

The two-compartment model describing mRNA and FABP synthesis that was used for the simulation is shown in Fig. 6-5. As mRNA and protein stability have been estimated before (mRNA: ($t_{1/2} = 2.3$ days), chapter 6.3.2; FABP: ($t_{1/2} = 34$ days), chapter 6.3.1), only K_M was unknown. Optimal match between the measured data and the simulated values was obtained for a K_M value of 0.2 %. This means that at the concentration of 1030 copies of pre-mRNA/ng of total RNA (0.2 % of the maximal value of 514,000 found on day 5), the mRNA synthesis/export rate is half of the maximal rate. As the pre-mRNA concentration increases, the mRNA synthesis rate approaches a maximum, while at lower pre-mRNA concentration, the synthesis of mRNA is almost proportional to the amount of pre-mRNA present (Fig. 6-6).

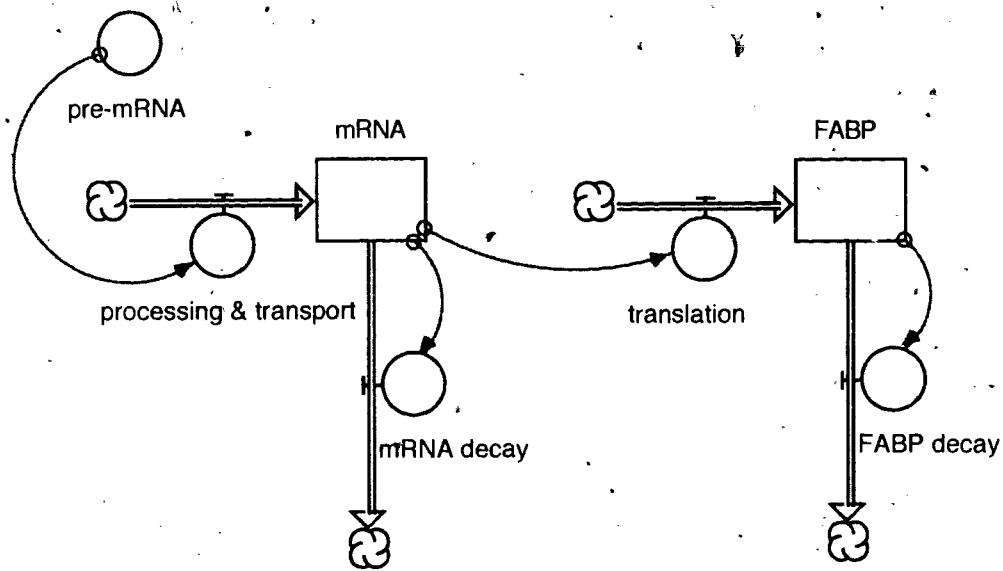


Fig. 6-5: Two-compartment model of FABP expression.

The complete process of simulation model of locust flight muscle FABP synthesis during development with STELLA II simulation program was constructed.

pre-mRNA: pre-mRNA values from nymph to day 20 adult were used in the model.

mRNA synthesis is the function of transcription and processing and transport.

FABP synthesis is the function of mRNA concentration.

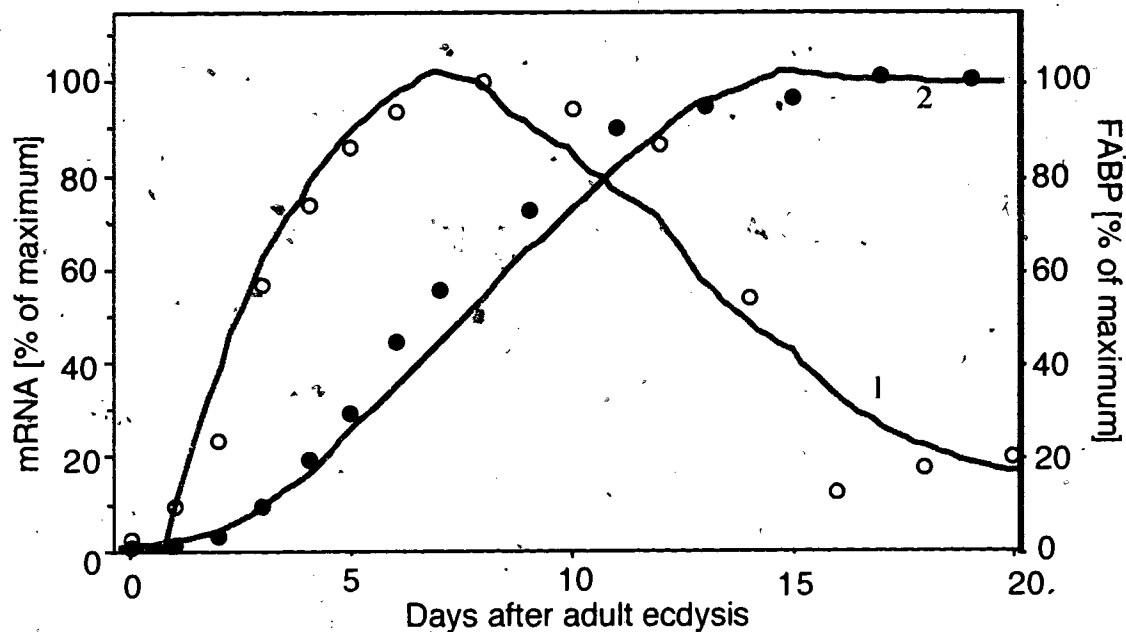


Fig. 6-6: Simulation of FABP expression.

The complete process of FABP expression was simulated with model shown in Fig. 6-5. The following parameters were used:

pre-mRNA = 0+STEP(1.397,1)+STEP(20.346,2)+STEP(48.319,3)+
STEP(29.938,5)-STEP(86.492,6)-STEP(12.632,7)-STEP(0.558,8)-STEP(0.122,10)-
STEP(0.136,12)-STEP(0.04,15)-STEP(0.035,20)

processing & transport = pre-mRNA/(pre-mRNA+0.2)

initial mRNA concentration = 0

mRNA decay = mRNA * (0.693/2.3)

mRNA half-life $t_{1/2}$ = 2.3 days

initial FABP concentration = 0

translation = mRNA * 1

FABP decay = FABP * (0.693/34)

FABP half-life $t_{1/2}$ = 34 days

curve 1: mRNA from simulation

curve 2: FABP from simulation

○ mRNA values from Haunerland et al., 1992

● FABP values from Haunerland et al., 1992

6.4. Discussion:

In order to investigate the interrelationship between primary transcript, mRNA, and FABP, models of FABP gene expression were constructed and the mRNA and FABP accumulation was analyzed by computer simulation. The rate of FABP translation appears to be proportional to the amount of mRNA present. Assuming that the low mRNA level present in fully grown, mature adults is sufficient for the replacement of decaying FABP, the half-life of FABP can be estimated to be 34 days. Hence, locust FABP is an extraordinary stable protein, a fact that is advantageous for maintaining the very high FABP levels found in fully differentiated flight muscles. FABP levels increase from 0 to 18 % of the total cytosolic proteins after FABP expression is turned on in adult locusts. The FABP concentration finally reaches a new steady state, where the gene is expressed at a rate needed to counteract FABP breakdown. Under steady state conditions of gene expression, the concentration a protein reaches in the cell depends only on its stability. Therefore, if the FABP gene was expressed always at the very low rate seen in insects older than 2 weeks, ultimately the FABP concentration would reach the same maximal value. However, since it takes approximately 5 times the half-life to establish a new steady state, this level would be reached only after almost half a year. It is obvious that with the long half-life of locust M-FABP and the relatively short life time of the animals a rapid increase in FABP can only be achieved through transient, high levels of expression. Through the rapid accumulation of much larger concentrations of mRNA, the final FABP concentration is reached within 2 weeks. At that time, however, the mRNA concentration must be reduced to the maintenance level.

Mammalian FABP genes, however, do not appear to be similarly controlled. In rat heart muscle, for example, the FABP concentration does increase during development,

from 1.2 mg/g cytosolic protein in neonatal heart to 5.7 mg/g protein in adults (van Nieuwenhoven, et al., 1995). This increase is the consequence of altered mRNA concentrations, that increase at the same time to a new steady state level. While the half-life of mammalian FABP is not known, the period to reach a new steady state should be small when compared with the life span of the animal. However, similar transient increases in gene expression have been observed in mammalian liver. For example, 3-hydroxy-3-methylglutaryl coenzyme A reductase (HMG-CoA reductase), its gene expression has been observed to increase the concentration up to 200-fold. It has been speculated that an "overshoot" of gene expression is necessary to assure a rapid change around birth (Hargrove, 1994).

The variations in FABP mRNA are clearly a consequence of dramatic changes in the expression of the FABP gene. Indeed, the number of primary transcript molecules measured from day 2 to day 6 of adult life is extremely high. The synthesis rate of mRNA is half-maximal at day 10 when the pre-mRNA concentration (1010 copies/ng RNA, see chapter 5) is similar to the K_M . From the simulation, the maximal rate is achieved between day 1 and 6, when pre-mRNA is at least 100-fold higher. Obviously, a vast overshoot in the transcription of the FABP gene occurs at the earlier days, as a huge excess of pre-mRNA is produced here. It should be interesting to study the details of the induction of the locust FABP gene once the upstream regions of this gene have been cloned, and to understand the reasons for these phenomena.

The results obtained in this chapter provide a plausible explanation for the observed changes in FABP gene expression. However, the fact that the simulation leads to results that are similar to the measured data does not prove that the current model is correct, as several assumptions have been made in the construction of the model. Least controversial is probably the linear relationship between mRNA and translation, which has been found for many other proteins. Much less quantitative data exist that link

expression rates with mRNA concentrations, but normally investigators also assume a simple first order relationship. In the case of locust muscle FABP, this relationship is unlikely to exist, because the observed pre-mRNA concentration reaches extremely high levels. At day 5, FABP pre-mRNA may account for as much as 0.2 % of all cellular RNA (Chapter 5.3), including all transcripts and the vast amounts of ribosomal RNA present in the cytosol. The half-life of nuclear transcripts is always very short, and many nucleases appear to be present that rapidly destroy these molecules. Although the processing and transport of mRNA is also rapid, the high primary transcript number may exceed the capacity of splicing enzymes and transport mechanisms. While the transport mechanisms are not very well understood, mRNA has to pass through nuclear pores in order to enter the cytosol, and these may limit the transport rate at high concentrations.

The proposed model does not take changes in stability of either pre-mRNA or mRNA into account. Such changes have been observed for other proteins, such as histone (Ross, 1988; Senshu and Ohashi, 1979; Ross and Kobs, 1986, Peltz and Ross, 1987), and it is possible that they occur in the locust muscle as well. However, stability changes alone cannot explain the observed data, unless multiple changes and extremely unlikely values are assumed. In contrast, the half-lives of mRNA and protein found here, while certainly long, are not unrealistic. These characteristics may be associated with the functions of FABP as free fatty acid transporter, as locusts need large amounts of FABP to acquire the ability to fly long distances throughout their adult life. FABP's functions in locust flight muscle are comparable to hemoglobin, the oxygen transporter in mammalian blood. Hemoglobin is also a very stable protein. In murine erythroleukemia cells, hemoglobin mRNA can accumulate to values as high as 90 % of total cellular mRNA, or 1-2 % of the total RNA (total mRNA accounts normally for less than 2 % of the total RNA). This high level can only be achieved from the relative stability of globulin mRNA, with a half-life of about 50 hours, and hemoglobin itself, which is stable in

mature blood cells (Hargrove and Schmidt, 1989; Krowczynska et al, 1985; Ganguly and Skoultchi, 1985; Ross and Sullivan, 1985; Bastos and Aviv, 1977). Hence, the stability of FABP and its mRNA are not without a precedent, and is certainly advantageous from a physiological standpoint.

Although the experimental data can be simulated with the models constructed here, the match between theoretical and experimental data is not always perfect. This may be a consequence of the small number of data points and the relatively large error, as discussed earlier (chapter 4.3). Hence, the parameters found for protein and mRNA stability and the K_M value for the processing and transport of mRNA are inaccurate. Experiments can now be designed to test and refine this model. Moreover, the model can be used as a starting point to simulate the changes in FABP expression in response to flight activity and increased lipid delivery, as reported by Chen and Haunerland (1994). Such studies on insect and mammalian muscle may provide further insights into the mechanisms that regulate muscle FABP gene expression.

CHAPTER 7: GENERAL DISCUSSION

Muscles that are engaged in endurance activities normally depend on fatty acids as an energy resource. Fatty acids are the preferred substrate for the continuously beating heart muscle of vertebrates, but also for flight muscles of migratory birds and insects, which encounter very high metabolic rates during migratory flight (Crabtree and Newsholme, 1975). The intracellular fatty acid transport is mediated by FABP, and its concentration seems to reflect the metabolic capacity of a muscle. In rat heart, for which a fatty acid oxidation rate of $0.3 \mu\text{mol}/\text{min.g}$ intact muscle has been reported, nearly 6 % of all cytosolic proteins is FABP, while in flight muscle of the migratory birds (metabolic rate = $0.6 \mu\text{mol}/\text{min.g}$ intact muscle) the FABP concentration is twice as high, about 12 % of the cytosolic protein. Locust flight muscle, with an even higher metabolic rate ($0.9 \mu\text{mol}/\text{min.g}$ intact muscle), possesses the highest FABP concentration found in any organism; FABP comprises more than 18 % of soluble total cytosolic proteins (Hauerland et al., 1992).

Locust flight muscle FABP is a truly adult specific protein. As immature locust nymphs have no wings, their mesothorax muscles are not used for flight activity, which becomes possible several days after adult ecdysis. Neither FABP nor its mRNA is detectable in nymphs. During the first two weeks of adult life, the FABP concentration gradually increases from zero to 18 % of total cytosolic protein, and this high level is kept for the entire adult life. Its mRNA concentration rapidly peaks after one week and declines rapidly during the second week; afterwards it is present only at very low levels. This developmental pattern indicates that FABP expression in locust flight muscle is effectively regulated.

There are many possibilities how the concentration of a protein in a cell can be regulated. Regulation can occur at each of the steps involved from the transcription of the

gene to the final breakdown of the translation product. For locust FABP, the mRNA concentration changes dramatically during development, indicating that the regulation of FABP expression occurs at the level of transcription or mRNA stability. Altered transcription is the most common mechanism to change mRNA concentrations, but it is also possible that the gene transcription occurs at a constant level, and that the observed rise and decline in mRNA levels is the consequence of altered mRNA stability. To decide whether altered gene transcription is responsible for the observed changes in FABP mRNA, it is necessary to measure the level of transcription at different times in development.

The goal of this thesis was to determine whether the developmental differences in FABP expression are caused by changes in the transcription of the FABP gene. The *in vitro* nuclear run-on assay is the most direct way to measure the ongoing rates of transcription of a gene, but experimental difficulties frequently limit its usefulness. Initially, it was attempted to measure FABP expression with a nuclear run-on assay in locust flight muscles. Nuclei were isolated by density gradient centrifugation techniques from flight muscles. They appeared to be intact, as seen by electron microscope, but the yield was relatively small, which further complicates reliable run-on assays. It was hoped that the high levels of FABP gene expression would compensate for the low yield of nuclei, but this proved not to be the case. Many run-on experiments carried out under a variety of conditions failed to give reliable results, and therefore an alternative technique was thought to measure the expression of the FABP gene.

Immediately following transcription, the primary transcript is rapidly processed within the nucleus, by capping the 5' end, splicing out the intron sequences and adding a poly A tail. The resulting nuclear mRNA is then released as mature mRNA into the cytosol. Because of the short half-life of primary transcripts, their concentrations reflect an

equilibrium between transcription and post-transcription processes. Hence, the amount of primary transcript can be used to determine relative rates of gene expression.

Because of the small levels of primary transcripts present in the nucleus, classical hybridization techniques are not sensitive enough for such measurements. It should be possible, however, to measure such low levels with PCR-based techniques. As unspliced primary transcripts contain not only the sequence of the expressed proteins but also introns, reverse transcription PCR with primers specific for introns of the gene in question can be used to amplify only unprocessed transcripts.

In this thesis, a reverse transcription PCR technique was developed for the quantification of flight muscle FABP primary transcript. Since PCR amplification is an exponential process, the amount of the PCR product is not linearly related to the number of template molecules. Many different techniques that have been reported to determine the number of template molecules from the PCR product. Competitive PCR with an internal standard was chosen in this thesis, in which known amounts of a standard RNA was added to a constant amount of total RNA containing the target primary transcript. As target and standard compete for the same primers, the ratio of band intensities was used to determine the number of target molecules present in the sample. This technique worked very well over a wide concentration range, allowing measurement of as few as 1000 copies of pre-mRNA in 3 μ g of total RNA, or as many as 500,000 copies in one ng of total RNA. Hence, it was used to measure pre-mRNA changes during adult locust development.

The data obtained indicate that FABP pre-mRNA was not expressed at a detectable level before the final ecdysis, as suspected from the reported mRNA and FABP levels. Immediately after adult metamorphosis, within a few hours, the FABP primary transcript became detectable, although at a low level of about 100 copies per ng total RNA. From day 2 to day 5 the expression is extremely high, at up to more than 10^5 pre-mRNA molecules per ng total RNA. This suggests a delay in the full activation of FABP transcription,

possibly due to the need to synthesize other factors required for the full activation of the gene. After day 5, the transcription level drops rapidly, finally reaching the low level of 10^2 copies/ng total RNA level.

The dramatic changes in the pre-mRNA are consistent with the observed levels of mRNA and protein. mRNA steadily increased between day 2 and day 8, before it drops gradually to a constant low level reached after day 15. FABP protein increases slowly between day 2 and day 15, where it reaches very high, stable high level (18 % of total cytosolic protein).

In order to get an insight into the kinetic interrelationship between the components on FABP expression, a computer simulation model was constructed. First a single-compartment model was used, which only includes FABP translation and protein degradation. The translation was assumed proportional to mRNA concentration. The simulation matched the experimental data best for the FABP half-life of 34 days. As protein stability ultimately determines the intracellular concentration of a protein, a protein that is present in an extremely large concentration should be expected to be very stable. Indeed, other proteins present in large amounts, such as hemoglobin, are known to be stable. Based on these result, a separate model was used to estimate the mRNA half-life, which was found to be approx. 2.3 days. While most mRNAs have considerably shorter half-lives, mRNAs encoding abundant, stable proteins are generally more stable (Hargrove, 1994).

Using the estimates for protein and mRNA stability, a two compartment model was constructed to simulate the entire process of FABP synthesis starting from the measured pre-mRNA concentrations. The mRNA concentration in the cell depends on mRNA synthesis and mRNA decay, as defined by its half-life. However, the simulation showed clearly that mRNA synthesis is not a linear function of pre-mRNA. Instead, good agreement between measured pre-mRNA and mRNA levels were found when assuming

non-linear, Michaelis-Menten kinetics. This assumption seems to be justified, as enzymatic reactions are involved in the processing of pre-mRNA, and the nuclear concentration of FABP pre-mRNA can reach extreme values. It hence is likely that at high substrate concentrations these enzymes are saturated.

It is interesting to note that FABP transcription is leading to a huge excess of pre-mRNA, obviously much more than what can be processed. While it may seem wasteful for a cell to grossly overproduce mRNA, this may be the consequence of the mechanisms that control FABP gene expression. Currently, little is known about how FABP expression is controlled. It has been shown (Chen et al., 1993) that FABP is never expressed in nymphs, but always expressed in adults. The gene, that may be transcribed at a basal level at all times in adult insects, possibly can be activated to a level of very high transcriptional rates at certain developmental periods, as demonstrated here. The activated gene is transcribed at very high levels, indicating that the FABP gene has a very strong promoter that can be efficiently regulated.

The gene is also induced in response to physiological stimuli. Chen and Haunerland (1994) demonstrated that flight and increased lipid delivery lead to a rapid increase in mRNA levels. Using the RT-PCR technique developed in this thesis it should now be possible to determine whether this activation is due to increased transcription. Accurate measurements of pre-mRNA changes in response to changing lipid delivery can be carried out, and this may lead to a better understanding whether and how fatty acids control the expression of FABP.

Detailed studies of the kinetics of FABP expression in response to increased extracellular fatty acid supply may not be possible in living locusts, but may require suspensions of isolated myocytes. The very sensitive transcription assay developed here appears to be well suited for such studies, as only minute amounts of cellular material are

required for the analysis. Data can be analyzed if such experiments could be carried out with computer simulation, using a model modified from the one developed here.

While present at much lower concentrations, FABP from mammalian heart muscle may be under similar control mechanisms. Its synthesis increases similarly in response to exercise or elevated lipid supply. Mammalian muscle FABP and its mRNA also increase during development, but only up to 3 fold over a period of several weeks. In contrast, locust mRNA increases more than 100 fold during the first week of adulthood. As the large concentration of FABP is needed for migratory flight, it is important to reach the final FABP concentration as soon as possible. This rapid rise and subsequent decline to about 15 % of its maximal mRNA value assures that the maximal FABP level is reached within two weeks. Apparently, a similar overshoot in FABP expression as observed for the locust is not necessary in mammals.

Quantitative measurements of FABP transcription has only been done in undifferentiated muscle cell lines. The technique used in this study should provide useful methodology for the measurement of transcription rates in differentiated mammalian muscle as well, particularly in response to exercise, other physiological stimuli, or even under pathological conditions. Thus, the current thesis provides new methodologies that should be useful to better understand the control of FABP expression and its function in health and disease.

REFERENCES

- Ando, S., Xue, X-H, Tibbits, G.F., and Haunerland, N.H. (1997) Cloning and sequencing of complementary DNA for fatty acid binding protein from rainbow trout heart. *Comp. Biochem. Physiol.*, in press
- Auboeuf, D., and Vidal, H. (1997) The use of the reverse transcription-competitive polymerase chain reaction to investigate the in vivo regulation of gene expression in small tissue samples. *Anal. Biochem.* **245**, 141-148
- Banaszak, L., Winter, N., Xu, Z., Bernlohr, D.A., Cowan, S., and Jones, T.A. (1994) Lipid-binding proteins: a family of fatty acid and retinoid transport proteins. *Adv. Protein Chem.* **45**, 89-151
- Bass, N.M. (1988) The cellular fatty acid binding proteins: aspects of structure, regulation, and function. *Int. Rev. Cytol.* **111**, 148-184
- Bass, N.M., and Manning, J.A. (1986) Tissue expression of three structurally different fatty acid binding proteins from rat heart muscle, liver and intestine. *Biochem. Biophys. Res. Commun.* **137**, 929-935
- Bastos, R.N., and Aviv, H. (1977) Theoretical analysis of a model for globin messenger RNA accumulation during erythropoiesis. *J. Mol. Biol.* **110**, 205-218
- Becker-Andre, M., and Hahlbroek, K. (1989) Absolute mRNA quantification using the polymerase chain reaction (PCR). A novel approach by a PCR aided transcript titration assay (PATTY). *Nucl. Acids Res.* **17**, 9437-9446
- Beenackers, A.M.Th., Van der Horst, D.J., and Van Marrewijk, W.J.A. (1985) Biochemical processes directed to flight metabolism. In: *Comprehensive Insect Biochemistry, Physiology, and Pharmacology* (Gilbert, L.I., and Kerkut, G., eds.) vol. 10, Pergamon, New York, pp. 451-486
- Bentley, D.L., and Groudine, M. (1986) A block to elongation is largely responsible for decreased transcription of *c-myc* in differentiated HL60 cells. *Nature* **321**, 702-706
- Carey, J.O., Neuffer, P.D., Farrar, R.P., Veerkamp, J.H., and Dohm, G.L. (1994) Transcriptional regulation of muscle fatty acid binding protein. *Biochem. J.* **298**, 613-617
- Casey, T.M. (1989) Oxygen consumption during flight. In: *Insect flight* (Goldsworthy, G.J. and Wheeler, C.H., ed.) CRC Press, Inc., 257-272
- Celano, P., Berchtold, C., and Casero, R.A. Jr. (1989) A simplification of the nuclear run-off transcription assay. *BioTechniques* **7**, 942-943
- Celi, F.S., Zenilman, M.E., and Shuldiner, A.R. (1993) A rapid and versatile method to synthesize internal standards for competitive PCR. *Nucl. Acids Res.* **21**, 1047

- Chelly, J., Kaplan, J.C., Maire, P., Gautron, S., and Kahn, A. (1988) Transcription of the dystrophin gene in human muscle and non-muscle tissue. *Nature* **333**, 858-860
- Chelly, J., Montarras, D., Pinset, C., Berwald-Netter, Y., Kaplan, J.C., and Kahn, A. (1990) Quantitative estimation of minor mRNAs by cDNA-polymerase chain reaction. Application to dystrophin mRNA in cultures myogenic and brain cells. *Eur. J. Biochem.* **187**, 691-698
- Chen, X., and Haunerland, N.H. (1994) Fatty acid binding protein expression in locust flight muscle: Induction by flight, adipokinetic hormone, and low density lipophorin. *Insect Biochem. Mol. Biol.* **24**, 573-579
- Chen, X., Wang, Z., and Haunerland, N.H. (1993) Flight muscle fatty acid binding protein synthesis in juvenile and adult forms of the desert locust, *Schistocerca gregaria*. *Insect Biochem. Molec. Biol.* **23**, 337-343
- Chino, H. (1985) Lipid transport, In: *Comprehensive Insect Physiology, Biochemistry, and Pharmacology* (Gilbert, L.I., and Kerkut, G., eds.) vol. 10, Pergamon, New York, pp. 115-135
- Chino, H., and Kitazawa, K. (1981) Diacylglycerol carrying lipoprotein of haemolymph of the locust and some insects. *J. Lipid Res.* **22**, 1042-1052
- Chomczynski, P., and Sacchi, N. (1987) Single step method of RNA isolation by acid guanidinium thiocyanate-phenol-chloroform extraction. *Anal. Biochem.* **162**, 156-159
- Cornelius, P., Marlowe, M., Lee, M.D., and Pekala, P.H. (1990) The growth factor-like effects of tumor necrosis factor-alpha. Stimulation of glucose transport activity and induction of glucose transporter and immediate early gene expression in 3T3-L1 preadipocytes. *J. Biol. Chem.* **265**, 20506-20516
- Crabtree, B., and Newsholme, E.A. (1975) Comparative aspects of fuel utilization and metabolism by muscle. In: *Insect Muscle* (Usherwood, P.N.R., ed.), Academic Press, London, pp. 405-491
- Crisman, T.S., Claffey, K.P., Saouaf, R., Hanspal, J., and Brecher, P. (1987) Measurement of rat heart fatty acid binding protein by ELISA. Tissue distribution, developmental changes and subcellular distribution. *Mol. Cell. Cardiol.* **19**, 423-431
- David, J.D., Fredrickson, R.L., and Peterson, G.R. (1978) Isolation and purification of myotube and myoblast nuclei from cultures of embryonic chick skeletal muscle. *Exp. Cell Res.* **117**, 63-70
- Dignam, J.D., Lebovitz, R.M., and Roeder, R.G. (1983) Accurate transcription initiation by RNA polymerase II in a soluble extract from isolated mammalian nuclei. *Nucl. Acids Res.* **11**, 1475-1489
- Downer, R.G.H., and Chino, H. (1985) Turnover of protein and diacylglycerol components of lipophorin in insect haemolymph. *Insect Biochem.* **15**, 627-630

- Edelman, J.C., Edelman, P.M., Knigge, K.M., and Schwartz, I.L. (1965) Isolation of skeletal muscle nuclei. *J. Cell Biol.* **27**, 365-378
- Elder, H.Y. (1975) In: Insect muscle (Usherwood, P.N.R., ed) Academic Press, New York, pp. 1-74
- Elferink, C.J., and Reiners, J.J., Jr. (1996) Quantitative RT-PCR on CYP1A1 heterogeneous nuclear RNA: a surrogate for the in vitro transcription run-on assay. *BioTechniques* **20**, 470-477
- Fournier, N.C., Geoffrey, M., and Deshusses, J. (1978) Purification and characterization of a long chain fatty acid binding protein supplying the mitochondrial β -oxidation system in the heart. *Biochim. Biophys. Acta* **533**, 457-464
- Ganguly, S., and Skoultchi, A.I. (1985) Absolute rates of globin gene transcription and mRNA formation during differentiation of cultured mouse erythroleukemia cells. *J. Biol. Chem.* **260**, 12167-12173
- Gilliland, G., Perrin, S., Blanchard, K., and Bunn, F.F. (1990) Analysis of cytokine mRNA and DNA: Detection and quantitation by competitive polymerase chain reaction. *Proc Natl. Acad. Sci. USA* **87**, 2725-2729
- Goldsworthy, G.H. (1983) The endocrine control of flight metabolism in locusts. In: *Advances in Insect Physiology*, vol. 17 (Berridge, M.J., Treherne, J.E., and Wigglesworth, V.B., eds.), Academic Press, New York, pp. 149-204
- Gondim, K.C., Atella, G.C., Kawooya, J.H., and Masuda, H. (1992) Role of phospholipids in the lipophorin particles of *Rhodnius prolixus*. *Arch. Insect Biochem. Physiol.* **20**, 303-314
- Gorski, K., Carneiro, M., and Schibler, U. (1986) Tissue-specific in vitro transcription from the mouse albumin promoter. *Cell* **47**, 767-776
- Guglielmo, C.G., Haunerland, N.H., and Williams, T.D. (1998) Fatty acid binding protein, a major protein in the flight muscle migrating Western Sandpipers. *Comp. Biochem. Physiol.*, in press
- Hahn, C.G., and Covault, J. (1990) Isolation of transcriptionally active nuclei from striated muscle using percoll density gradients. *Anal. Biochem.* **190**, 193-197
- Hargrove, J.L. (1993) Microcomputer-assisted kinetic modeling of mammalian gene expression. *FASEB J.* **7**, 1163-1170
- Hargrove, J.L. (1994) Kinetic modeling of gene expression. R.G. Landes, Austin
- Hargrove, J.L., and Schmidt, F.H. (1989) The role of mRNA and protein stability in gene expression. *FASEB J.* **3**, 2360-2370
- Haunerland, N.H. (1997) Transport and utilization of lipids in insect flight muscles. *Comp. Biochem. Physiol.* **117B**, 475-482

- Hauerland, N.H., and Chisholm, J.M. (1990) Fatty acid binding protein in flight muscle of the locust, *Schistocerca gregaria*. *Biochim. Biophys. Acta* **1047**, 233-238
- Hauerland, N.H., Andolfatto, P., Chisholm, J.M., Wang, Z, and Chen, X. (1992) Fatty-acid-binding protein in locust flight muscle, Developmental changes of expression, concentration and intracellular distribution. *Eur. J. Biochem.* **210**, 1045-1051
- Heer, A.H., Keyszer, G.M., Gay, R.E., and Gay, S. (1994) Inhibition of RNA polymerase by Digoxigenin-labeled UTP. *BioTechniques* **16**, 54-55
- Heintz, N., Sive, H.L., and Roeder, R.G. (1983) Regulation of human histone gene expression: kinetics of accumulation and changes in the rate of synthesis and in the half-lives of individual histone mRNAs during the HeLa cell cycle. *Mol. Cell. Biol.* **3**, 539-550
- Held, I.R., Rodrigo, R.T., Yeoh, H.C., and Tonaki, H. (1977) Isolation of nuclei from red and white skeletal muscles of the adult rat. *Exp. Cell Res.* **105**, 191-197
- Holtke, H.L., and Kessler, C. (1990) Non radioactive labeling of RNA transcripts in vitro with the hapten digoxigenin (DIG): hybridization and ELISA-based detection. *Nucl. Acids Res.* **18**, 5843-5851
- Jackowski, G., and Liew, C.C., (1980) Fractionation of rat ventricular nuclei. *Biochem. J.* **188**, 363-373
- Jones, P.D., Carne, A., Bass, N.M., and Grigor, M.R. (1988) Isolation and characterization of fatty acid binding protein from mammary tissue of lactating rats. *Biochem. J.* **251**, 919-925
- Jutsum, A.R., and Goldsworthy, G.J. (1976) Fuels for flight in *Locusta*. *J. Insect Physiol.* **22**, 243-249
- Kaufman, M., Simoneau, J.A., Veerkamp, J.H., and Pette, D. (1989) Electrostimulation-induced increases in fatty acid-binding protein and myoglobin in rat fast-twitch muscle and comparison with tissue levels in heart. *FEBS Lett.* **245**, 181-184
- Klebe, R.J., Grant, G.M., Grant, A.M., Garcia, M.A., Giamberti, T.A., and Taylor, G.P. (1996) RT-PCR without RNA isolation. *Biotechniques* **21**, 1094-1100
- Krowczynska, A., Yenofsky, R., and Brawerman, G. (1985) Regulation of messenger RNA stability in mouse erythroleukemia cells. *J. Mol. Biol.* **181**, 231-239
- Linial, M., Gunderson, N., and Groudine, M. (1985) Enhanced transcription of c-myc in bursal lymphoma cells requires continuous protein synthesis. *Science* **230**, 1126-1132
- Manley, J.L., and Gefter, M.L. (1981) Transcription of mammalian genes in vitro. *Gene Amplif. Anal.* **2**, 369-382
- Marzluff, W.F., and Huang, R.U.C.C. (1984) in: Transcription and translation: a practical approach (Hames, D.B., and Higgins, S.F., eds.), IRL Press, Oxford, pp. 89-129

- McCully, J.D., and Liew, C.C. (1988) RNA transcription in myocardial-cell nuclei during postnatal development, the study establishing an assay system for transcription *in vitro*. *Biochem. J.* **256**, 441-445
- McEwen, B.S., and Zigmond, R.E. (1972) Research methods in neurochemistry (Marks, N., and Rodnight, R., eds.) vol. 1, Plenum Press, New York, pp. 139-161
- Mellon, I., and Bhorjee, S. (1982) Isolation and characterization of nuclei and purification of chromatin from differentiating cultures of rat skeletal muscle. *Exp. Cell Res.* **137**, 141-154
- Merscher, S., Hanselmann, R., Welter, C., and Dooley, S. (1994) Nuclear Runoff transcription analysis using chemiluminescent detection. *BioTechniques* **16**, 1024-1026
- Miller, W.C., Hickson, R.C., and Bass, N.M. (1988) Fatty acid binding proteins in three types of rat skeletal muscle. *Proc. Soc. Exp. Biol. Med.* **189**, 183-189
- Mitra, D., and Laurence, J. (1997) Quantitative RT-PCR for human Fas (CD95) expression. *BioTechniques* **22**, 442-446
- Mullis, K.B., and Faloona, F.A. (1987) Specific synthesis of DNA *in vitro* via a polymerase-catalyzed chain reaction. *Methods Enzymol.* **155**, 335-350
- Nevins, J.R. (1987) Isolation and analysis of nuclear RNA. *Methods Enzymol.* **152**, 234-241
- Ockner, R.K., Manning, J.A., Poppenhausen, R.B., and Ho, W.K.L. (1972) A binding protein for fatty acids in cytosol of intestinal mucosa, liver, myocardium, and other tissues. *Science* **177**, 56-58
- Orchard, I., and Lange, A.B. (1983) The hormonal control of haemolymph lipid during flight in *Locusta migratoria*. *J. Insect Physiol.* **29**, 639-642
- Owczarek, C.M., Enriquez-Harris, P., and Proudfoot, N.J. (1992) The primary transcription unit of the human $\alpha 2$ globin gene defined by quantitative RT/PCR. *Nucl. Acids Res.* **20**, 851-858
- Parker, C.S., and Topol, J. (1984a) A *Drosophila* RNA polymerase II transcription factor contains a promoter region-specific DNA-binding activity. *Cell* **36**, 357-369
- Parker, C.S., and Topol, J. (1984b) A *Drosophila* RNA polymerase II transcription factor binds to the regulatory site of an hsp 70 gene. *Cell* **37**, 273-283
- Peltz, S. W. And Ross, J. (1987) Autogenous regulation of histone mRNA decay by histone proteins in a cell free system. *Mol. Cell Biol.* **7**, 4345-4356
- Phelan, C.M., Larsson, C., Baird, S., Futreal, P.A., Rutledge, M.H., Morgan, K., Tonin, P., Hung, H., Korneluk, R.G., Pollak, M.N., Narod, S.A. (1996) The human mammary-derived growth inhibitor (MDGI) gene: genomic structure and mutation analysis in human breast tumors. *Genomics* **34**, 63-68

- Price, H.M., Ryan, R.O., and Haunerland, N.H. (1992) Primary structure of locust flight muscle fatty acid binding protein. *Arch. Biochem. Biophys.* **297**, 285-290
- Rainey, R.C. (1989) Migration and Meteorology. Clarendon Press, Oxford, p. 12
- Rappolee, D., Wang, A., Mark, D., and Werb, Z. (1989) Novel method for studying mRNA phenotypes in single or small numbers of cells. *J. Cell Biochem.* **39**, 1-11
- Robinson, M., and Simon, M. (1991) Determining transcript number using the polymerase chain reaction: PGK-2, mP2, and PGK-2 transgene mRNA levels during spermatogenesis. *Nucl. Acids Res.* **19**, 1557-1562
- Ross, J. (1988) Messenger RNA turnover in eukaryotic cells. *Mol. Biol. Med.* **5**, 1-14
- Ross, J. And Kobs, G. (1986) H4 histone messenger RNA decay in cell free extracts initiates at or near the 3' terminus and proceeds 3' to 5'. *J. Mol. Biol.* **188**, 579-593
- Ross, J., and Sullivan, T.D. (1985) Half-lives of beta and gamma globin messenger RNAs and of protein synthetic capacity in cultured human reticulocytes. *Blood* **66**, 1149-1154
- Saiki, R.K., Scharf, S., Faloona, F., Mullis, K.B., Horn, G.T., Erlich, H.A., and Arnheim, N. (1985) Enzymatic amplification of β -globin genomic sequences and restriction site analysis for diagnosis of sickle cell anemia. *Science* **230**, 1350-1354
- Saric, T., and Shain, S.A. (1997) Semiquantitative RT-PCR: enhancement of assay accuracy and reproducibility. *BioTechniques* **22**, 630-636
- Sarzani, R., Claffey, K.P., Chobanian, A.V., and Brecher, P. (1988) Hypertension induces tissue specific gene suppression of a fatty acid binding protein in rat aorta. *Proc. Natl. Acad. Sci. USA* **85**, 7777-7781
- Schneeberger, C., and Zeillinger, R. (1996) PCR-mediated synthesis of exogenous competitors for quantitative RT-PCR. *BioTechniques* **20**, 360-362
- Senshu, T. and Ohashi, M. (1979) Fate of newly synthesized histones shortly after interruption of DNA replication. *J. Biochem.* **86**, 1259-1267
- Shapiro, D.J., Sharp, P.A., Wahli, W.W., and Keller, M.J. (1988) A high efficiency HeLa cell nuclear transcription extract. *DNA* **7**, 47-55
- Sierra, F. (1990) A laboratory guide to in vitro transcription. (Azzi, A., Polak, J.M., and Saluz, H.P., eds.) Birkhäuser Verlag, Basel
- Singer-Sam, J., Robinson, M., Bellve, A., Simon, M., and Riggs, A. (1990) Measurement by quantitative PCR of changes in HPRT, PGK-1, PGK-2, APRT, Mtase, and Zfy gene transcripts during mouse spermatogenesis. *Nucl. Acids Res.* **18**, 1255-1259
- Smuckler, E.A., Koplitz, M., and Smuckler, D.E. (1976) Subnuclear components. preparation and fractionation (Birnie, G.D., ed.) Butterworths, London, pp. 1-57

- Souaze, F., Ntodou-Thome, A., Tran, C.Y., Rostene, W., and Forgez, P. (1996) Quantitative RT-PCR: limits and accuracy. *BioTechniques* **21**, 280-285
- Specht, B., Bartetzko, N., Hohoff, C., Kuhl, H., Franke, R., Börchers, T., and Spener, F. (1996) Mammary derived growth inhibitor is not a distinct protein but a mix of heart type and adipocyte type fatty acid binding protein. *J. Biol. Chem.* **271**, 19943-19949
- STELLA II, High Performance Systems, Inc., Hanover, NH
- Surholt, B., Goldberg J., Schulz, T.K.F., Beenakker, A.M.Th., and van der Horst, D.J. (1991) Lipoproteins act as a reusable shuttle for lipid transport in the flying death's head hawkmoth *Acherontia atropos*. *Biochim. Biophys. Acta* **1086**, 15-21
- Tarnuzzer, R.W., Macauley, S.P., Farmerie, W.G., Caballero, S., Ghassemifar, M.R., Anderson, J.T., Robinson, C.P., Grant, M.B., Humphreys-Beher, M.G., Franzen, L., Peck, A.B., and Schultz, G.S. (1996) Competitive RNA templates for detection and quantitation of growth factors, cytokines, extracellular matrix metalloproteinases by RT-PCR. *BioTechniques* **20**, 670-674
- Tata, J.R. (1974) Isolation of nuclei from liver and other tissues. *Methods Enzymol.* **31**, 253-262
- Treuner, M., Kozak, C.A., Gallahan, D., Grosse, R., and Müller, T. (1994) Cloning and characterization of the mouse gene encoding mammary derived growth inhibitor/heart fatty acid binding protein. *Gene* **147**, 237-242
- Tsai, S.J., and Wiltbank, M.C. (1996) Quantification of mRNA using competitive RT-PCR with standard curve Methodology. *BioTechniques* **21**, 862-866
- Uvarov, B.P. (1977) Grasshoppers and Locusts. A handbook of general acridology, vol. 2, Center for Overseas Pest Research, London.
- Van den Heuvel, J.P., Tyson, F.L., and Bell, D.A. (1993) Construction of recombinant RNA templates for use as internal standards in quantitative RT-PCR. *BioTechniques* **14**, 395-398
- Van den Hondel-Franken, M.A.M., and Flight, W.F.G. (1981) tracheolization and the effects of implantation of corpora allata on the invagination of tracheoblasts into the developing flight muscle fibers of *Locusta migratoria*. *Gen. Comp. Endocrinol.* **43**, 503-518
- Van der Horst, D.J., Van Doorn, J., and Beenackers, A.M. Th. (1978) Dynamics in the haemolymph trehalose pool during flight of the locust, *Locusta migratoria*, *Insect Biochem.* **8**, 413-416
- Van der Horst, D.J., Van Doorn, J.M., Passier P.C.C.M., Vork, M.M., and Glatz J.F.C. (1993) Role of fatty acid binding protein in lipid metabolism of insect flight muscle. *Mol. Cell Biochem.* **123**, 145-152

- Van Heusden, M.C., Van der Horst, D.J., Kawooya J.K., and Law J.H. (1991) *In vivo* and *in vitro* loading of lipid by artificially lipid-depleted lipophorins: evidence for the role of lipophorin as a reusable lipid shuttle. *J. Lipid Res.* **32**, 1789-1794
- Van Heusden, M.C., Van der Horst, D.J., Voshol, J., and Beenackers, A.M.Th. (1987) The recycling of protein components of the flight specific lipophorin in *Locusta migratoria*. *Insect Biochem.* **17**, 771-776
- van Nieuwenhoven, F.A., Verstijnen, C.P.H.J., Abumrad, N.A., Willemsen, P.H.M., van Eys, G.J.J.M., van der Vusse, G.J., and Glatz, J.F.C. (1995) Putative membrane fatty acid translocase and cytoplasmic fatty acid-binding protein are co-expressed in rat heart and skeletal muscles. *Biochem. Biophys. Res. Commun.* **207**, 747-752
- Veerkamp, J.H., and Maatman, R.G. (1995) Cytoplasmic fatty acid-binding proteins: their structure and genes. *Prog. Lipid Res.* **34**, 17-52
- Veerkamp, J.H., and van Moerkerk, H.T.B. (1993) Fatty acid binding protein and its relation to fatty acid oxidation. *Mol. Cell Biochem.* **123**, 101-106
- Veerkamp, J.H., Paulussen R.J., Peeters, R.A., Maatman, R.G., van Moerkerk, H.T., and van Kuppevelt, T.H. (1990) Detection, tissue distribution and (sub)cellular localization of fatty acid binding protein types. *Mol. Cell Biochem.* **98**, 11-18
- Wang, A.M., Doyle, M.V., and Mark, D.F. (1989) Quantitation of mRNA by the polymerase chain reaction. *Proc. Natl. Acad. Sci. USA* **86**, 9717-9721
- Wang, Z., Chen, X., and Haunerland, N.H. (1993) Flight muscle development in juvenile and adult forms of the desert locust, *Schistocerca gregaria*. *J. Insect Physiol.* **39**, 325-333
- Wheeler, C.H. (1989) Mobilization and transport of fuels to the flight muscles. In: *Insect flight* (Goldsworthy, G.J. and Wheeler, C.H., ed.) CRC Press, Inc., 273-303
- Wiesner, R.J. (1992) Direct quantification of picomolar concentrations of mRNAs by mathematical analysis of a reverse transcription/exponential polymerase chain reaction assay. *Nucl. Acids Res.* **20**, 5863-5864
- Wigglesworth, V.B. (1983) The physiology of insect tracheoles, In: *Advances in Insect Physiology*, vol. 17 (Berridge, M.J., Treherne, J.E., and Wigglesworth, V.B., eds.), Academic Press, New York, pp. 85-148
- Yokoi, H., Natsuyama, S., Iwai, M., Noda, Y., Mori, T., Mori, K.J., Fujita, K., Nakayama, H., and Fujita, J. (1993) Non-radioisotopic quantitative RT-PCR to detect changes in mRNA levels during early mouse embryo development. *Biochem. Biophys. Res. Commun.* **195**, 769-775
- Zahradka, P., Larson, D.E., and Sells, B.H. (1989) RNA polymerase II-directed gene transcription by rat skeletal muscle nuclear extracts. *Exp. Cell Res.* **185**, 8-20